UNIVERSITÄT ZU LÜBECK

From the institute of Nutrition Medicine

of the University of Lübeck

Director: Prof. Dr. Sina

Development of differentially glycosylated IgG antibodies

Dissertation for Fulfillment of

Requirements for the Doctoral Degree

of the University of Lübeck

from the Department of Natural Sciences

Submitted by

Simon Eschweiler

from Stolberg

Lübeck 2017

First referee: Prof. Dr. Marc Ehlers

Second referee: Prof. Dr. Tamás Laskay

Date of oral examination: 15.08.2017

Approved for printing. Lübeck, 21.08.2017

Table of contents

Project summary

Class switched antibodies (Abs) are key mediators of the humoral immune response. They effectively bind, block, opsonize and facilitate killing of specific pathogens via different mechanisms. While these effector functions are pivotal for an effective immune response, exaggerated or flawed B cell clone selection can have detrimental effects, resulting in tissue damage or autoimmunity. The expansion of autoreactive clones is being hindered during the germinal center (GC) response. GCs form in response to a T cell dependent (TD) antigen, and substantially contribute to an effective immune reaction by development of memory B cells and Ab-secreting plasma cells. This process is being controlled by T follicular helper cells, which facilitate B cell help and ultimately induce the humoral Ab response. Two factors are known to influence the IgG Ab structure and therewith its effector functions. First, the IgG subclass, and second the varying N-linked glycosylation of the Fc region. Both define or alter the Ab conformation and thereby its affinity for type I and type II Fc receptors. Several studies indicate that especially sialylated IgG Abs facilitate anti-inflammatory properties, while agalactosylated and asialylated IgG^+ Abs act in a pro-inflammatory manner. Terminal Fc galactosylation and sialylation are facilitated by β,1-4 galactosyltransferase I (B4galt1) and α,2-6-sialyltransferase I (St6gal1), respectively.

Although the immunomodulatory potential of these differentially glycosylated IgG Abs has been intensively investigated, the mechanism by which IgG Fc-glycosylation is regulated remains poorly understood. This work evaluated the impact of different co-stimuli (either pro- or low-inflammatory), T-cell subsets and its produced cytokines for the generation of differentially glycosylated IgG Abs.

I found that the Fc-glycosylation of antigen-specific IgG Abs is regulated within the GC and that it is influenced by T follicular helper cells (Tfh), T follicular regulatory cells (Tfr), their produced cytokines, as well as expression of co-inhibitory receptors. In more detail, I could show that the expression of B4galt1 and St6gal1 in GC B cells and differentiated plasma cells is being modulated by the ratio of Tfh/Tfr cells. I modified this ratio of stimulatory/inhibitory cells by either depleting or massively inducing suppressive Tfr cells. A depletion of Tfr cells during an immune response against a low-inflammatory TD-model-antigen significantly altered the ensuing IgG glycosylation towards a higher abundance of pro-inflammatory (agalactosylated and asialylated) IgG Abs. A vast induction of Tfr cells during a pro-inflammatory immune reaction had opposing effects and resulted in a higher abundance of anti-inflammatory galactosylated and sialylated IgG Abs.

Furthermore, I delineated potential suppressive mechanisms of Tfr cells, by demonstrating substantial production of anti-inflammatory cytokines and a direct inhibiting effect on GC B cells. This regulatory action was facilitated by the expression of the co-inhibitory receptor Cytotoxic T-lymphocyte-associated protein 4 (CTLA-4) on Tfr cells and resulted in a direct inhibition of CD28 mediated Tfh cell activation by downregulating CD86 on GC B cells.

Thus, IgG Ab glycosylation seems to be regulated during the GC response and can be actively modulated by altering the Tfh/Tfr ratio, which could have a great impact on the treatment of autoimmune diseases, as well as vaccination strategies.

Projektzusammenfassung

Immunglobuline sind die zentralen Mediatoren der humoralen Immunantwort. Sie binden, blocken, opsonisieren und vermitteln das Abtöten pathogener Keime durch verschiedene Effektormechanismen. Obwohl diese Effektorfunktionen ausschlaggebend für eine effektive Immunantwort sind, können unkontrollierte oder fehlerhafte Selektionsmechanismen autoreaktiver B-Zell Klone zu Gewebeschädigungen oder Autoimmunität führen. Die Expansion solcher autoreaktiver B-Zell Klone wird während der Keimzentrumsreaktion verhindert. Keimzentren formen sich als Antwort auf T-Zell abhängige Antigene und tragen durch die Entwicklung von *memory* B-Zellen und Antikörper sekretierender Plasmazellen entscheidend zu einer erfolgreichen Immunantwort bei. Dieser Prozess wird maßgeblich von T follikulären Helferzellen reguliert, die B-Zell Hilfe vermitteln und schließlich die humorale Immunantwort induzieren. Es gibt 2 Faktoren, die Einfluss auf die Antikörperstruktur und damit auf ihre Effektorfunktionen ausüben können. Erstens, die IgG Subklasse und zweitens die konservierte Glykosylierung an der Fc Region der Antikörper. Beide sind in der Lage, die Antikörperkonformation zu verändern und somit auch ihre Affnitität zu Typ I und Typ II Fc Rezeptoren. Verschiedene Studien deuten darauf hin, dass vor allem sialinisierte IgG Antikörper anti-inflammatorische Eigenschaften vermitteln, während agalaktosylierte und asialinisierte IgGs pro-inflammatorisch agieren. Terminale Galaktosylierung und Sialinisierung werden von den Enzymen β,1-4 galaktosyltransferase I (B4galt1) and α,2-6-sialyltransferase I (St6gal1) katalysiert.

Obwohl das immunomodulatorische Potenzial dieser unterschiedlich glykosylierten IgG Antikörper intensiv erforscht wurde, ist sehr wenig über die Regulation dieses Prozesses bekannt. Diese Arbeit untersucht daher den Einfluss unterschiedlicher Co-Stimuli (pro- und gering-inflammatorisch), T-Zell Populationen und der von ihnen sekretierten Zytokine auf die Entwicklung unterschiedlich glykosylierter IgG Antikörper.

Ich konnte zeigen, dass die IgG Fc-Glykosylierung nach unterschiedlich inflammatorischen T-Zell abhängigen Immunreaktionen im Keimzentrum reguliert wird und dass sie von T-follikulären Helferzellen (Tfh), T-follikulären regulatorischen Zellen (Tfr), ihren produzierten Zytokinen und der Expression co-inhibitorischer Rezeptoren beeinflusst wird. Im Einzelnen konnte ich zeigen, dass die Expression der Enzyme B4galt1 und St6gal1 in B-Zellen im Keimzentrum und Plasmazellen durch das Verhältnis von Tfh/Tfr Zellen moduliert wird. Dieses Verhältnis von

stimulatorischen/inhibitorischen Zellen konnte durch Depletion oder Induktion regulatorischer Tfr Zellen verändert werden. Eine Depletion von Tfr Zellen während einer gering-inflammatorischen Immunreaktion gegen ein T-Zell abhängiges Modellantigen resultierte in der Produktion eines größeren Anteils pro-inflammatorischer (agalaktosylierter und asialinisierter) IgG Antikörper. Eine starke Induktion regulatorischer Tfr Zellen während einer pro-inflammatorischen Immunreaktion resultierte hingegen in einem erhöhten Anteil anti-inflammatorischer galaktosylierter und sialinisierter IgG Antikörper. Zudem konnte ich potentielle suppressive Mechanismen von Tfr Zellen aufzeigen. Diese bestanden in hoher Produktion anti-inflammatorischer Zytokine und direkter Inhibiton von B-Zellen im Keimzentrum. Dieser inhibitorische Mechanismus wurde von dem Rezeptor *Cytotoxic T-lymphocyte-associated protein 4* (CTLA-4) auf Tfr Zellen vermittelt und resultierte in einer aktiven Herrunterregulierung des co-stimulatorischen Rezeptors CD86 auf B-Zellen im Keimzentrum.

Zusammengefasst konnte gezeigt werden, dass die IgG Fc-Glykosylierung während der Keimzentrumsreaktion durch das Verhältnis von Tfh/Tfr Zellen aktiv moduliert werden kann. Dies könnte einen großen Einfluss auf die Behandlung verschiedener Autoimmunkrankheiten und dem Design neuer Vakzinierungsmethoden haben.

1 Introduction

1.1 Immune system

The immune system effectively detects and eradicates harmful pathogens, while simultaneously maintaining tolerance towards harmless self- and foreign antigens. In order to properly process these opposing immune reactions and ensuing effector functions, the immune system needs to be tightly regulated. While the innate immune system is a first line of defense against a broad spectrum of pathogens, the adaptive immune system develops over time and is specific for distinct antigens. If an infection cannot be cleared initially by innate immunity and the antigen burden rises, adaptive immune responses are being triggered. This requires an effective interplay between antigen presenting cells (APCs) and T lymphocytes. T cells with a specific T cell receptor (TCR) get activated, proliferate and differentiate upon antigen-presentation and form the primary cell based immune reaction.

1.2 T lymphocytes

$CD4^+$ T cells form a diverse group of either helper cells (Th) or regulatory cells (Treg), all of which secrete specific cytokines, which elicit effector functions. While natural Tregs (nTregs) derive from the thymus in response to self-antigen, peripheral Tregs (iTregs) derive from naïve $CD4^+$ T cells in peripheral tissues (Kasper et al. 2016). Both Treg populations require stable forkhead-box-protein 3 (FoxP3) expression for their development and TGF-β and IL-2 have been shown to effectively maintain FoxP3 expression (Fontenot et al. 2003; Zheng et al. 2007). Moreover, it has been reported that iTregs also require a specific cytokine milieu consisting of TGF-β and a lack of pro-inflammatory cytokines like Interleukin-4 (IL-4), Interleukin-6 (IL-6) or Interferon-γ (IFN-γ) for differentiation (Kasper et al. 2016; Chen et al. 2003). They develop upon antigen-encounter through MHC-II presentation of antigen-presenting cells (APCs). Apart from the classical Th and Treg populations, recent studies underlined the importance of another subset of T cells, T follicular helper (Tfh) cells and $FoxP3^+$ T follicular regulatory (Tfr) cells (Crotty 2011; Wing et al. 2014; Sage et al. 2015; Weinstein et al. 2016). These cells are thought to control the germinal center (GC) response, which forms in response to T cell dependent (TD) antigens and to control B cell differentiation (Wing et al. 2014; Sage & Sharpe 2016; Aloulou et al. 2016).

1.3 B lymphocytes

B cells can be subdivided into 3 distinct groups. Marginal zone (MZ) B cells and B1 cells are able to efficiently respond to T cell independent (TI) antigens, whereas follicular B cells seem to preferentially react to TD antigens (Allman & Pillai 2008; Carsetti et al. 2004; Nutt et al. 2015). Cross-linking of antigen-specific B cell receptors (BCR) then leads to activation of these cells (Pali-Schöll & Jensen-Jarolim 2016). When follicular B cells are being activated by a TD antigen, the cells migrate to the T cell-B cell (T-B) border or interfollicular (IF) region of secondary lymphoid organs, ultimately differentiating either into Ab-secreting plasma blasts, unswitched memory B cells (MBCs) or re-entering the follicle and become GC B cells (Gatto & Brink 2010; Victora & Nussenzweig 2012; Takemori et al. 2014). The germinal center reaction culminates in the production of memory B cells and high-affinity Ab-secreting plasma cells (PCs), a hallmark of the humoral immune response.

1.4 Germinal center reaction

An effective humoral immune response against TD antigens requires a complex interplay between a variety of different cell types (Crotty 2011; Goodnow et al. 2010; Baumjohann et al. 2013). B cells, activated by exogenous antigen within the follicle migrate to the T-B border or IF region within secondary lymphoid organs and form transient or long-lasting interactions with antigen-specific T cells, which were primed by antigen-presenting Dendritic cells (DCs) (**Figure 1**) (Vinuesa & Cyster 2011; Qi 2016). As mentioned above, not all activated B cells return to the follicle, where they form GCs, but a subset of them, supposedly those with high affinity for the antigen, move to the medullary chords, proliferate and differentiate into short-lived plasma blasts or unswitched and unmutated MBCs (Gatto & Brink 2010; Victora & Nussenzweig 2012; Kaji et al. 2012; Paus et al. 2006; O'Connor et al. 2006). This process is heavily dependent on co-stimulatory T cell signals, especially between CD40 and CD40L (Cunningham et al. 2004), and prolonged interactions are thought to preferentially drive the expansion of extrafollicular plasma blasts (Chan et al. 2009; Schwickert et al. 2011). From the remainder B cells, only those with the highest relative affinity for the antigen re-enter the follicle to establish the GC, probably due to competition for T cell help (**Figure 1**) (Shih et al. 2002; Schwickert et al. 2011).

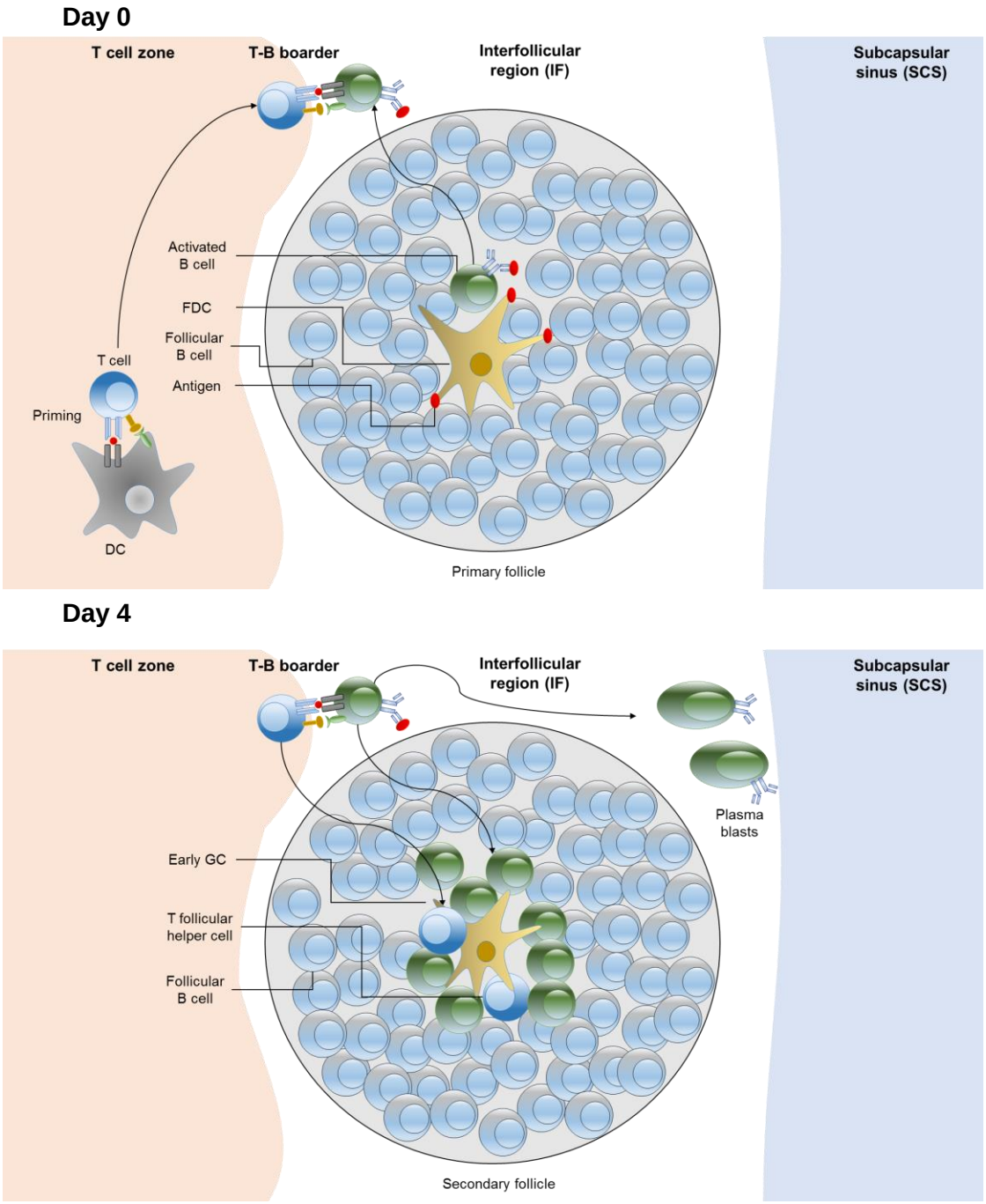

Figure 1: Initiation of the germinal center reaction and early GC formation. On day 0, naïve T cells are primed by DCs and migrate to the T-B boarder or the IF zone where they form long lasting interactions with activated B cells. By day 4, those activated B cells proliferated and either differentiated into Ab-secreting plasma blasts or re-entered the follicle where they initiate the GC reaction. Primed T cells, which acquired a Tfh cell phenotype are able to migrate into the follicle via a CXCL13 gradient, where they facilitate B cell help. Modified from (De Silva & Klein 2015).

Not all B cells within the GC are antigen-specific. Instead, a high abundance of GC B cell population is composed of so called bystander B cells, which have no specificity for the cognate antigen (Qi 2016). Due to that, they receive no stimulatory signals and eventually go into apoptosis. Activated T cells, which acquire a Tfh phenotype are able to migrate and enter the GC due to a CXCL13 gradient and facilitate B cell help (Sage, Alvarez, et al. 2014; Shulman et al. 2013). Only those GC B cells, which possess a high affinity BCR and are therefore able to efficiently present the cognate antigen via MHC-II, receive positive selection signals from Tfh cells and can therefore re-enter into the dark zone, where they undergo iterative cycles of proliferation and somatic hypermutation (SHM) (Victora et al. 2010). This process ensures somatic hypermutation, affinity maturation and class switch recombination (CSR) of GC B cells, with an initially high affinity for the cognate antigen and eventually leads to the differentiation of memory B cells and long lived plasma cells (LLPCs) (Baumjohann et al. 2013; McHeyzer-Williams et al. 2012; Tarlinton & Good-Jacobson 2013). Interestingly, a recent study unraveled the sequential order, in which the GC produces these effector cells. Through the utilization of BrdU pulse experiments, it became apparent that LLPCs are produced very late in the GC response, preceded by the production of unswitched and switched MBCs (Weisel et al. 2016). Interclonal competition for antigen and thereby T cell help promote affinity maturation (Zhang et al. 2013).

While self-tolerance should prevent the proliferation of self-reactive clones, it was shown in numerous studies, that this regulatory mechanism is often flawed, leading to autoimmunity (Kao et al. 2014; Schwab et al. 2015; Esplugues et al. 2011; Holmdahl et al. 2014). In this regard, recent studies unveiled the importance of FAS expression as well as self-antigen expression for the survival of self-reactive GC B cells. Self-reactive GC B cells fail to survive, if they express sufficient amounts of FAS, whereas FAS deficient mice and humans produce large amounts of self-reactive IgE (Butt et al. 2015). Furthermore, several studies highlight the GC microenvironment as another key factor in regulating autoreactive B cells. A study in Bxd-2 mice, which spontaneously develop arthritis underlined the importance of Interleukin-17 (IL-17) in the induction of GCs and autoreactive Abs. Mice, in which IL-17 signaling was blocked or mice that lacked IL-17Receptor (IL-17R) expression were less prone to produce autoreactive GC B cells and Abs (Hsu et al. 2008). Other studies clearly delineated the dependence of Interferon-γ Receptor I (IFN-γRI) expression on B cells for the induction of spontaneous GCs, Tfh cells and production of auto-reactive Abs. B cell specific IFN-γRI depletion was sufficient to efficiently reduce spontaneous GC formation and Tfh numbers in a murine model for autoimmunity (Domeier et al. 2016). Accordingly, IFN-γRI signaling

was identified to substantially contribute to pathogenesis, in a murine model of systemic lupus erythematosis (SLE) (Jackson et al. 2016).

Taken together, GCs form in response to a T cell dependent (TD) antigen, and substantially contribute to an effective immune reaction by development of memory B cells and Ab-secreting plasma cells. This process is being controlled by T follicular helper cells, which facilitate B cell help and ultimately induce the humoral Ab response.

1.5 T follicular helper cells

Tfh cells characterize a specialized subset of effector T cells, which provide B cell help during GC reactions to induce memory B cells and Ab-secreting PCs (Tangye et al. 2013; Sage et al. 2015). Recent studies revealed striking similarities between murine and human Tfh cells (Schmitt et al. 2014). They are defined by their expression of the transcription factor B-cell lymphoma 6 (Bcl-6), the chemokine receptor CXC receptor 5 (CXCR5), inducible T cell co-stimulator (ICOS) and programmed cell death protein 1 (PD-1) (Sage, Paterson, et al. 2014; Shulman et al. 2014; Ramiscal&Vinuesa2013;Crotty2015) (**Table 1**). They differentiate into early Tfh cells through cognate interactions with DCs and migrate into the GC through a CXCL13 gradient (Crotty 2015). Their differentiation is induced in the IF zone, where they form long lasting interactions with GC B cells and upregulate Bcl-6, as well as CXCR5 and PD-1 and differentiate into Tfh cells (Kerfoot et al. 2011). BLIMP-1 expression represses Bcl-6 and accordingly also suppresses Tfh induction (Johnston et al. 2009). While GC B cells don't seem to be necessary for the primary induction of the Tfh cell phenotype, they are crucial for the maintenance of this phenotype, once the Tfh cells enter the follicle (Goenka et al. 2011; Crotty 2014). The maintenance of the Tfh cell phenotype also requires continuous antigen supply, as well as constant, yet transient interactions with GC B cells (Baumjohann et al. 2013). Although Tfh cells have a clear phenotype, it doesn't seem to be static but substantially flexible (Cannons et al. 2013). Cytokines, secreted by DCs activate STAT3 (Fazilleau et al. 2009) and STAT4 (Nakayamada et al. 2011), which induce Bcl-6 (Yu et al. 2009; Nurieva et al. 2009). Several cytokines have been linked to the induction of Tfh cells. While IL-6, IL-21 and IL-27 seem to successfully induce a Tfh cell phenotype in mice, IL-6 is indicated to play a minor role in Tfh differentiation in humans (Schmitt et al. 2014). Here, IL-12, IL-21 and IL-27 appear to be the major inducers. Moreover, TGF-β has recently been identified as an important factor in Tfh cell differentiation in humans. Together with IL-12 and IL-23, it is able to induce the

expression of CXCR-5,ICOS and Bcl-6, while simultaneously repressing BLIMP-1 (Schmitt et al. 2014).

Table 1: Comparison of Tfr, Treg, Tfh and T naïve phenotypes, adapted from (Sage & Sharpe 2015)

	Tfr	Treg	Tfh	T naïve
CD4	++	++	++	++
CXCR5	++	-	+++	-
FoxP3	++	++	-	-
ICOS	+++	+	++	+
PD-1	++	-, +	++	-
Bcl-6	+	-	++	-
Blimp-1	+	+	-	-
CTLA-4	+++	++	+	-
CD25	++	+++	-	-
GITR	+++	++	-	-
KI-67	++	-, +	+++	-, +
CD44	++	-	++	-
IL-21	-	-	+	-

Tfh cells are critical for the GC formation, as they facilitate B cell help and B cell selection and induce differentiation into high affinity memory B cells and plasma cells through constant transient interactions (Weinstein et al. 2016). It has been shown that Tfh cells are able to produce specific cytokines, which regulate the GC response and also contribute to isotype switching. They are able to produce IL-21, IL-4, IFN-γ and other cytokines (Sage, Alvarez, et al. 2014; Carola G Vinuesa et al. 2016). While IL-21 has been identified as a key modulator of the GC response, IL-4 and IFN-γ have been shown to induce class switch recombination (CSR) in response to certain pathogens (Weinstein et al. 2016). Mice deficient in IL-4 or IL-4Rα resulted in reduced production of IgG1 and IgE (King & Mohrs 2009; Kühn et al. 2013; Ballesteros-Tato et al. 2016; Fairfax et al. 2015). On the other hand, deficiency of IL-21 results in flawed affinity maturation of B cells and LLPC generation (Zotos et al. 2010; Linterman et al. 2010). Furthermore, it has been suggested that IL-21 secreting Tfh cells enable high-affinity clone selection while IL-4 secreting Tfh cells induce plasma cell differentiation (Weinstein et al. 2016). Apart from co-determining the cytokine

milieu in the GC, Tfh cells interact with GC B cells through TCR-MHCII complex, ICOS-ICOSL and CD-CD40L signaling (Crotty 2011; Gitlin et al. 2014). CD40L is mainly stored in intracellular vesicles but can be rapidly transported to the cell surface upon ICOS co-stimulation, which facilitates a so called entangled contact (Qi 2016; Liu et al. 2015) (**Figure 2**). This process is characterized by a high interacting surface area and possibly explains why high affinity GC B cells outcompete their lower affinity counterparts, since a higher interacting area can provide a higher abundance of co-stimulatory signals (Liu et al. 2015).

Taken together, these cell-cell interactions support GC B cell survival (Crotty 2011), aid in B cell selection (Gitlin et al. 2014) and activate activation-induced cytidine deaminase (AID) in B cells (Reinhardt et al. 2009; Dedeoglu et al. 2004). Altogether, interaction of Tfh cells with GC B cells regulates somatic hypermutation, affinity maturation and CSR (Sage & Sharpe 2015) (**Figure 3**). Interestingly, Tfh cells seem to be able to freely migrate between different GCs and facilitate B cell help to regulate mutation and differentiation, a mechanism which is implied to amplify antigenic variation while ensuring distribution of T cell help throughout the GCs (Shulman et al. 2013). While Tfh cells are necessary to mount and efficient humoral response, recent studies indicate that exaggerated Tfh cell numbers as well as continuous Tfh cell signaling can lead to defective clone selection, production of auto-antibodies and thereby autoimmunity (Linterman et al. 2009; Vinuesa et al. 2005; Baumjohann et al. 2013). Furthermore, new studies indicate that exaggerated Tfh cell numbers and possible autoimmune reactions stem from deficiencies in the T follicular regulatory (Tfr) cell compartment, which regulate the GC B cells and Tfh cells (Sage et al. 2015; Wu et al. 2016; Sage & Sharpe 2016; Wing et al. 2014; Sage & Sharpe 2015).

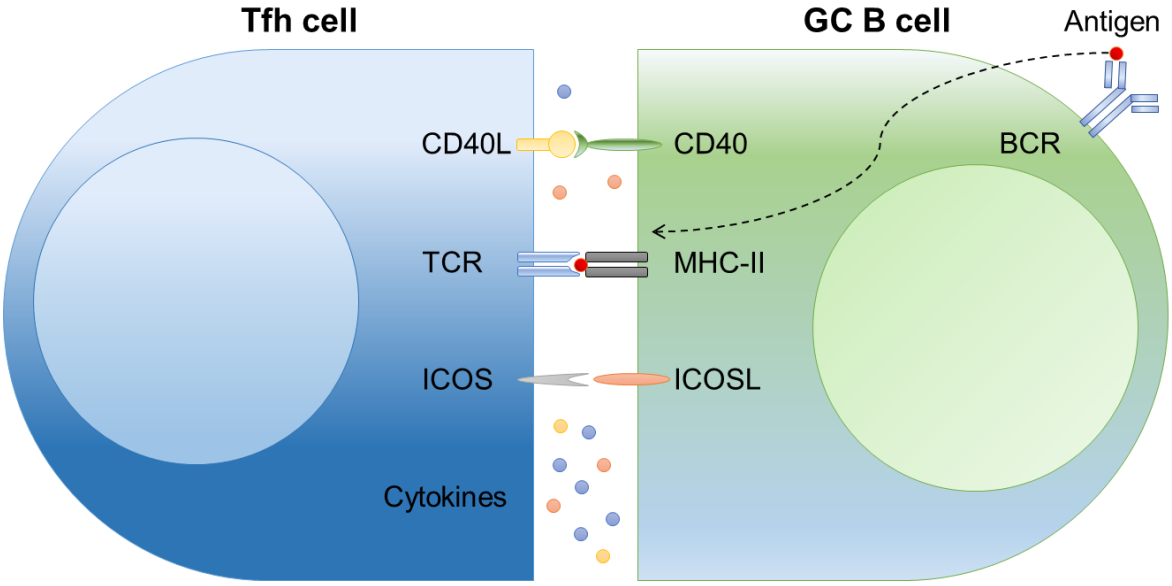

Figure 2: Tfh – GC B cell interactions in the germinal center. Antigen-specific light zone B cells form transient interactions with Tfh cells via MHC-II – TCR binding and receive additional co-stimulatory signals facilitating positive clone selection, SHM, affinity maturation and CSR. Tfh cells on the other hand receive positive signals to maintain their Tfh cell phenotype. Modified from (Qi 2016).

1.6 T follicular regulatory cells

Tfr cells control the GC reaction through inhibition of GC B cells and Tfh cells, thereby limiting GC B cells, excessive Tfh cell proliferation and production of self-reactive Abs (Sage & Sharpe 2015). Tfr cells are phenotypically similar to Tfh cells due to their expression of CXCR5, ICOS, PD-1 and Bcl-6, but unlike Tfh cells, they additionally express FoxP3, CD25 and GITR, while they lack expression of CD40L, IL-21 and IL-4 (**Table 1**) (Aloulou et al. 2016; Linterman et al. 2011; Chung et al. 2011; Wollenberg et al. 2011; Sage et al. 2013). While Tfh cells originate from naïve T cells (Crotty 2011), Tfr cells can either arise from nTreg (Linterman et al. 2011; Chung et al. 2011) or peripheral iTreg precursors (Aloulou et al. 2016). Tfr cells and Treg cells represent distinct subsets, since they display a different transcriptional profile and lack of Bcl-6 or B cells resulted in profoundly reduced Tfr cells, while the abundance of Treg cells remained unchanged (Linterman et al. 2011; Chung et al. 2011; Wollenberg et al. 2011). New studies imply, that Tfr might be directed against the immunizing antigen (either foreign- or self-antigen), rather than possessing a skewed TCR against self-antigens (Aloulou et al. 2016). As for Tfh cells, Tfr cells depend on DCs for differentiation, since a DC depletion leads to profoundly reduced Tfr cells (Sage, Alvarez,

et al. 2014) and similar to Tfh cells they require B cell stimulation for differentiation and expansion (Linterman et al. 2011; Sage, Alvarez, et al. 2014; Kerfoot et al. 2011). Moreover, they require co-stimulatory signals to efficiently differentiate, as CD28 induces FoxP3 (Tai et al. 2005) and $CD28^{-/-}$ mice show marked reductions in the Tfr compartment in secondary lymphoid organs and in the blood (Linterman et al. 2011; Sage et al. 2013). Further co-stimulation in form of ICOS signaling is required for optimal differentiation, since ICOS mediates expression of Bcl-6 and a lack of ICOS results in similar Tfr cell defects as in $CD28^{-/-}$ mice (Sage et al. 2013). Adoptive transfer models, in which Tfh cells were transferred either alone or in combination with Tfr cells, revealed the suppressive capacity of Tfr cells to inhibit antigen-specific IgG production (Sage et al. 2013). Accordingly, *in vitro* studies confirmed that Tfr cells are able to restrain Ab production significantly better than Treg cells (Sage, Alvarez, et al. 2014; Sage et al. 2013). Moreover, Tfr cells efficiently suppress Tfh cell activation, defined as reduction in Ki-67 expression, without changing their transcriptional profile, as well as secretion of Tfh specific cytokines IL-21, IL-4 and IFN-γ and inhibited formation of GC B cells and CSR (Sage, Alvarez, et al. 2014). Although it is still unclear, how these regulatory functions are exerted, several mechanisms have been proposed. These suppressive effects might involve mechanical disruption of GC B-Tfh cell interactions or secretion of regulatory cytokines IL-10 and TGF-β (Sage & Sharpe 2015). CTLA-4 has been identified as a key regulatory molecule, due to its inherently high affinity for B7-1 and B7-2. Selective depletion of CTLA-4 on Treg cells leads to profoundly enhanced GC responses, while depletion of CTLA-4 on Tfr cells results in a substantial loss of suppressive capacity (Paterson et al. 2015; Wing et al. 2014).

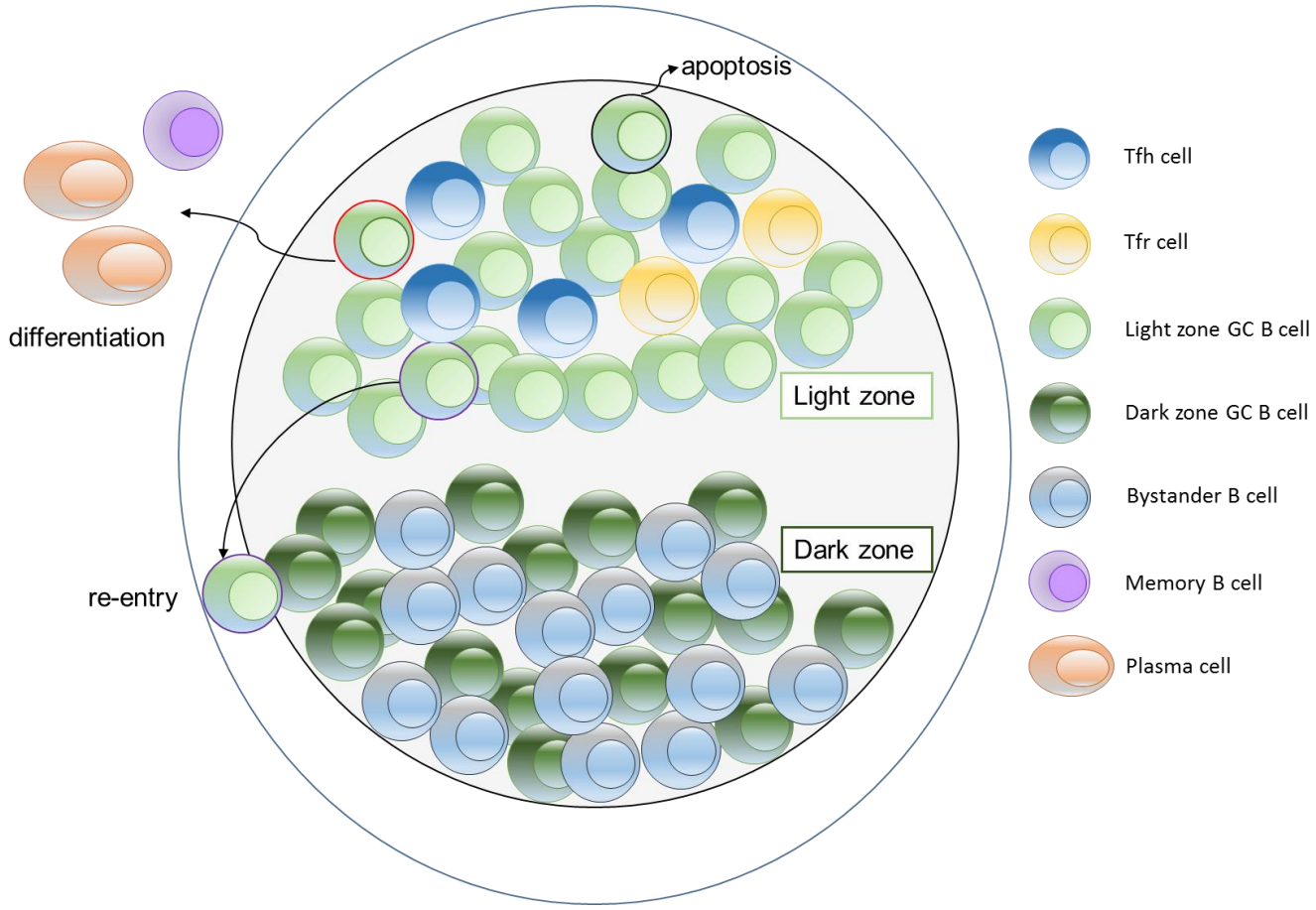

Figure 3: GC reaction in response to a TD antigen. The germinal center is divided into the dark zone and the light zone. Most of the B cells within the GC bear no specificity for the cognate antigen (bystander B cells). Dark zone germinal center B cells undergo multiple round of cell division and somatic hypermutation and migrate to the light zone, where they interact with Tfh and Tfr cells. Light zone GC B cells compete with each other for T cell help and antigen acquisition. Cells, which don't receive sufficient positive selection signals go into apoptosis (black circled), while positively selected cells (lilac circled) can re-enter the dark zone to repeat cell division and somatic hypermutation. Tfr cells are supposed to not only be able to suppress Tfh cells, but also GC B cells, adding an additional layer of competition for T cell help. Ultimately, B cells with a high affinity BCR differentiate into plasma cells or memory B cells (red circled). Modified from (Qi 2016).

1.7 Co-inhibitory receptors

Co-stimulation has been postulated to explain why T cells are able to react to pathogens, while maintaining tolerance to self and harmless foreign antigens. It has been demonstrated, that positive or co-stimulatory signals promote T cell activation, while negative or co-inhibitory signals are key mediators of tolerance (Kamphorst et al. 2017; Anderson et al. 2016). Multiple of these co-inhibitory receptors have been identified recently, among them programmed death-1 (PD-1), lymphocyte activation gene-3 (LAG-3), T cell Ig and mucin containing domain-3 (TIM-3), CLTA-4, and others.

PD-1 is inducibly expressed by $CD4^+$ and $CD8^+$ T cells, natural killer cells, macrophages, B cells and DC cell subsets during inflammation or immune activation (Schildberg et al. 2016). While it is usually transiently expressed and rapidly downregulated upon antigen clearance, sustained PD-1 expression defines an exhausted T cell state, characterized by decreased functionality (Blackburn et al. 2009). Interestingly, in the case of Tfh and Tfr cells, PD-1 expression is sustained without marking these cells as exhausted (**Table 1**). It interacts with its two ligands programmed death ligand 1 (PD-L1) and PD-L2, with the latter ligand having an approximately 3-fold higher affinity for PD-1 (Schildberg et al. 2016). While PD-L1 is expressed by a variety of different cells, PD-L2 expression is mainly limited to macrophages and DCs, but has been demonstrated to also be expressed on GC B cells (Kamphorst et al. 2017; Schildberg et al. 2016). Pro-inflammatory cytokines, especially IFN-γ, but also IL-10 and common γ-chain cytokines upregulate the expression of these ligands as a means of a negative feedback loop to control local inflammation (Schildberg et al. 2016). When PD-1 becomes phosphorylated on its ITIM and ITSM tyrosine motifs upon ligation, it recruits SHP-1 and SHP-2 phosphatases, which dephosphorylate CD28, thereby effectively limiting cell activation and cytokine production (Kamphorst et al. 2017).

The co-inhibitory receptor CTLA-4 is constitutively expressed on Treg and Tfr cells, to a lesser degree on Tfh cells and readily induced upon activation in naïve T cells (Walker 2013; Sage, Paterson, et al. 2014; Linterman et al. 2011; Wing et al. 2014). It has a much higher affinity for B7 molecules than CD28 and effectively competes with it for ligand binding (Sage, Paterson, et al. 2014). Germline deletion of CTLA-4 is fatal and mice die rapidly after birth, due to exaggerated autoimmune symptoms and Ab production (Tivol et al. 1995; Waterhouse et al. 1995; Walker et al. 2003; Sage, Paterson, et al. 2014). Moreover, germline deletion leads to excessive CD28 signaling due to lack of competition with CTLA-4 (Walker & Sansom 2015). Conditional gene

deletion of CTLA-4 (CTLA-4 CKO mice) results in autoimmunity, even when housed under pathogen free (SPF) conditions. This is accompanied by spontaneous formation of GCs and expansion of Tfh cells, as well as higher abundances of Treg and Tfr cells, suggesting that CTLA-4 expression on Treg and Tfr cells is necessary for effective GC regulation (Wing et al. 2014). Surprisingly, recent studies demonstrate, that drug induced deletion of CTLA-4 on Treg cells during adulthood does not induce autoimmunity, but efficiently prevents experimental autoimmune encephalomyelitis (EAE) (Paterson et al. 2015). Due to the lethality of germline deletion of CTLA-4, massive organ inflammation upon Treg specific deletion, as well as failure of anti-CTLA-4 Abs to target specific cell types, it is hard to unravel how CTLA-4 confers its suppressive effects (Sage, Paterson, et al. 2014).

Although a variety of studies have investigated the suppressive effects elicited by CTLA-4, no definitive mode of action has been demonstrated so far, but rather multiple possible ways, including cell-intrinsic as well as cell extrinsic T-cell effects of CTLA-4 (Walker & Sansom 2015; Paterson et al. 2015; Sage, Paterson, et al. 2014). Cell intrinsic effects are conferred through the intracellular domain of CTLA-4, which recruits the phosphatases SHP-2 and PP2A and subsequently inhibits downstream signaling of TCR (Paterson et al. 2015; Marengère et al. 1996; Cilio et al. 1998). Cell extrinsic effects on the other hand involve direct interactions between CTLA-4 and its ligands CD80 and CD86 on APCs, which can either inhibit CD28 mediated signaling and subsequent activation due to a higher affinity of CTLA-4 to its ligands, or actively downregulate B7 molecules on DCs and B cells through transendocytosis (Onishi et al. 2008; Qureshi et al. 2011; Sage, Paterson, et al. 2014; Wing et al. 2014). Nonetheless, the use of heterozygous CTLA-$4^{flox/wt}$ mice, in which Treg cells express slightly less CTLA-4, compared to wildtype mice, revealed an expansion in splenic Tfh cells, as well as antigen-specific GC B cells, plasma cells, and memory B cells after vaccination with NP-OVA in alum (Wing et al. 2014). Thus, Treg and Tfr cells mediate its suppressive effects at least in part through CTLA-4 and act on DCs, GC B cells, as well as Tfh cells, thereby influencing plasma cell numbers and Ab production.

Apart from CTLA-4 mediated suppressive effects, it has been demonstrated that the abundance of Interleukin-2 (IL-2) critically influences GC formation by altering the abundance of Tfh cells. Due to its immense immunomodulatory potential and the ability to selectively engage either stimulatory or regulatory pathways, IL-2 has been efficiently used to treat a variety of autoimmune diseases.

1.8 IL-2 therapy

IL-2 is a ~16kDa, pleiotropic molecule, able to exert various immunomodulatory actions (Arenas-Ramirez et al. 2015). It signals via the IL-2R, which can consist of different subunits CD25 (IL-2Rα), CD122 (IL-2β) and CD132 (IL-2Rγ, also referred to as the common γ-chain, γ_C), and can therefore be either mono-, di- or trimeric, depending on the cell type on which it is expressed (Boyman & Sprent 2012; Malek & Castro 2010; Liao et al. 2013). The signaling cascade comprises 3 major pathways. First, binding of IL-2 to the trimeric receptor activates the Janus family tyrosine kinases JAK1 and JAK3, which activate each other and subsequently act on downstream targets, ultimately activating STAT1, STAT3 and STAT5, which promote cell activation, proliferation and differentiation (Friedmann et al. 1996; Lin et al. 2012; Arenas-Ramirez et al. 2015). Second, IL-2 binding activates phosphoinositide 3-kinase-AKT signaling pathway, facilitating cell growth and survival (Dibble & Cantley 2015). Third, activation of mitogen-activated protein kinase (MAPK), which promotes cell growth (Liao et al. 2013).

Interestingly, IL-2 cannot signal through CD25 or CD122 alone, but requires CD132 (Arenas-Ramirez et al. 2015). Accordingly, dimerization of CD122 and CD132 ensues a low affinity IL-2R (K_D~10^{-9} M), whereas trimerization of CD25, CD122 and CD132 results in a high affinity IL-2R (K_D~10^{-11} M), increasing its affinity 10-100-fold, compared with the dimeric receptor (Arenas-Ramirez et al. 2015; Liao et al. 2013; Klatzmann & Abbas 2015). This implies a key role for CD25 expressing cells like Treg cells, rendering them substantially more sensitive to IL-2 activity. In support of this notion, IL-2 drives Treg expansion and mice and humans lacking either IL-2 or CD25 lack Tregs and develop autoimmunity (Arenas-Ramirez et al. 2015). IL-2 alone, or in conjunction with other cytokines, promotes the differentiation of a variety of cell types. A cytokine milieu, consisting of IL-2 and IL-12 promotes Th1 cells, while IL-2 with IL-4 leads to differentiation into Th2 cells and IL-2 with TGF-β results in the induction of Tregs (Arenas-Ramirez et al. 2015). Of note, several studies have shown that IL-2 signaling inhibits Tfh cell differentiation and thereby GC formation through a STAT5 dependent activation of BLIMP-1, which inhibits Bcl-6 expression (Johnston et al. 2012; Ballesteros-Tato et al. 2012; Nurieva et al. 2012).

Recently, a variety of studies have rekindled the interest in IL-2 as a tool for immunotherapy of various autoimmune diseases (Saadoun et al. 2011; Yu et al. 2015; von Spee-Mayer et al. 2015; Long et al. 2012; Hartemann et al. 2013), cancer (Rosenberg 2014) or viral infections (Cunningham-Rundles et al. 1992; Kovacs et al. 1996; Abrams et al. 2009). Mechanistically, low-

dose IL-2 therapy is thought to selectively activate and expand Tregs, due to their massively enhanced sensitivity for this cytokine, whereas a high-dose IL-2 therapy appears to stimulate $CD8^+$ T cells and NK cells (Arenas-Ramirez et al. 2015). Apart from dosage-dependent effects, IL-2, complexed with monoclonal anti-IL-2 IgG Abs, seem to selectively induce stimulatory or regulatory activities in mice, dependent on the complexing Ab (Boyman & Sprent 2012; Boyman et al. 2006). A complex of IL-2 with monoclonal (mAb) S4B6 Ab (IL-2/S4B6) occludes the CD25 binding site of IL-2, thus promoting preferential activation of $CD122^{high}$ cells, like cytotoxic $CD8^+$ T cells and NK cells. Complexing IL-2 with JES6-1 (IL-2/JES6-1) on the other hand blocks the CD122 and/or CD132 binding site, thereby facilitating efficient activation of $CD25^{high}$ cells, like Tregs (Boyman & Sprent 2012; Boyman et al. 2006). Several studies have successfully utilized this opposing IL-2 effects for the treatment of various diseases. IL-2/S4B6 complexes have shown promising results in various cancer models (Krieg et al. 2010; Levin et al. 2012; Tomala et al. 2009), as well as models of infectious diseases (Molloy et al. 2009; Hamilton et al. 2010).

IL-2/Jes6-1 complexes, which substantially and selectively increase the abundance of Tregs (7-15-fold) (Arenas-Ramirez et al. 2015), were used in the treatment of several autoimmune diseases in mice, such as collagen-induced arthritis (Lee et al. 2012), type I diabetes (Tang et al. 2008) or autoimmune encephalomyelitis (Webster et al. 2009), as well as prevention allograft rejection (Webster et al. 2009; Vokaer et al. 2013).

Of note, the IgG subclass of the used anti-IL-2 mAbs differs between the two main formulations (S4B6 and JES6-1), indicating a possible role of the Fc region for their modes of action (Boyman et al. 2006; Arenas-Ramirez et al. 2015). IL-2/mAb formulations have several advantages compared to just dosage dependent IL-2 activity. First, a massively increased half-life, due to complexation and interactions with the FcRn and second an increased specificity for either stimulatory or regulatory pathways (Létourneau et al. 2010; Phelan et al. 2008). This is especially apparent with high-dose IL-2 therapy, since $CD25^{high}$ cells get saturated first, due to their expression of the high affinity IL-2R, resulting in activation of both stimulatory $CD8^+$ T cells, NK cells, as well as Treg cells. Altogether, IL-2 therapy, either alone or in conjunction with a mAb, holds an immense immunomodulatory and therapeutic potential.

1.9 IgG antibodies

The production of high-affinity antibodies by plasma cells is an integral part of the humoral immune response and dependent on a variety of factors. While a protective reaction with sufficient Ab production needs to be assured, excessive or flawed immune responses can have detrimental effects. Therefore, a complex interplay between different cell types, co-stimulatory and co-inhibitory factors, as well as cytokines is required. Abs consist of a Fc (Fragment crystallizable) part, which exerts its immunomodulatory effector functions and of a Fab (Fragment antigen binding) part, which binds to the cognate antigen. IgGs have a tetrameric structure with pairs of identical heavy and light chains. The heavy chains compose of three constant domains (C_H1, C_H2 and C_H3) and a variable domain (V_H), while the light chain comprises one constant (C_L) and one variable (V_L) domain (**Figure 4**).

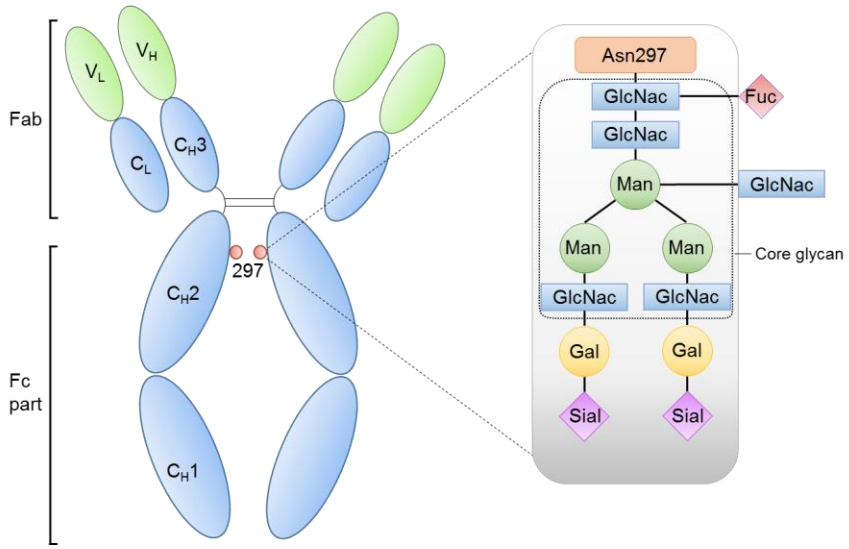

Figure 4: IgG Ab structure, comprising the conserved N-linked glycan at Asn297. The core glycan bound to Asn297 is comprised N-Acetyl-glucosamine (blue) and Mannose (green), but can be further diversified by additional N-Acetyl-glucosamine or fucose (red) addition. This moiety can be further modulated by addition of terminal galactose (yellow) and sialic acid (magenta). Modified from (Chan & Carter 2010)

During the course of a GC reaction, the Ab repertoire and also its affinity for the cognate antigen increases massively, due to SHM and affinity maturation (Tangye et al. 2013). During SHM, the

variable (V), diversity (D) and joining (J) gene segments recombinate through interaction of recombination activating gene (RAG) 1 and RAG2 with recombination signal sequences (RSSs) (Schatz & Ji 2011). This process takes place in B cells, which are located in the dark zone of the GC and results in greatly enhanced affinity of their BCRs and Abs. SHM and affinity maturation of GC B cells are being facilitated through cell-cell contacts with Tfh cells, which reside in the light zone of the GC. Thereby, Tfh cells actively influence GC B cells through co-stimulation and cytokine secretion and also impact CSR, a process which further amplifies the immunomodulatory potential of Abs (Baumjohann et al. 2013; Reinhardt et al. 2009; Shulman et al. 2013). Abs exert their effector functions through interactions of their Fc region with Fc Receptors on target cells. They are able to induce antibody-dependent cell mediated cytotoxicity (ACCC), antibody-dependent cellular phagocytosis (ADCP) and complement-dependent cytotoxicity (CDC) (Wieland et al. 2015; Chan & Carter 2010). Moreover, interactions of the FC region with FcRn (neonatal Fc receptor) modulate the half-life of IgG Abs. Thus, IgG Abs have a tremendous therapeutic potential. Accordingly, numerous Abs were approved for therapy and even more are in clinical trials for treatment of autoimmunity, cancer, inflammation and others (Chan & Carter 2010; Reichert 2016). There are four distinct IgG subclasses in humans (IgG1, IgG2, IgG3 and IgG4), as well as in mice (IgG1, IgG2a, IgG2b and IgG3) (Anthony et al. 2012). Since the IgG subclasses differ in their Fc part, they also differ in their elicited effector functions, due to their inherently diverse affinity for Fc gamma receptors (FcγRs) (**Table 2**) (Anthony et al. 2012; Irani et al. 2015). In regard of function, human IgG1 resembles murine IgG2a, whereas human IgG4 resembles murine IgG1 (Vidarsson et al. 2014; Bruhns & Jönsson 2015). FcγRs bind IgG Abs in the form of immune complexes (ICs). ICs crosslink the FcγRs, which are expressed on most immune cells, and lead to a phosphorylation of immunoreceptor tyrosine based activating motifs (ITAMs) or immunoreceptor tyrosine based inhibitory motifs (ITIMs) (Smith & Clatworthy 2010; Nimmerjahn & Ravetch 2008; Pincetic et al. 2014; Bakema & Egmond 2014). Most FcγRs bear an ITAM, with the single exclusion of FcγRIIB, which bears an ITIM. Humans and mice both possess the high affinity receptor FcγRI and the inhibitory receptor FcγRIIB, and both have several unique low-affinity FcγRs (FcγRIIA, FcγRIIC, FcγRIIIA and FcγRIIIB in humans, and FcγRIII and FcγRIV in mice) (Nimmerjahn & Ravetch 2008; Smith & Clatworthy 2010). The ratio of activating to inhibitory FcγRs (A/I ratio) sets a threshold for cell activation and dictates, together with the affinity of IgG subclass Abs, the subsequent immune response (Anthony et al. 2012).

Table 2: Human and murine FcγRs. Modified from (Smith & Clatworthy 2010; Furness et al. 2014)

Human	**FcγRI**	**FcγRIIA**	**FcγRIIC**	**FcγRIIIA**	**FcγRIIB**
Binding motif	ITAM	ITAM	ITAM	ITAM	ITIM
Binding affinity	IgG1>>>IgG2, IgG3&IgG4	IgG1 & IgG3 >>IgG2>IgG4	IgG1>IgG3>> IgG4>IgG2	IgG1>>IgG2 & IgG3>IgG4	IgG1>IgG3>> IgG4>IgG2
Mouse	**FcγRI**		**FcγRIII**	**FcγRIV**	**FcγRIIB**
Binding motif	ITAM		ITAM	ITAM	ITIM
Binding affinity	IgG2a>IgG2b >IgG1		IgG2a>IgG2b >IgG1	IgG2a>IgG2b >IgG1	IgG1>IgG2b> IgG2a

The affinity of the IgG subclasses for the different FcγRs is highly diverse. Therefore, all IgG subclasses possess an individual A/I ratio, depending on their affinity for the respective activating and inhibitory FcγRs. Murine IgG1 has a very low A/I ratio of 0.1, while murine IgG2a has an A/I ratio of 70 (Nimmerjahn & Ravetch 2005; Nimmerjahn et al. 2005). These differences stem from the fact, that IgG1 has a high affinity for the inhibitory receptor FcγRIIB and a low affinity for the other activating FcγRs, whereas IgG2a has a low affinity for FcγRIIB and a high affinity for FcγRI, FcγRIII and FcγRIV (**Table 2**).

Most cells express multiple types of FcγRs, except B cells, which only express the inhibitory receptor FcγRIIB (Amigorena et al. 1989). Here, IC binding leads to crosslinking of FcγRIIB to the BCR, resulting in ITIM phosphorylation by the kinase LYN and ensuing binding of SH-2-domain-containing inositol phosphatases (SHIPs), which effectively dephosphorylate downstream targets to inhibit the induction of an activating signal transduction (Masao et al. 1997; Ono et al. 1996; Smith & Clatworthy 2010).

Another factor besides the IgG subclass, which is able to alter the affinity of an IgG Ab for its FcγR, is glycosylation of the IgG Fc part. Recent studies suggest that variations in the glycosylation profile of IgG Abs modify its structure and therewith its affinity for their cognate FcRs

(Matsumiya et al. 2007; Kaneko et al. 2006; Boyd et al. 1995; Pincetic et al. 2014). Accordingly, different glycoforms of murine IgG1 Abs have been shown to differ greatly in the A/I ratio, depending on the abundance of α,2-6-sialylated forms, which lead to a 10-fold decrease in the A/I ration upon sialylation, due to its decreased affinity for FcγRIIB (Kaneko et al. 2006; Smith & Clatworthy 2010). Accordingly, IgG Abs can be differentially glycosylated and therefore exert varying immunomodulatory effects to further fine-tune the antibody-dependent immune response against certain antigens.

1.10 IgG glycosylation

IgG Abs possess a conserved glycosylation site at Asparagine (Asn) 297 at the C_H2 domains, which consists of a core glycan and can be further varied by addition of terminal galactose or terminal galactose and sialic acid, a process taking place in the trans-Golgi (Anthony et al. 2012) (**Figure 4**). Addition of terminal galactose and sialic acid is facilitated by the enzymes B4GalT1 and ST6Gal1, respectively (Anthony et al. 2012; Ohmi et al. 2016; Onitsuka et al. 2012; Warnock et al. 2005; Wang et al. 2015). Moreover, the core glycan can carry optional fucose or N-Acetylglucosamine residues, while the core glycan itself is a heptasaccharide consisting of N-Acetylglucosamine and Mannose molecules. These different Fc glycosylations are accompanied by conformational changes of the IgG Abs, which also affect the affinity for their cognate FcγRs (Pincetic et al. 2014). Their obtained data indicate, that IgG Abs can mainly adopt two distinct structural forms, which enable them to preferentially bind to either type I or type II FcRs (Pincetic et al. 2014). IgG Abs, which only contain the core glycan usually maintain an open conformation, resulting in preferential engagement of type I FcRs, whereas especially terminally sialylated IgG Abs alter between an open and a closed conformation, thus enabling them to access type II FcRs (Pincetic et al. 2014). IgG Abs, in which the core glycan was removed enzymatically completely fail to bind its cognate FcRs, possibly due to a collapsed Fc structure (Albert et al. 2008; Pincetic et al. 2014; Jefferis & Lund 2002). Type I FcRs consist of the classical FcγRs FcγRI, FcγRIIB and FcγRIIA, FcγRIIC, FcγRIIIA and FcγRIIIB in humans, and FcγRIII and FcγRIV in mice, whereas type II FcRs (e.g. CD23 and CD209) belong to the C-type lectin receptors (Nimmerjahn & Ravetch 2008; Pincetic et al. 2014).

Thus, these distinct conformational states result in differential effector functions, ultimately influencing the IgG Ab activity. A low abundance of fucose residues increases the affinity of human IgG1 and murine IgG2b for FcγRIII, leading to enhanced ADCC (Shields et al. 2002; Nimmerjahn

& Ravetch 2005). Furthermore, it has been suggested that IgG glycoforms, which lack terminal galactose and sialic acid are more pro-inflammatory (Parekh et al. 1985; Rademacher et al. 1994; Ercan et al. 2010).

The impact of IgG1 galactosylation was recently demonstrated in a murine autoimmune model of epidermolysis bullosa aquisita (EBA), in which ICs of galactosylated IgG Abs and TNP-OVA promote the conjunction of FcγRIIB and CD209, thereby efficiently protecting mice from EBA (Karsten et al. 2012). Studies with murine monoclonal anti-platelet IgG switch variants revealed a significant decrease in cytotoxicity upon sialylation (Kaneko et al. 2006).

The necessity of sialylated glycoforms for its anti-inflammatory activity was further confirmed in a murine model for rheumatoid arthritis, in which the protective effects of intravenous immunoglobulin (IVIG) were abrogated upon desialylation, whereas an enrichment of the sialylated fraction of IVIG substantially increased its protective potential (Kaneko et al. 2006; Nimmerjahn & Ravetch 2007). It was found that the anti-inflammatory activity of sialylated IVIG is dependent on the expression of the C-type lectin receptor SIGN-RI on splenic macrophages, since receptor blockage or deletion abrogated its suppressive effects (Anthony, Wermeling, et al. 2008). Accordingly, sIVIG binding to DC-SIGN on effector cells results in increased IL-33 production, further amplifying its immunosuppressive effects (Schwab & Nimmerjahn 2013). Moreover, in an auto-antibody driven humanized mouse model for immunothrombocytopenia (ITP), the sialylated IgG glycoforms was essential for the protective effects of IVIG (Schwab et al. 2015). A study with influenza virus vaccinations delineated the effects of sialylated Abs in positive selection of B cell clones. They found that binding of ICs, consisting of sialylated IgG Abs and vaccine Ag, to CD23 on B cells substantially upregulated FcγRIIB expression on activated B cells and concluded that this leads to an activated threshold for B cell activation in the GC and ensuing interclonal competition, thereby increasing the affinity of produced antigen-specific IgG Abs (Wang et al. 2015). Accordingly, another recent study demonstrated, that antigen-specific sialylated IgG Abs not only attenuated disease progression, but were also to suppress disease development in a collagen-induced arthritis model (Ohmi et al. 2016). Studies, in which antigen-specific sialylated IgG Abs were transferred or induced, showed decreases in B cell activation and delayed type hypersensitivity (DTH) (Hess et al. 2013; Oefner et al. 2012). Moreover, IgG Fc sialylation of human IgG1 has been shown to reduce its efficiency to induce CDC (Quast et al. 2015). Furthermore, decreased abundances of sialylated auto-antibodies correlate with disease flares in several autoimmune diseases, such as anti-citrullinated peptide (ACPA) in rheumatoid arthritis and anti-PR3 Abs

in granulomatosis (de Man et al. 2008; Espy et al. 2011; Scherer et al. 2010; Rombouts et al. 2015; van de Geijn et al. 2009). Thus, IgG glycosylation can be utilized as an important biomarker to predict autoimmune disease progression, as well as being modified to selectively engage pro- or anti-inflammatory signaling cascades.

To summarize, a complex interplay between B- and T-lymphocytes is essential to mount an effective immune response against TD-antigens. T-cells enable the induction of an early and protective Ab production by plasma blasts, while simultaneously initiating a long-lived memory and humoral immune response in the form of MBCs and LLPCs. Therefore, Tfh cells provide stimulatory signals for GC B cells during the GC response, facilitating the production of class switched, high-affinity Abs. This process is being regulated by Tfr cells, which are thought to directly inhibit Tfh, as well as GC B cells. The ensuing humoral immune response is characterized by high abundances of immunomodulatory IgG Abs, which elicit pro- or anti-inflammatory effector functions, depending on their Fc glycosylation.

Up to this point, it is not yet clear how exactly Tfr cells control the GC response or how the IgG glycosylation process is being regulated.

1.11 Aim of Dissertation

IgG Abs are key mediators of the humoral immune response and pivotal for the efficient eradication of most pathogens. Their broad spectrum of field of applications makes them a prime tool for the efficacious treatment of inflammation, cancer, autoimmunity and other diseases, as evidenced by the sheer amount of already approved and in trial Ab therapeutics (Chan & Carter 2010). IVIG is one of the most prominent examples for the routinely used Ab formulations and recent studies have highlighted the importance of the sialylated fraction for its clinical efficacy (Nimmerjahn & Ravetch 2007; Anthony, Nimmerjahn, et al. 2008). Moreover, enzymatically sialylated IVIG (s4IVIG) shows an up to 10-fold increase in anti-inflammatory activity, compared with IVIG (Washburn et al. 2015). Furthermore, recent studies have delineated the importance of IgG Fc glycosylation and modulation for cancer treatment with checkpoint inhibitors, either alone in combination therapy (Arlauckas et al. 2017; Arce Vargas et al. 2017).

The aim of this study was to unravel the mechanism, by which the type of IgG glycosylation is determined. We hypothesized that the immunogenicity of a TD antigen in conjunction with an adjuvant controls IgG glycosylation. Pro-inflammatory TD immune reactions would therefore induce agalactosylated IgG Abs, whereas non/low-inflammatory TD immune reactions would result in a higher abundance of galactosylated and additionally sialylated IgG Abs.

Therefore, I established two multicolor FACS panels (up to 14 fluorescent parameters) to efficiently deduce cell types, cytokine production and enzyme expression, all of which might influence IgG Ab glycosylation. Furthermore, I utilized various mouse models and evaluated the immunomodulatory potential of different pro- or low-inflammatory co-stimuli in altering the Fc-glycosylation by measuring glycosyltransferase expression in antigen-specific GC B cells and plasma cells and the glycosylation pattern of antigen-specific IgG Abs in the serum. Next, I exploited different mouse strains and immunization patterns to specifically deduce, which cell types and cytokines contribute to an altered IgG glycosylation. Furthermore, I also tested, if the glycosylation of antigen-specific IgG Abs is maintained over longer periods of time by screening glycosyltransferase expression of LLPCs in the bone marrow (BM) and the glycoprofiles of serum IgG Abs upon antigen re-exposure. Finally, I evaluated the impact of Treg/Tfr depletion or induction on the GC reaction and the ensuing IgG response. Altogether, being able to modulate the Fc-glycosylation in vivo might provide new therapeutic angles for the treatment of the aforementioned diseases.

2 Materials & Methods

Mice

C57BL/6 wildtype mice were either purchased from Charles River Laboratories or bred in the in-house facility of the UKSH Lübeck in accordance to institutional guidelines. Exclusively 8-12-week-old female or male mice of the following strains were analyzed and no gender specific differences were observed.

Mice
C57BL/6
DEREG
IL-17RA$^{-/-}$
IL-17RA$^{-/-}$/IFN-γRI$^{-/-}$
Vert-X (IL-10 eGFP Reporter)

2.1 Materials

2.1.1 Antibodies

Antibody	Clone	Fluorochrome	Supplier
anti-B220	RA3-6B2	BV786	BD Biosciences
anti-CD138	281-2	BV711	BD Biosciences
anti-CD16/CD32	2.4G2	BV605	BD Biosciences
anti-CD95	Jo-2	BV510	BD Biosciences
anti-IL-17A	TC11-18H10	BV605	BD Biosciences
anti-IFN-γ	XMG1.2	PE-Texas Red	BD Biosciences
anti-GL-7	GL-7	PerCP-Cy5.5	Biolegend

Antibody	Clone	Fluorochrome	Supplier
anti-CD4	RM4-5	BV711	Biolegend
anti-CXCR5	L138D7	Biotin, PE-Dazzle594	Biolegend
anti-ICOS	C396.4A	PE-Cy7	Biolegend
anti-CD8	53-6.7	A700	Biolegend
anti-LAP-1	TW7-16B4	BV421	Biolegend
Streptavidin	-	PE-Dazzle594 BV421	Biolegend
anti-IL-2	Jes6-1	Purified	Biolegend
anti-IgG1	RMG1-1	BV421	Biolegend
anti-CTLA-4	UC10-4B9	PE	Biolegend
anti-IgM	eB121-15F9	PE-Cy7	eBioscience
anti-FoxP3	FJK16s	APC	eBioscience
anti-IgA	Poly4053	A700	eBioscience
anti-ST6Gal1	polyclonal	Biotin	R&D Systems
anti-B4GalT1	polyclonal	Biotin	R&D Systems
anti-IgG	polyclonal	PE, HRP	Bethyl
anti-IgG1	polyclonal	HRP	Bethyl
anti-IgG2b	polyclonal	HRP	Bethyl
anti-IgG2c	polyclonal	HRP	Bethyl
anti-IgG3	polyclonal	HRP	Bethyl

Antibody	Clone	Fluorochrome	Supplier
Labeled OVA	-	Alexa647	ThermoFisher Scientific

2.1.2 Cell culture media and supplements

Medium	Supplier
Cell Stimulation Cocktail containing PMA/Ionomycin, Brefeldin-A and Monensin	eBioscience
Dulbecco´s Phosphate buffered saline	ThermoFisher Scientific
Fetal bovine serum	ThermoFisher Scientific
HEPES (N-(2-Hydroxyethyl)piperazin-N'-(2-ethansulfonacid))	ThermoFisher Scientific
Penicillin Streptomycin	ThermoFisher Scientific
RPMI1640 (L-Glutamine)	ThermoFisher Scientific
β-Mercaptoethanol	Sigma

Cell Activation Medium:

RPMI1640 Medium (L-Glutamine)

+ 1% Penicillin Streptomycin

+10% Fetal bovine serum

+1mM HEPES

+50µM β-Mercaptoethanol

2.1.3 Chemicals

Chemical	Supplier
Ammonium chloride (NH_4Cl)	Sigma
Bovine Serum Albumin (BSA)	GE Healthcare
Carbonate-bicarbonate	Sigma
Cytofix/Cytoperm	BD Biosciences
Ethylenediaminetetraacetic acid (EDTA)	Sigma
Fixation Buffer	Biolegend
FoxP3 / Transcription Factor Staining Buffer Set	eBioscience
Gelatin from cold water fish	Sigma
IC Fixation Buffer	eBioscience
Isopropanol (2-Propanol)	Otto Fischar
Potassium dihydrogen phosphate (KH_2PO_4)	Carl Roth
Saponin	Sigma
Sodium acetate ($C_2H_3NaO_3$)	Sigma
Sodium azide (NaN_3)	Sigma
Sodium chloride (NaCl)	Carl Roth
Sodium hydrogen carbonate ($NaHCO_3$)	Carl Roth
Sodium phosphate dibasic (Na_2HPO_4)	Sigma
TMB Substrate Reagent Set	BD Biosciences
Trizma Base (Tris-HCl)	Sigma

Chemical	Supplier
Tween 20	Sigma

2.1.4 Kits

Kit	Supplier
Biotin – XX Microscale Protein Labeling Kit	ThermoFisher Scientific
Pierce™ Dye Removal Columns	ThermoFisher Scientific

2.1.5 Antigens and Adjuvants

Antigen or Adjuvant	Supplier
Albumin from chicken egg white (Ovalbumin)	Sigma
Freund´s Adjuvant Incomplete	Sigma
Freund´s Adjuvant Complete	Sigma
Mycobacterium tuberculosis H37 RA, Desicatted	BD Biosciences

2.1.6 Buffers and Solutions

Buffer	Components
ELISA Blocking Buffer	3 % BSA (w/v) 0.1 % Gelatine (w/v) 3 mM EDTA in 1x PBS
ELISA Coating Buffer	50 mM Carbonate-bicarbonate Buffer in ddH_20

Buffer	Components
ELISA Wash Buffer	0.05 % Tween 20 (v/v) in 1x PBS
FACS Buffer	0.5 % BSA 0.05% NaN_3 in 1x PBS
Perm/Wash:	0.05x PBS 0.05 % Saponin 0.01 % NaN_3 in ddH_20
Phosphate-Buffered Saline (PBS):	137 mM NaCl 2.7 mM KCl 72 mM Na_2HPO_4 1.8 mM KH_2PO_4 in ddH_20, pH 7.4
RBC (Red blood cell) Lysis Buffer	0.15M NH_4Cl 1mM $NaHCO_3$ 0.1mM EDTA in ddH_2O, pH=7.2

2.1.7 Consumables

Product	Supplier
Cell strainer (70µm)	BD Biosciences
Costar Assay plates (24, 96) well	Corning
Falcon tubes (15, 50 ml)	Greiner Bio-one
Pipette tips (10, 200, 1000 µl)	Sarstedt

Product	Supplier
Reaction tubes (1.5, 2.0 ml)	Sarstedt
Serological pipettes (5, 10, 25, 50 ml)	Sarstedt
Single-use syringes, 1ml	Braun

2.1.8 Equipment

Device	Supplier
Analytic Scale	Sartorius
Autoclave	Webeco
Centrifuge 5424R	Eppendorf
Centrifuge 5810R	Eppendorf
Direct Heat CO2 Incubator	Integra
Flow cytometer LSRII	BD Biosciences
Fluostar Omega	BMG Labtech
Microscope Wilovert	Helmut Hund GmbH
Nanopure Barnstead	ThermoScientific
Nanodrop ND-1000	pegLab Biotechnologie GmbH
pH-meter SevenEasy	Mettler-Toledo
Pipetboy	Integra
Sterile hood NU-437-600E	Integra
Thermomixer Compact	Eppendorf
Vacusafe and Vacuboy	Integra

2.1.9 Software

Software
BD FACSDiva v8.01
FlowJo X 10.0.7r2
GraphPad Prism 6.0
Mendeley
ND1000

2.2 Methods

2.2.1 Fluorescence-associated cell sorting (FACS)

A single cell suspension of spleen or bone marrow cells of immunized and untreated mice was generated by smashing through a 70µm cell strainer. These or cultured cells were counted and normalized to $2.5x10^7$ cells/sample. 400µl FACS buffer was added to the cells and they were centrifuged for 5min at 4°C and 400×g.

For extracellular staining, the cells were then resuspended in 100ul FACS Buffer containing the particular Abs with the specific concentration. The cells were stained for 20min at 4°C in the dark. To exclude dead cells, fixable viability dye was added in a concentration of 1:1000. The cells were again resuspended in 400µl FACS Buffer and subsequently centrifuged for 5min at 4°C and 400×g.

For intracellular staining, the cells were stained extracellularly and then fixed for 25 min with Fixation Buffer, followed by addition of 400µl Perm/Wash Buffer and centrifuged for 5min at 4°C and 400×g after 5min of incubation. The cells were then resuspended in 400µl Perm/Wash Buffer containing the particular Abs at the specific concentrations. The cells were stained for 20min at 4°C in the dark, followed by addition of 400µl FACS Buffer, centrifuged for 5min at 4°C and 400×g and resuspended in 400µl FACS Buffer. If a Biotin/Streptavidin combination was used, an additional intracellular staining step was added.

For intranuclear staining, the cells were stained extracellularly and then fixed for 30min with Fixation Buffer and centrifuged for 5min at 4°C and 400×g. The cells were then resuspended in 400µl Fixation/Permeabilization solution for 1h, followed by addition of 400µl Permeabilization Buffer and centrifuged for 5min at 4°C and 400×g. The cells were then resuspended in 100µl Permeabilization Buffer containing the particular Abs at the specific concentrations and stained for 2h at room temperature in the dark, followed by addition of 400µl FACS Buffer, centrifuged for 5min at 4°C and 400×g and resuspended in 400µl FACS Buffer for analysis.

For intracellular cytokine analysis, cells were stimulated for 5h at 37°C with cell stimulation cocktail, containing PMA, Ionomycin, Brefeldin-A and Monensin, followed by extracellular staining at 37°C for 30min, subsequent fixation and intracellular staining.

To maintain the eGFP signal during intracellular and intranuclear stainings, the cells were fixed with Fixation Buffer (without Permeabilization solution).

2.2.2 Glycan analysis of purified (OVA-specific) IgG Abs via HPLC

N-glycans were isolated from purified OVA-specific or total IgG Abs and were treated with endoglycosidase S (EndoS) for 2 h at 37° C and 300 rpm to cleave off N-glycans. The resulting N-glycans were purified by solid phase extraction using home-made Carbograph^{TM} graphitized carbon columns. Based on the terminal sugar moiety, the peaks were assigned to one of the following nine groups: G0+bisecting GlcNAc, G0-bisecting GlcNAc, G1+bisecting GlcNAc, G1-bisecting GlcNAc, G2+bisecting GlcNAc, G2-bisecting GlcNAc, G1S1, G2S1 and G2S2. Peaks containing sialic acid and bisecting GlcNAc were not detected. The proportion of each group was calculated by dividing the value of the specific peak area by the total area of all peaks in the nine groups. The resulting percentages of the bisecting GlcNAc versions of G0, G1 and G2 were added to the percentages of the G0, G1 and G2 versions without bisecting GlcNAc, respectively, to herein describe six groups totaling 100%: G0, G1, G2, G1S1, G2S1 and G2S2. Ab purification and analysis of N-glycans were performed by Yannic Bartsch in our laboratory via affinity-chromatography and HILIC-HPLC, respectively. The glycoprofiles were measured with a Dionex Ultimate 3000.

2.2.3 OVA-reactive ELISA

To measure the quantitiy of the OVA-specific Abs in the sera of immunized mice, ELISA plates were coated with 10 µg/ml OVA and stored at 4°C for 24h. After blocking of the plates, sera with indicated concentrations were added. After 1h of incubation, 0.1µg of HRP-coupled polyclonal goat anti-mouse Ig isotype or subclass-specific Abs was added per well in a volume of 100µl. Finally, TMB substrate was added and the optical density (450nm) was measured with Fluostar Omega.

2.2.4 Fluorochrome coupling to Abs

To couple Biotin or A647 to B4GalT1 and IgA respectively, Protein Labeling kits and Dye Removal Columns were used. The Ab was diluted 1:10 with 1M Carbonate/Bicarbonate Buffer and Fluorochrome was added drop-wise at optimal concentrations (according to manufacturer's instructions). The solution was transferred to columns to remove excessive dye. To determine the concentration of the fluorochrome labelled Ab, the solution was analyzed with the Nanodrop ND-1000.

2.2.5 IL-2/Jes6-1 complexing

To complex recombinant IL-2 with the anti-IL-2 antibody Jes6-1, 1µg of IL-2 and 5µg anti-IL-2 were incubated for 30 minutes at 37°C in 200µl sterile PBS.

2.2.6 Experimental setups for immunization

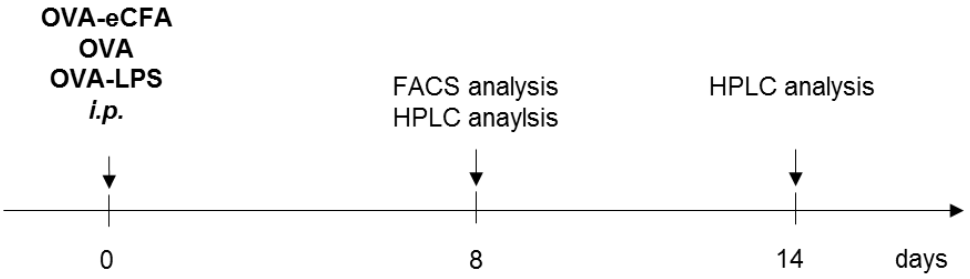

On day 0, mice of indicated strains were immunized intraperitoneally (i.p.) with either 100µg OVA emulsified in enriched CFA, 5mg OVA or 100µg OVA in 30µg LPS. FACS analysis of splenic cells was performed at day 8 after indicated immunizations and serum samples were taken at day 8 or day 14 via cardiac puncture under anesthesia.

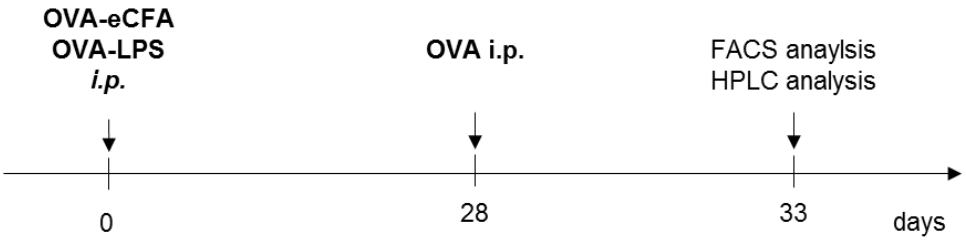

To deduce effects upon antigen re-exposure, mice of indicated strains were immunized intraperitoneally (i.p.) with either 100µg OVA emulsified in enriched CFA or 100µg OVA in 30µg LPS at day 0. At day 28, mice were challenged with 100µg OVA i.p. FACS analysis of splenic cells and BM cells was performed at day 33 after indicated immunizations and serum samples were taken via cardiac puncture under anesthesia.

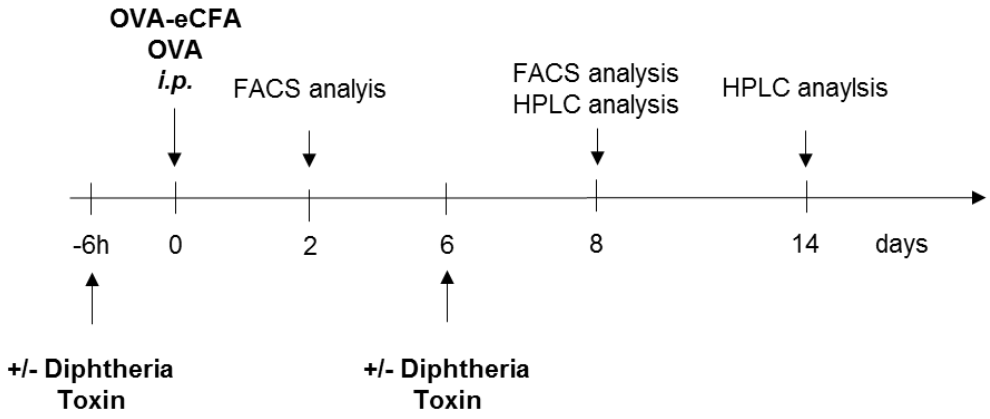

To transiently deplete Treg and Tfr cells, mice of indicated strains were immunized *i.p.* with 1µg DT followed by immunization with 5mg OVA 6h later and another DT treatment at day 6. FACS analysis of splenic cells was performed at day 8 after indicated immunizations and serum samples were taken at day 8 or day 14 via cardiac puncture under anesthesia.

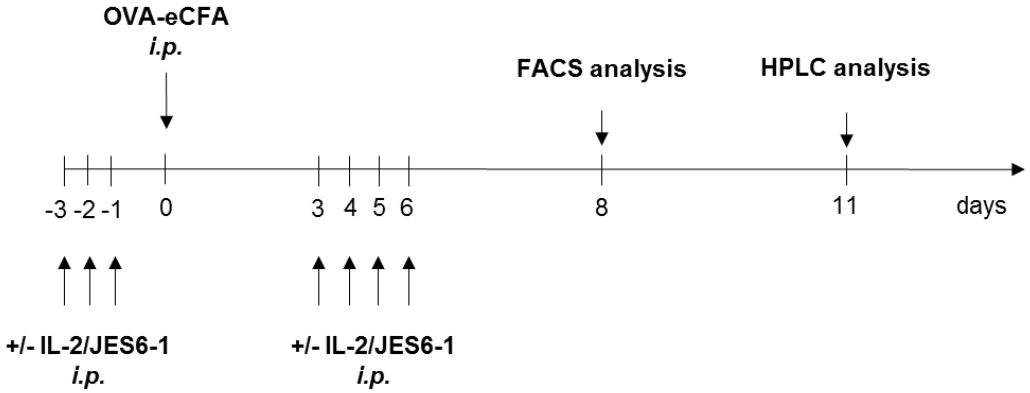

To massively induce Treg and Tfr cells, mice of indicated strains were were immunized i.p. with 100 µg OVA emulsified in enriched CFA at day 0, or 3 times with IL-2/Jes6-1 (day -3, -2 and -1) followed by 100 µg OVA emulsified in enriched CFA (day 0) and 4 additional IL-2/Jes6-1 (day 3-6) immunizations. FACS analysis of splenic cells was performed at day 8 after indicated immunizations and serum samples were taken at day day 11 via cardiac puncture under anesthesia.

2.2.7 Statistical Analysis

Statistical analysis was performed using Graph Pad Prism version 6.0. With regard to small sample sizes, normal distribution was assumed. To analyze differences between two normally distributed groups, a two-tailed t-test was used. Comparison of the means of more than two normally or non-normally distributed groups was done by one-way analysis of variance (ANOVA) with TUKEY post-test to adjust for multiple comparisons. If not stated otherwise, data were taken from 2–4 individual experiments or combined of multiple experiments and data are presented as mean values ± standard error of mean (SEM), *P < 0.05, **P < 0.01, ***P < 0.001 and ****P<0.0001.

3 Results

IgG Abs alone or in conjunction with further pharmaceuticals are a pivotal therapeutic tool for the treatment of various diseases, ranging from cancer over viral infections to autoimmunity. The elicited effector functions of these therapeutic Abs are heavily dependent on antigen-specificity, subclass, as well as Fc-glycosylation. While agalactosylated and asialylated IgG Abs are associated with pro-inflammatory effector functions (Ackerman et al. 2013), such as IgG auto-Abs in patients with rheumatoid arthritis (Campbell et al. 2014; Matsumoto et al. 2000), especially sialylated IgG Abs exert anti-inflammatory properties (Ohmi et al. 2016; Quast et al. 2015; Wang et al. 2015; Schwab et al. 2015). Terminal galactosylation and sialylation of the IgG Fc region takes place in the trans golgi and is being facilitated by the enzymes B4galt1 and St6gal1, respectively (Anthony et al. 2012; Ohmi et al. 2016; Onitsuka et al. 2012; Warnock et al. 2005; Wang et al. 2015; Shade & Anthony 2013). Although the immunomodulatory functions of these differentially glycosylated IgG Abs have been started to be investigated, few studies have dealt with the IgG Fc glycosylation process.

Since high affinity IgG Abs are the product of a successful GC response towards a TD-antigen, I tested if the IgG glycosylation is being modified by the antigen immunogenicity and by the microenvironment within the GC. Therefore, I first assessed the immunomodulatory potential of different pro- or low-inflammatory co-stimuli in conjunction with a model TD-antigen in altering the IgG Ab Fc-glycosylation. Accordingly, I measured B4galt1 and St6gal1 expression in class-switched antigen-specific GC B cells and PCs and the glycosylation pattern of antigen-specific IgG^+ Abs.

3.1 Different co-stimuli result in robust induction of the germinal center response

To determine if different co-stimuli in conjunction with the model antigen Ovalbumin (OVA) result in altered immune responses, I first assessed the strength of the splenic germinal center response under pro-inflammatory (OVA-eCFA) and low-inflammatory conditions (OVA-LPS or pure OVA) by measuring the frequency of splenic GC B cells. I characterized these cells as $B220^+CD138^-FAS^+GL\text{-}7^+$ (**Figure 5** A-D, left and middle panel). OVA-eCFA treatment resulted in a substantial induction of GC B cells (~7%). Although OVA-LPS and OVA immunization induced lower GC B cell frequencies than OVA-eCFA (~4% and ~1%, respectively), both were profoundly higher compared with untreated mice (**Figure 5** A-D, middle panel and **Figure 6** A). Of note, OVA treated mice showed nearly double the percentage of GC B cells compared with untreated control

mice, although it didn't reach statistical significance. This indicates, that all tested stimuli induce a robust germinal center response. Next, I tested whether the GC response is directed against the antigen used for immunization by analyzing the amount of OVA-specific GC B cells. Interestingly and in accordance with the magnitude of the GC response, OVA-eCFA treated mice showed the highest percentage of OVA^+ GC B cells (~4%), compared with OVA-LPS (~1.5%) and pure OVA (~0.35%) (**Figure 5** A-D, right panel and **Figure 6** B).

Approximately 40-50% of the OVA^+ GC B cells after all tested immunizations were $IgG1^+$ (**Figure 6** C), implying that the GC B cells have undergone iterative circles of proliferation, SHM, affinity maturation, as well as CSR. To test if this IgG1 poised GC subset is being translated into $IgG1^+$ PCs and $IgG1^+$ Abs, I next assessed the abundance of class switched splenic PCs and the IgG subclass distribution in the sera of differently treated mice.

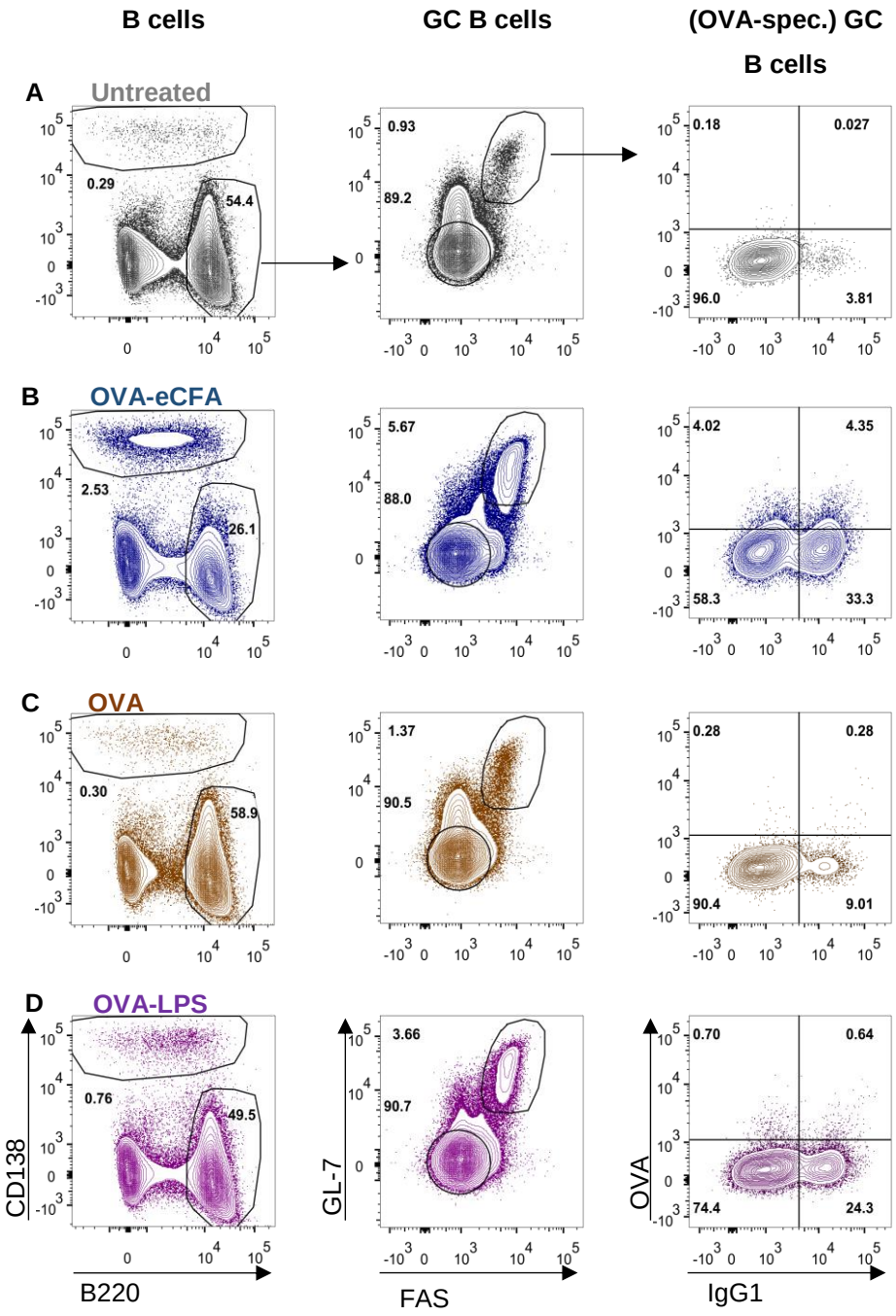

Figure 5: Different co-stimuli result in robust induction of germinal center response. C57BL/6 mice were immunized *i.p.* with 100 µg OVA emulsified in enriched CFA, 5mg OVA or 100 µg OVA in 30 µg LPS, n=4-5 per group. Gating strategy to identify splenic $B220^+FAS^+GL\text{-}7^+OVA^+IgG1^+$ GC B cells of either untreated (A) or immunized mice (B)-(D) at day 8 after vaccination. Data are representative of at least 2 independent experiments.

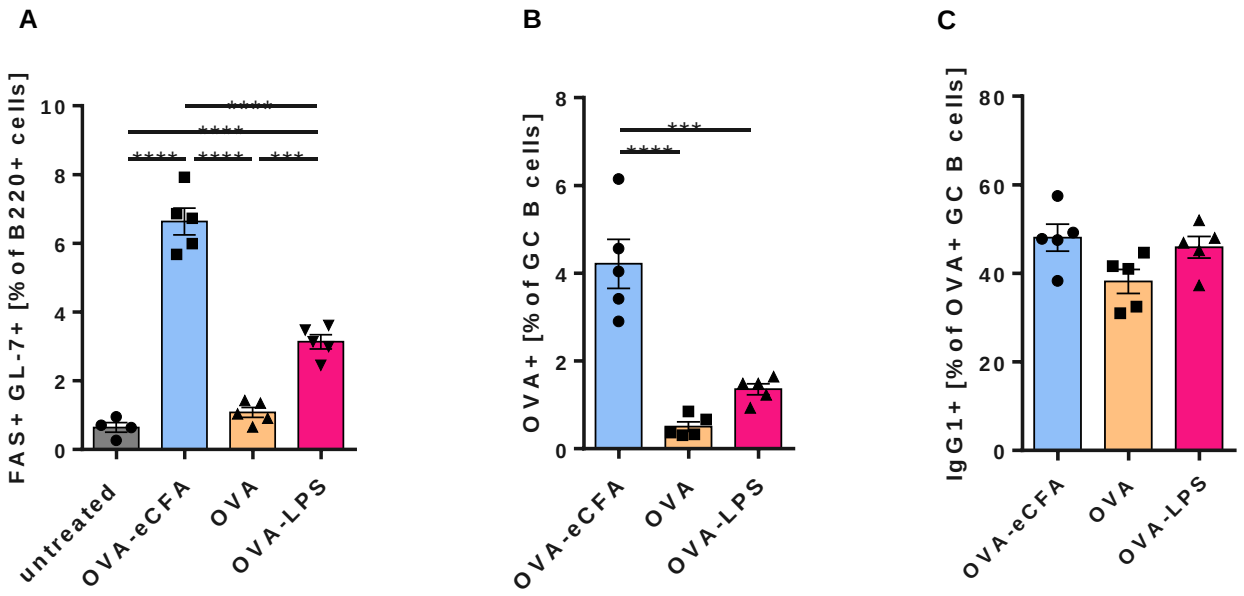

Figure 6: OVA-eCFA treatment results in enhanced GC B cells. C57BL/6 mice were immunized *i.p.* with 100 µg OVA emulsified in enriched CFA, 5mg OVA or 100 µg OVA in 30 µg LPS, n=4-5 per group. Frequencies of B220$^+$ FAS$^+$ GL-7$^+$ cells (A), OVA$^+$ B220$^+$ FAS$^+$ GL-7$^+$ cells (B) and IgG1$^+$ OVA$^+$ B220$^+$ FAS$^+$ GL-7$^+$ cells (C), at day 8 after vaccination. Data are representative of at least 2 independent experiments. One-way ANOVA test was used for all comparisons and data are presented as mean +/- SEM, *P < 0.05, **P < 0.01, ***P < 0.001 and ****P<0.0001

3.2 TD antigens with different co-stimuli induce predominantly IgG1 Abs

To delineate whether the strength of the GC reaction corresponds with the amount of produced Abs, I first analyzed the frequency of PCs, characterized as CD138$^+$ cells of living lymphocytes, upon the different vaccinations. FACS analysis of murine spleen cells after OVA-eCFA and OVA-LPS immunizations showed significantly higher PC frequencies compared to OVA and untreated control mice (**Figure 5** A-D, left panel and **Figure 8** A). After OVA-eCFA and OVA-LPS treatment, a very high percentage of all PCs (~35% and 30%, respectively) were directed against OVA (**Figure 8** B). Although OVA-immunized and untreated mice showed comparable percentages of total plasma cells (both ~0.3%), the OVA-immunized mice had a significantly higher percentage of OVA-specific PCs (~6% to 1%) (**Figure 8** A and **Figure 7** A, C, left panel). These data suggest that although pure OVA isn't as immunogenic as OVA-eCFA or OVA-LPS, the mice still mount an antibody response against the pure protein, likely due to small traces of impurities, like LPS. To verify this, I immunized C57BL/6J mice with either 100 µg of endotoxin free OVA in 3 µg LPS or

with endotoxin free OVA without LPS. As expected, the mice immunized with the endotoxin free OVA failed to mount an antibody response against the protein, whereas 3µg of LPS resulted in similar OVA^+ plasma cells frequencies as 30 µg of LPS (data not shown). This implies that even low concentrations of LPS suffice to induce a GC reaction directed against the protein.

To test whether the high percentage of $IgG1^+$ GC B cells is directly being translated to the PC compartment, I measured the frequencies of OVA-specific -$IgG1^+$, -IgG^+ (IgG2b, IgG2c and IgG3), -IgM^+ and -IgA^+ PCs. As expected from the obtained GC data (**Figure 5** right panel and **Figure 6** C), all immunizations led to a profound OVA^+IgG1^+ Ab response (**Figure 7** B-D, middle panel and **Figure 8** C). Although the ratio of OVA-specific -IgM and -IgA was comparable between all groups, OVA treatment resulted in a higher percentage of these cells, compared with the other treatments (**Figure 7** B-D, middle panel). This is probably due to the decreased immunogenicity of Ovalbumin without a further co-stimulus, since the antibody ratio of OVA-treated mice resembles the steady state conditions of untreated mice (**Figure 7** A, C). To verify these results, I measured the distribution of OVA-specific IgG subclasses in the sera of mice 14 days upon vaccination. Interestingly, all immunizations resulted in a comparable distribution, with IgG1 as the predominant subclass, followed by IgG2b, IgG2c and IgG3 (**Figure 9** A-C). Only the pro-inflammatory OVA-eCFA resulted in slightly higher levels of IgG2b, compared with OVA-LPS and OVA treated mice (**Figure 9** A-C). Taken together, this indicates that different co-stimuli in conjunction with OVA induce similar regulatory processes within the GC.

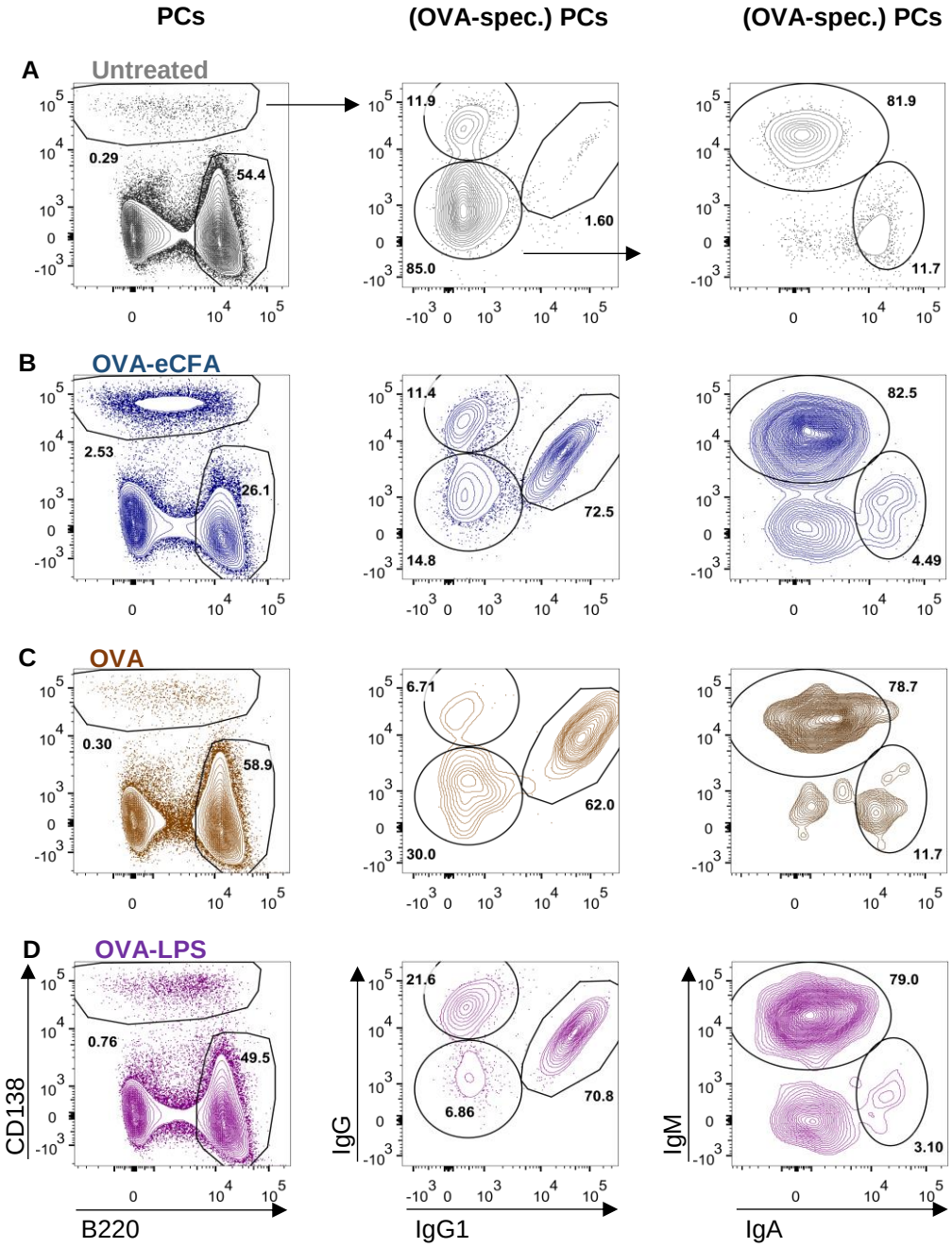

Figure 7: **Different co-stimuli result in substantial production of antigen-specific IgG1**. C57BL/6 mice were immunized *i.p.* with 100 µg OVA emulsified in enriched CFA, 5mg OVA or 100 µg OVA in 30 µg LPS, n=4-5 per group. Gating strategy to identify splenic OVA^+ -IgG^+, -$IgG1^+$, -IgM^+ and -IgA^+ PCs, respectively at day 8 after vaccination. Mice were immunized *i.p.* with indicated stimuli. Data are representative of at least 2 independent experiments.

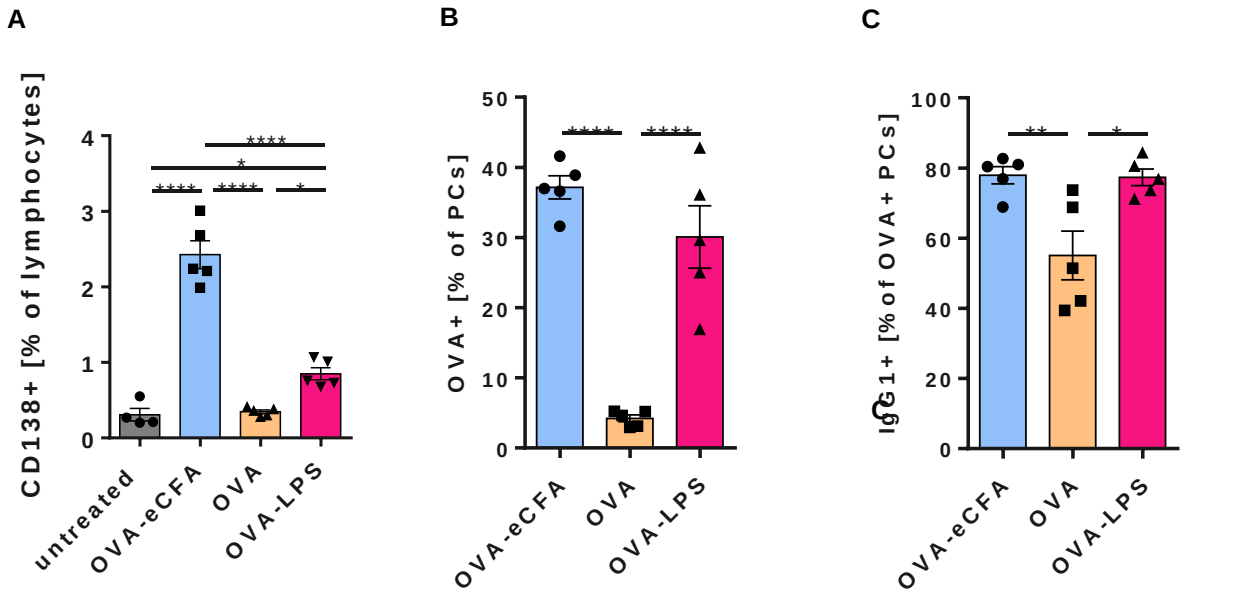

Figure 8: Ovalbumin alone or in conjunction with different co-stimuli predominantly induces IgG1$^+$ Abs. C57BL/6 mice were immunized i.p. with 100 µg OVA emulsified in enriched CFA, 5mg OVA or 100 µg OVA in 30 µg LPS, n=4-5 per group. (A) Frequencies of CD138$^+$ PCs, OVA-specific cells of PC (B), or IgG1 positive cells of OVA$^+$ PCs (C), at day 8 after vaccination. Data are representative of at least 2 independent experiments. One-way ANOVA test was used for all comparisons and data are presented as mean +/- SEM, *P < 0.05, **P < 0.01, ***P < 0.001 and ****P<0.0001

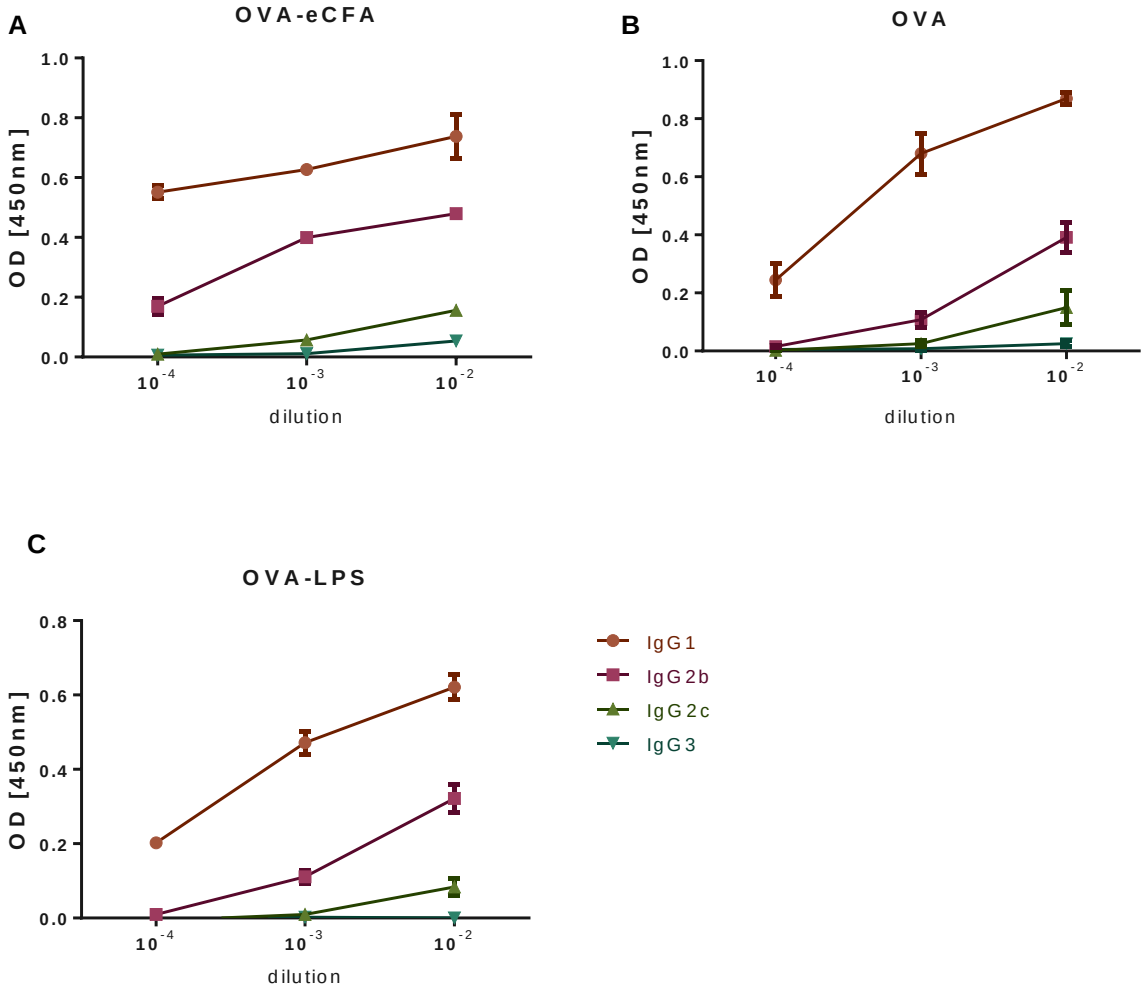

Figure 9: Different co-stimuli result in substantial production of antigen-specific IgG1. C57BL/6 mice were immunized *i.p.* with 100 µg OVA emulsified in enriched CFA, 5mg OVA or 100 µg OVA in 30 µg LPS, n=4 per group. (A-C) Quantification of OVA-specific serum Ab levels for all IgG subclasses at day 14 after indicated immunizations. Plates were coupled with 10ug OVA and serum was diluted at indicated concentrations. Antibody subclasses were identified by HRP-coupled anti-subclass Abs. Data are presented as mean +/- SEM

3.3 Antibody galactosylation and sialylation are possibly regulated in GC B cells

Since most OVA^+ GC B cells belonged to the IgG1 subclass (**Figure 5**, right panel, **Figure 6** C), I next examined if this population is phenotypically distinct upon the various immunizations by assessing the expression of the glycosyltransferases B4galT1 and St6gal1. These enzymes have been demonstrated to be responsible for antibody galactosylation and sialylation, respectively (Anthony et al. 2012; Ohmi et al. 2016; Onitsuka et al. 2012; Warnock et al. 2005; Wang et al. 2015; Shade & Anthony 2013). Importantly, OVA induced a robust GC response throughout all tested stimuli and a substantial part of the GC B cells were specific for this cognate antigen. Moreover, most of these cells had undergone a class switch towards IgG1 (**Figure 5** B-D, **Figure 6** A-C). Therefore, I investigated if the glycosyltransferases are differentially expressed in splenic OVA^+IgG1^+ GC B cells.

Interestingly, the pro-inflammatory co-stimulus eCFA resulted in significantly decreased expression levels of both glycosyltransferases, compared with the low-inflammatory co-stimulus LPS and pure OVA without any co-stimulus (**Figure 10** A-D). OVA immunization alone or in conjunction with LPS resulted in nearly identical expression levels of both enzymes (**Figure 10** A-D).

Strikingly, naïve B cells, characterized as $B220^+CD138^-FAS^-GL\text{-}7^-$, showed no detectable expression of B4galt1 and St6gal1 (**Figure 10** A, B). Taken together, this indicates that the expression levels of those enzymes are actively regulated in the GC microenvironment and that GC B cells, which are generated in response to TD-antigens in conjunction with certain co-stimuli express distinct and variable levels of B4galt1 and St6gal1. This implies that antigen-specific GC B cells are subject to regulatory processes within the GC, which do not only affect their abundance, but also their phenotype.

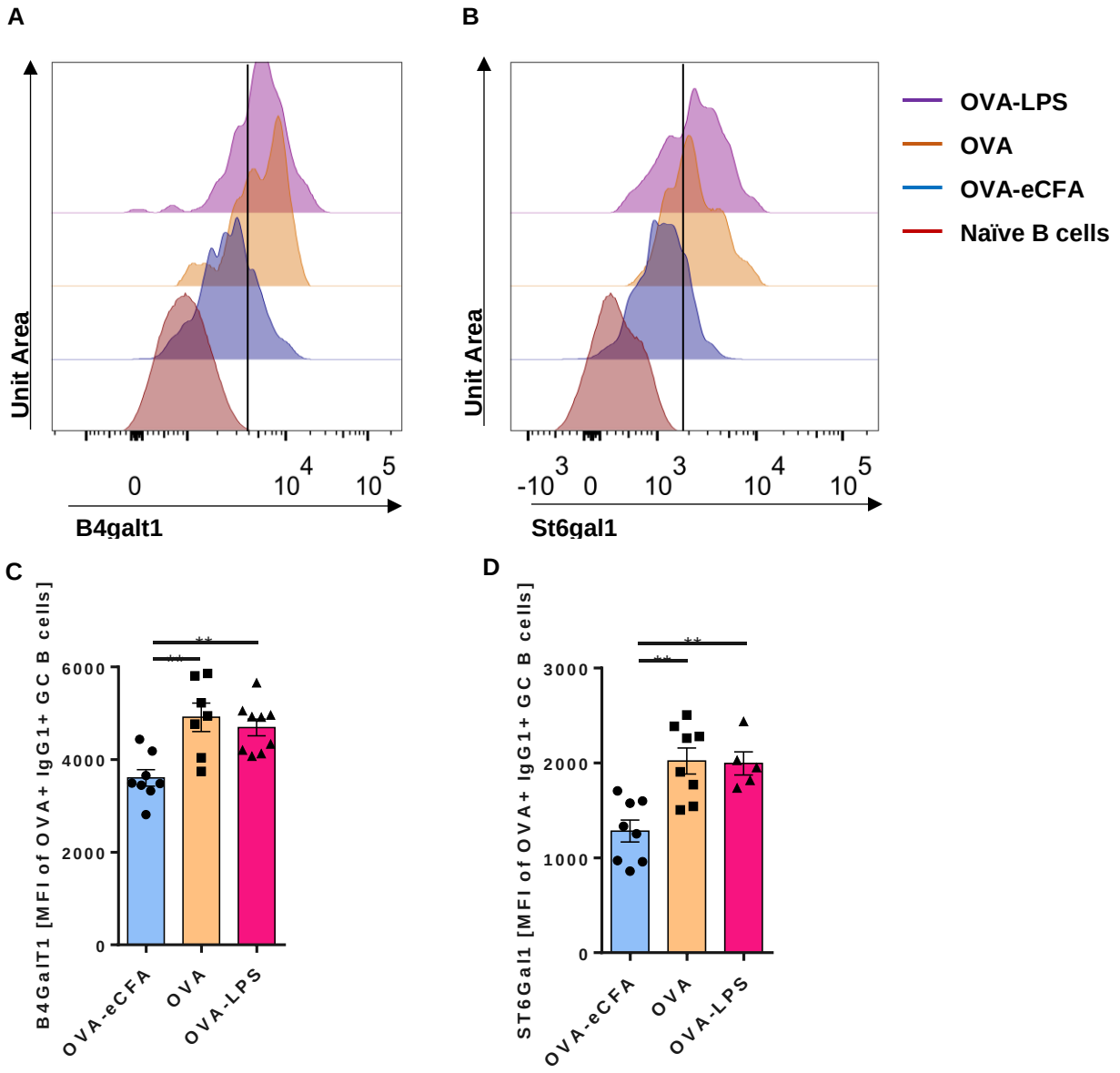

Figure 10: B4galt1 and St6gal1 expression are regulated within GC B cells. C57BL/6 mice were immunized *i.p.* with 100 µg OVA emulsified in enriched CFA, 5mg OVA or 100 µg OVA in 30 µg LPS. (A, B) Histogram overlays of B4galt1 and St6gal1 expression in splenic naïve B cells and OVA^+IgG1^+ GC B cells at day 8 after vaccination. (C, D) MFI of B4galt1 and St6gal1 in OVA^+IgG1^+ GC B cells at day 8 after vaccination. Data are representative of at least 2 independent experiments and data in C and D were pooled from 2 independent experiments, with n=7-9 per group. One-way ANOVA test was used for all comparisons and data are presented as mean +/- SEM, *P < 0.05, **P < 0.01, ***P < 0.001 and ****P<0.0001.

Since the OVA$^+$IgG1$^+$ GC B cell compartment were effectively translated into OVA$^+$IgG1$^+$ PCs (**Figure 6** B, C and **Figure 8** B, C), I next compared expression levels of B4galt1 and St6gal1 in these two cell types. As shown before (**Figure 10** A, B), naïve B cells showed no detectable expression of either glycosyltransferase (**Figure 11** A, B).

Under steady state conditions in untreated mice, naïve B cells (red histogram) showed substantially lower B4galt1 and St6gal1 expression levels, compared with IgG1$^+$ GC B cells (green histogram) and IgG1$^+$ PCs (blue histogram), which the latter two being comparable in their enzyme expression (**Figure 11** A, B).

Interestingly, these data imply that the expression levels of B4galt1 and St6gal1 are similar in IgG1$^+$ GC B cells and IgG1$^+$ PCs (**Figure 11** A, B). Of note, this points to regulatory processes, which modulate IgG Ab glycosylation during the GC response through differential expression of the responsible enzymes B4galt1 and St6gal1 in antigen-specific class switched GC B cells. Since these distinct expression levels are mostly maintained in OVA$^+$IgG1$^+$ PCs, this further suggests that the enzyme expression remains steady even after differentiation into fully matured Ab-secreting PCs. Although I cannot exclude, that a fraction of the OVA-specific PCs is generated extrafollicularly, these data suggest that a profound part of this population stem from GC B cell progenitor cells.

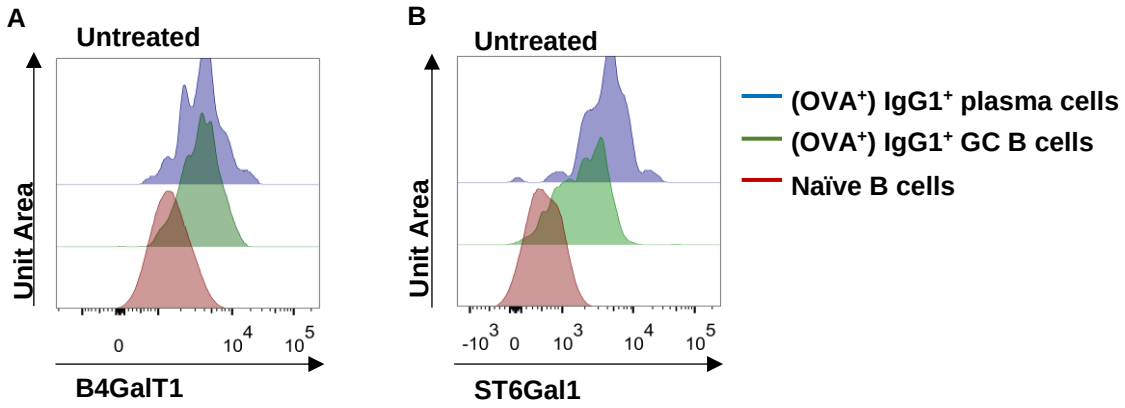

Figure 11: B4galt1 and St6gal1 expression in GC B cells are mostly maintained upon differentiation into PCs. Histogram overlays of B4galt1 and St6gal1 expression in splenic naïve B cells, IgG1$^+$ GC B cells and IgG1$^+$ PCs. Data are representative of at least 2 independent experiments.

To further verify these results, I analyzed the glycosyltransferase expression in OVA^+IgG1+ PCs upon immunization and compared it with the expression under steady state conditions in total $IgG1^+$ PCs in untreated control mice. As expected, analysis of the expression levels of both B4galt1 and St6gal1 produced similar results as in GC B cells. When gated on PCs (**Figure 12** A, C), OVA-eCFA treated mice showed substantially less glycosyltransferase expression than OVA- and OVA-LPS treated mice, whereas the latter two showed comparable enzyme expression levels as under steady state conditions in untreated mice.

Most OVA^+ PCs showed little expression of B4galt1 (A) and St6gal1 (C) upon OVA-eCFA vaccination (**Figure 12** A and C, blue contour blot). A high frequency of the PCs was not specific for OVA, indicating that these plasma cells produce IgG Abs against other antigens. Interestingly, a portion of these PCs had markedly higher expression of B4galt1 and St6gal1, which could stem from two possibilities. Either those cells present a distinct population with an inherently high expression of both glycosyltransferases and produce Ab of the same isotype and subclass, or those cells produce Abs of another isotype. To delineate between those possibilities, I gated on $IgG1^+$ PCs, which do not contain other subclasses or isotypes (**Figure 12** B, D). Since the population of cells with high glycosyltransferase expression vanished, I could confirm the latter possibility. Furthermore, I verified that those cells produced IgM^+ and IgA^+ Abs (data not shown). When gated on $IgG1^+$ PCs, most them were antigen-specific (70.9% (B) and 66.4% (D)) and expressed low amounts of both glycosyltransferases upon OVA-eCFA treatment.

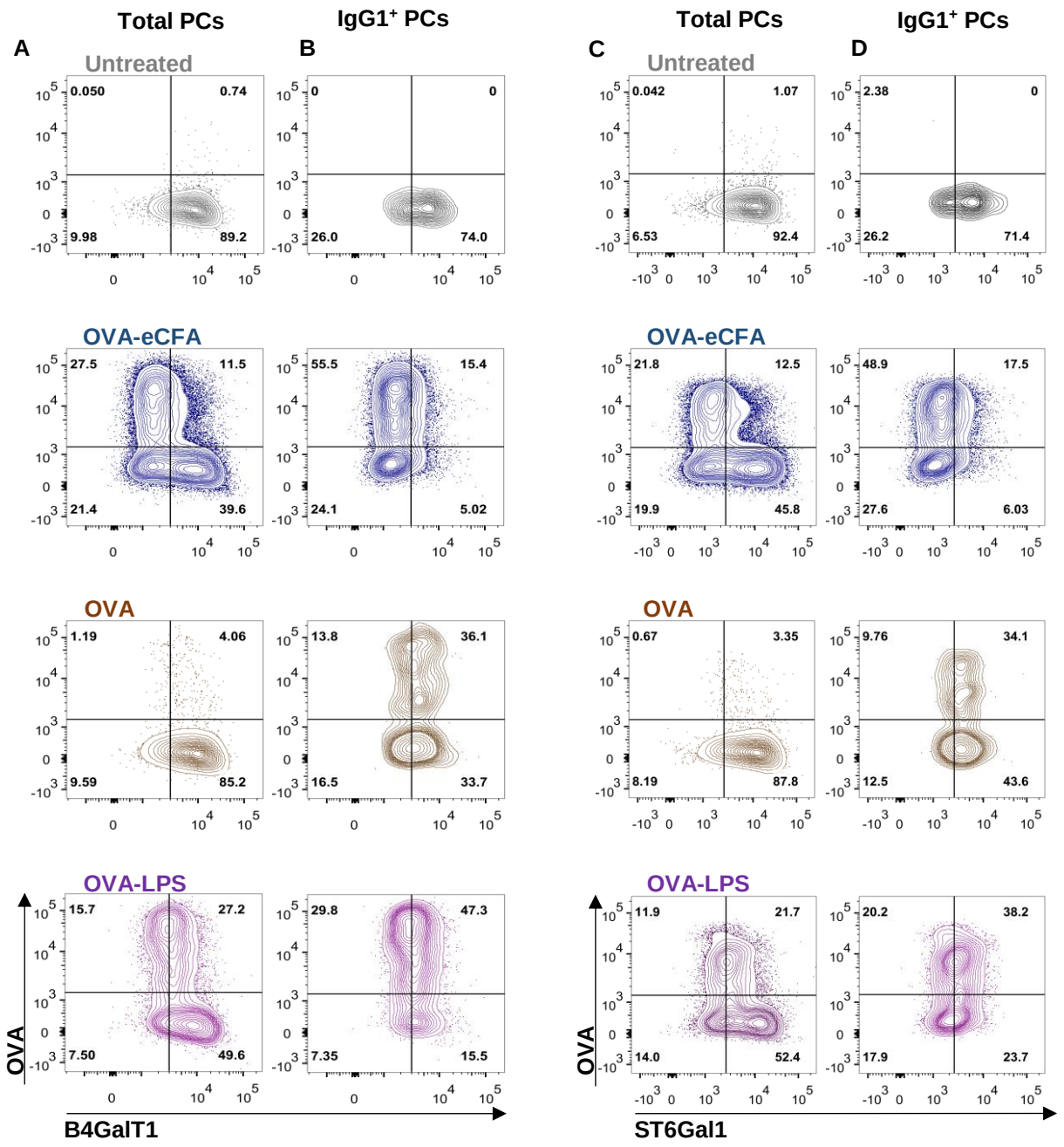

Figure 12: B4GalT1 and ST6Gal1 are differentially expressed in PCs. C57BL/6 mice were immunized *i.p.* with 100 µg OVA emulsified in enriched CFA, 100 µg OVA in 30 µg LPS or 5mg OVA and sacrificed at d8, n=5 per group. (A, C) Comparison of intracellular B4GalT1 (A) and ST6Gal1 (C) expression in splenic CD138$^+$ cells after indicated immunizations, (B, D) Comparison of intracellular B4GalT1 (B) and ST6Gal1 (D) expression in splenic CD138$^+$IgG1$^+$ cells after indicated immunizations. Data are representative for at least 2 independent experiments.

Treatment with pure OVA resulted in glycosyltransferase expression levels comparable to steady state conditions in untreated mice. Nearly all OVA^+ PCs upon OVA and OVA-LPS immunization showed markedly higher B4galt1 and St6gal1 expression, when compared with OVA-eCFA treated mice, even when gated on $IgG1^+$ PCs (**Figure 12** A-D).

When compared more specifically, it becomes evident that OVA^+IgG1^+ PCs possess distinct expression levels of B4galt1 and St6gal1 upon different immunizations. While OVA-eCFA treated mice showed a very low transferase expression, which was comparable to those of naïve B cells (blue and red histograms), OVA and OVA-LPS treatment (orange and magenta histograms) resulted in significantly higher expression, which was comparable with the steady state conditions in untreated mice (grey histograms) (**Figure 13** A, B). The expression levels of B4galt1 and St6gal1 in OVA^+IgG1^+ PCs upon OVA and OVA-LPS immunization and in $IgG1^+$ PCs in untreated mice were nearly 2-fold as high as of OVA^+IgG1^+ PCs upon OVA-eCFA immunization (**Figure 13** C, D).

Taken together these data suggest that the distinct glycosyltransferase expression levels observed in OVA^+IgG1^+ GC B cells are also apparent in OVA^+IgG1^+ PCs. Importantly, this implies that IgG Fc glycosylation is actively regulated during the GC response, and could therefore be influenced by a variety of factors.

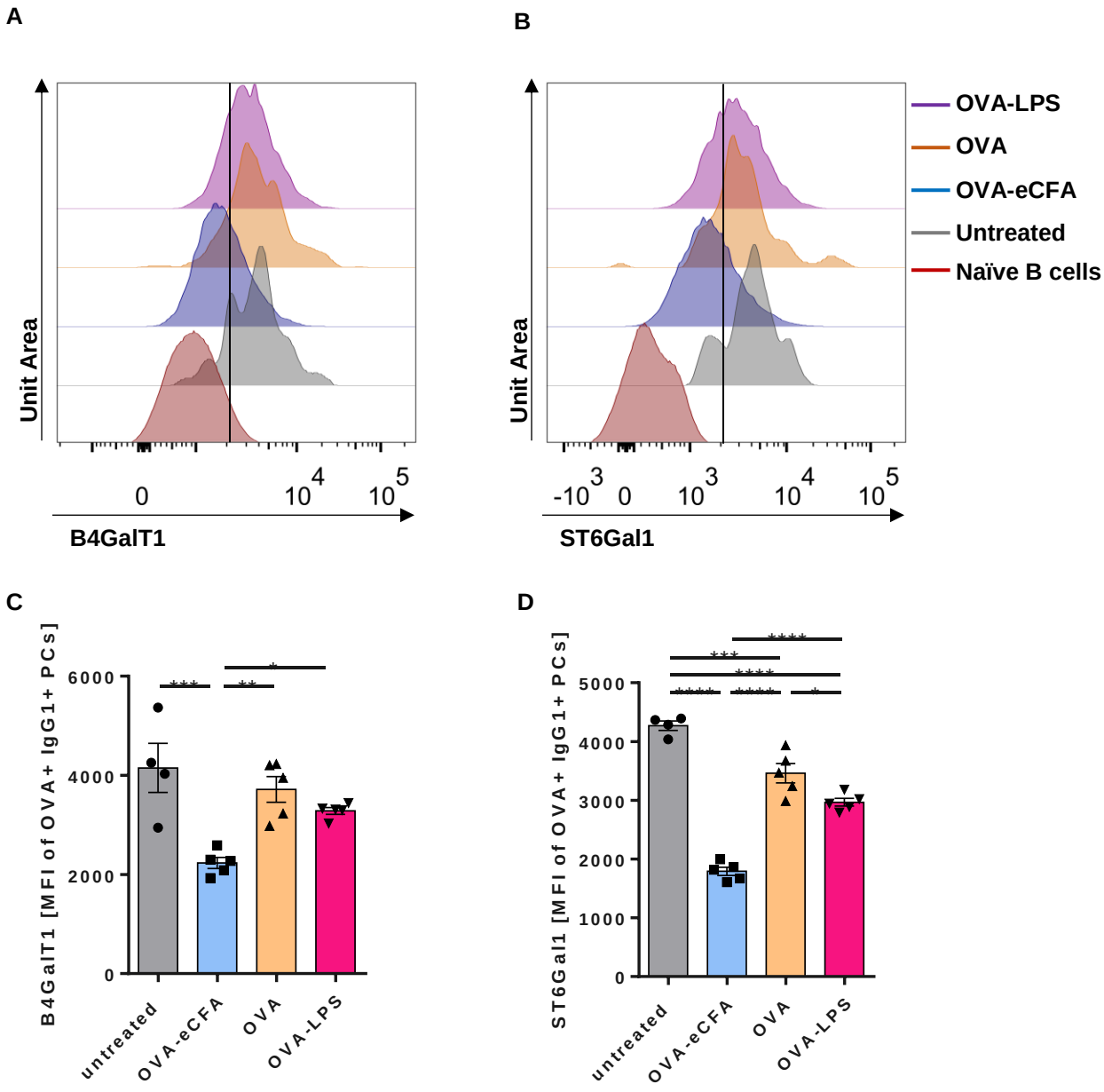

Figure 13: B4GalT1 and ST6Gal1 are differentially expressed in PCs. C57BL/6 mice were immunized *i.p.* with 100 µg OVA emulsified in enriched CFA, 5mg OVA or 100 µg OVA in 30 µg LPS, n=4-5 per group. (A, B) Comparison of intracellular B4GalT1 (A) and ST6Gal1 (B) expression in splenic $OVA^{+}IgG1^{+}$ PCs at day 8 after vaccination, data are presented as histogram overlays of one representative mouse per group. (C, D) Comparison of intracellular B4GalT1 (C) and ST6Gal1 (D) expression in splenic $OVA^{+}IgG1^{+}$ PCs. Data are representative of at least 2 independent experiments. One-way ANOVA test was used for all comparisons and data are presented as mean +/- SEM, *P < 0.05, **P < 0.01, ***P < 0.001 and ****P<0.0001

To rule out that plasma cells producing other IgG subclass Abs differ in their glycosyltransferase expression, I analyzed and compared the expression of B4galt1 and St6gal1 in OVA^+IgG^+ PCs (which don't contain IgG1 but all other subclasses, see also (**Figure 7** A-D, middle panel) and OVA^+IgG1^+ PCs. As expected, PCs producing OVA-specific IgG2b, IgG2c and IgG3 and PCs producing OVA-specific IgG1 had comparable transferase expression (**Figure 14** A, B). Since IgM and IgA producing plasma cells showed a significantly higher transferase expression, compared with IgG and IgG1 producing PCs, this indicates an inherent and isotype specific glycosylation process independent of antigen or co-stimuli.

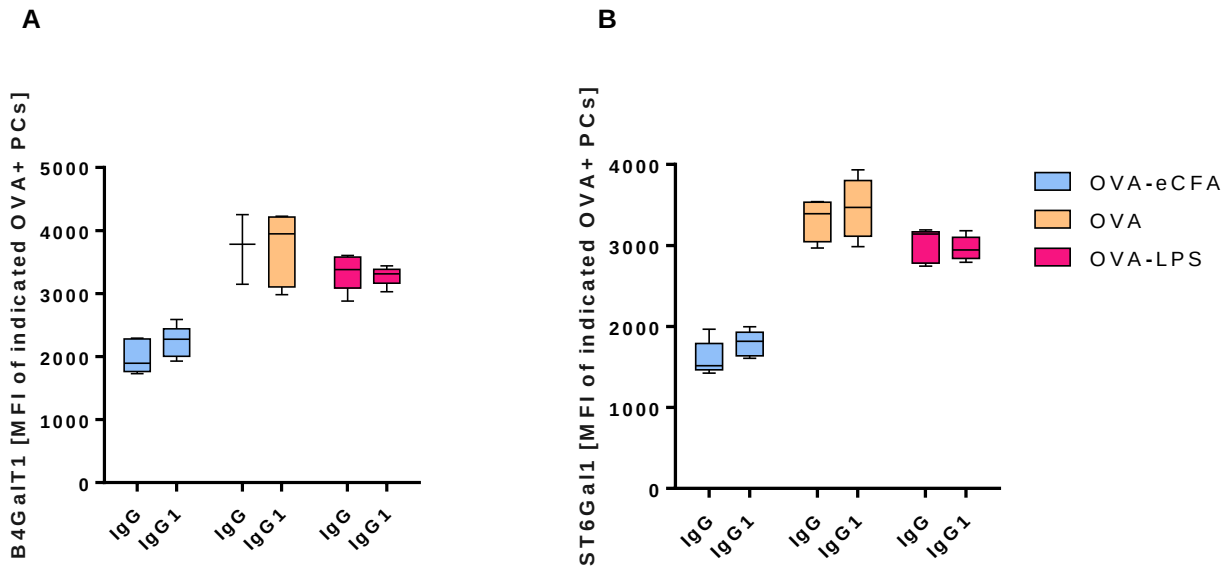

Figure 14: PCs producing IgG and PCs producing IgG1 express comparable B4galt1 and St6gal1 levels. C57BL/6 mice were immunized *i.p.* with 100 µg OVA emulsified in enriched CFA, 5mg OVA or 100 µg OVA in 30 µg LPS, n=3-5 per group (A, B) Comparison of intracellular B4galt1 (A) and St6gal1 (B) expression in splenic OVA^+IgG^+ PCs and OVA^+IgG1^+ PCs at day 8 after vaccination. Data are representative of at least 2 independent experiments and are presented as dot and are presented as 10-90 percentile.

To verify, that the expression levels of B4galt1 and St6gal1 in OVA^+IgG1^+ GC B cells and PCs correlate with Ab glycosylation, the sera of immunized and untreated control mice were used for glycoanalysis of OVA^+IgG^+ Abs (for immunized mice) or total IgG^+ Abs (for untreated mice) via HPLC. We found that the glycoprofiles of OVA^+IgG^+ Abs after OVA and OVA-LPS immunization

were similar to those of total IgG under steady state conditions in untreated control mice (**Figure 15**). The G0 content, defined as IgG Abs, which don't possess any residual galactose or sialic acid residues, was with ~25% stable among all 3 groups (untreated, OVA and OVA-LPS), whereas the G0 content of OVA-eCFA treated mice was with ~40% substantially higher (**Figure 15**, blue bars). The amount of galactosylated IgG Abs (G1 and G2), which do not contain any residual sialic acid residues were comparable between all tested groups (~40% galactosylated glycoforms), with only a slight increase in the G1 content of OVA-eCFA treated mice (~45% galactosylated glycoforms), compared with the other groups (**Figure 15** bright and dark yellow bars). The terminal sialic acid content (G1S1, G2S1 and G2S2) of OVA^+IgG^+ Abs was significantly lower in OVA-eCFA treated mice (~10% sialylated glycoforms), compared with OVA and OVA-LPS treated mice (~25% sialylated glycoforms). None of the analyzed groups showed any substantial amount of G2S2 IgG Abs (**Figure 15**, magenta bars). Taken together, pro-inflammatory OVA-eCFA treatment results in a markedly higher abundance of pro-inflammatory agalactosylated and asialylated IgG^+ Abs, compared with low-inflammatory OVA-LPS and pure OVA treatment.

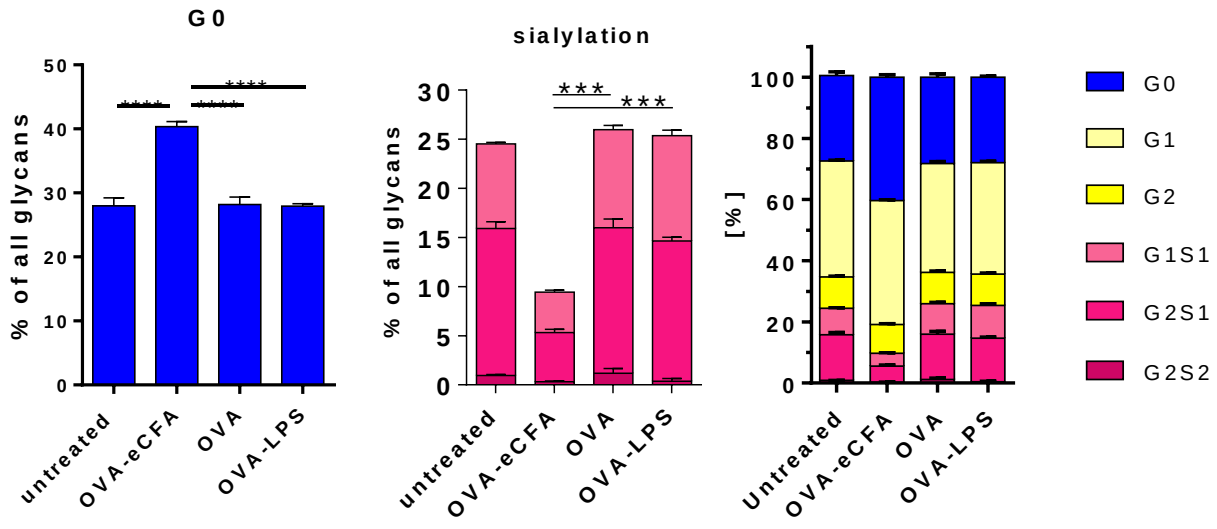

Figure 15: Antibody galactosylation and sialylation are regulated in GC B cells and correlate with expression of the glycosyltransferases B4GalT1 and ST6Gal1. C57BL/6 mice were immunized *i.p.* with 100 µg OVA emulsified in enriched CFA, 5mg OVA or 100 µg OVA in 30 µg LPS. Comparison of OVA^+IgG^+ glycoprofiles at day 14 after vaccination. Data are presented as mean +/- SEM of n=24 for untreated, n=19 for OVA-eCFA-, n=14 for OVA- and n=9 for OVA-LPS- treated groups.

These data demonstrate that IgG antibody galactosylation and sialylation correlate with the expression levels of their respective glycosyltransferases B4galt1 and St6gal1. Since the expression levels of both transferases in OVA^+IgG1^+ GC B cells and OVA^+IgG1^+ PCs were significantly higher than in naïve B cells, this further indicates that IgG Ab glycosylation is actively regulated during the germinal center response. Since many vaccines use boost injections to intensify the ensuing Ab response, it is of interest if the Ab glycosylation is also maintained upon antigen re-exposure, when memory B cells form new GCs and LLPCs produce large amounts of protective Abs. Therefore, I next tested whether splenic OVA^+IgG1^+ PCs, which are formed upon secondary antigen exposure, show a comparable glycosyltransferase expression to those formed upon first antigen contact. Since enzyme expression are only relative values, I furthermore assessed the glycoprofile of OVA^+IgG^+ Abs, 5 days after the boost immunization with 100ug OVA.

3.4 IgG antibody glycosylation is maintained upon re-exposure to antigen

To test if antibody glycosylation is maintained throughout longer time periods, I immunized mice with either OVA-LPS or OVA-eCFA at d0, challenged them 28d later with 100 µg OVA and analyzed the expression of B4galt1 and St6gal1, as well as the glycoprofiles at day 5 after the boost immunization (**Figure 16**). Since the serum half-life of IgG antibodies is ~21 days, most of the initially generated Abs shouldn't be detectable anymore by this time point. Moreover, plasma blasts, which could also contribute to the Ab repertoire, are relatively short lived and only a small percentage of them undergo CSR, implying an only a minor impact of these cells and Abs. To delineate between newly formed PCs and LLPCs, I additionally analyzed whether any of the LLPCs in the bone barrow were antigen-specific after the OVA challenge. To further quantify the amount of present IgG^+ Abs in the sera of the immunized mice, I did an ELISA analysis of total IgG and all IgG subclasses.

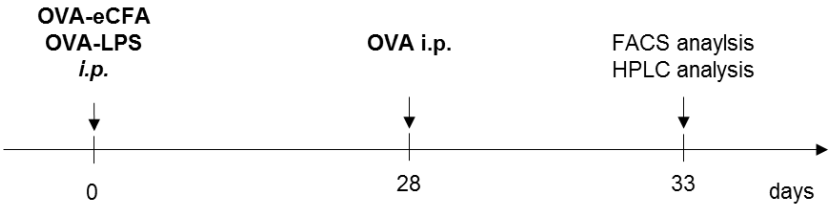

Figure 16: Experimental setup of long term immunization and subsequent challenge. Vert-X mice were immunized *i.p.* with 100 µg OVA emulsified in enriched CFA or 100 µg OVA in 30 µg LPS and 28d later challenged with 100 µg OVA. 5d later the mice were sacrificed, serum was taken for HPLC analysis and ELISA analysis and spleen and bone marrow were collected for FACS analysis.

I found that OVA-eCFA treated mice induced significantly more splenic PCs (~3%) than OVA-LPS treated mice (~1%) upon antigen re-exposure. Although, the frequency of OVA$^+$ PCs was more than 3 times higher in OVA-eCFA treated mice, compared with OVA-LPS treated mice, the frequency of OVA$^+$IgG1$^+$ PCs was comparable (**Figure 17** A-C).

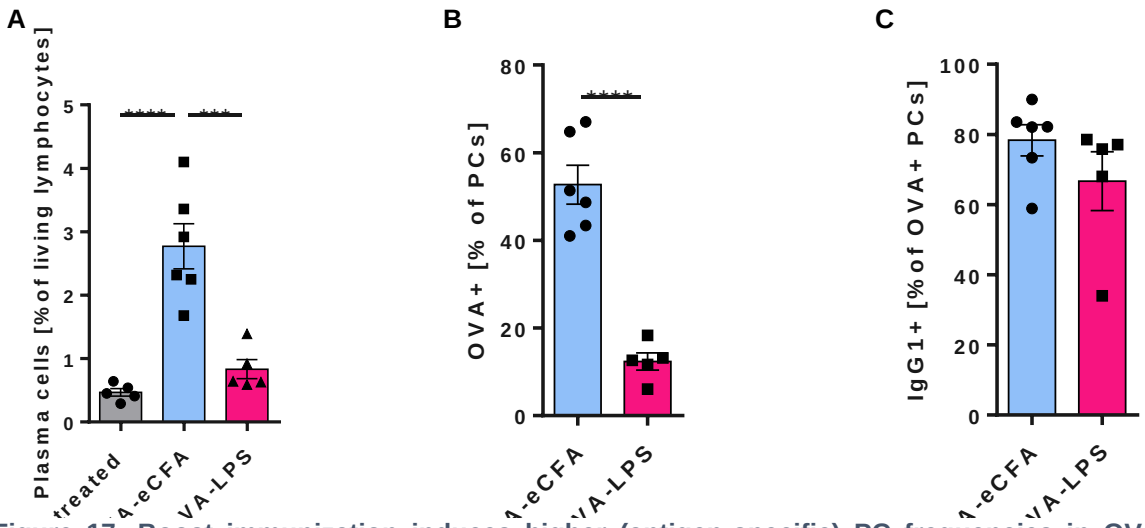

Figure 17: Boost immunization induces higher (antigen-specific) PC frequencies in OVA-eCFA treated mice than in OVA-LPS treated mice. Vert-X mice were immunized *i.p.* with 100 µg OVA emulsified in enriched CFA or 100 µg OVA in 30 µg LPS and 28 days later challenged with 100 µg OVA, n=5-6 per group. (A-C) Comparison of the frequencies of PCs (A), OVA$^+$ PCs (B) and OVA$^+$IgG1$^+$ PCs (C). Data are representative of 2 independent experiments. Students unpaired t-test (B, C) or One-way ANOVA test (A) were used for comparisons and data are presented as mean +/- SEM, *P < 0.05, **P < 0.01, ***P < 0.001 and ****P<0.0001

To test, whether the differences in OVA$^+$ PC frequencies result in distinct amounts of produced OVA$^+$IgG$^+$ Abs, I analyzed the sera of OVA-eCFA and OVA-LPS treated mice 5 days upon the boost immunization. As expected from the frequency of OVA$^+$ PCs, OVA-eCFA treatment resulted in significantly increased IgG production throughout all subclasses (**Figure 18**). Since IgG1 is the most predominant subclass after OVA-eCFA and after OVA-LPS immunization, as evidenced by the flow cytometric data, it is likely that the biggest differences in total IgG stem from differences in IgG1 production.

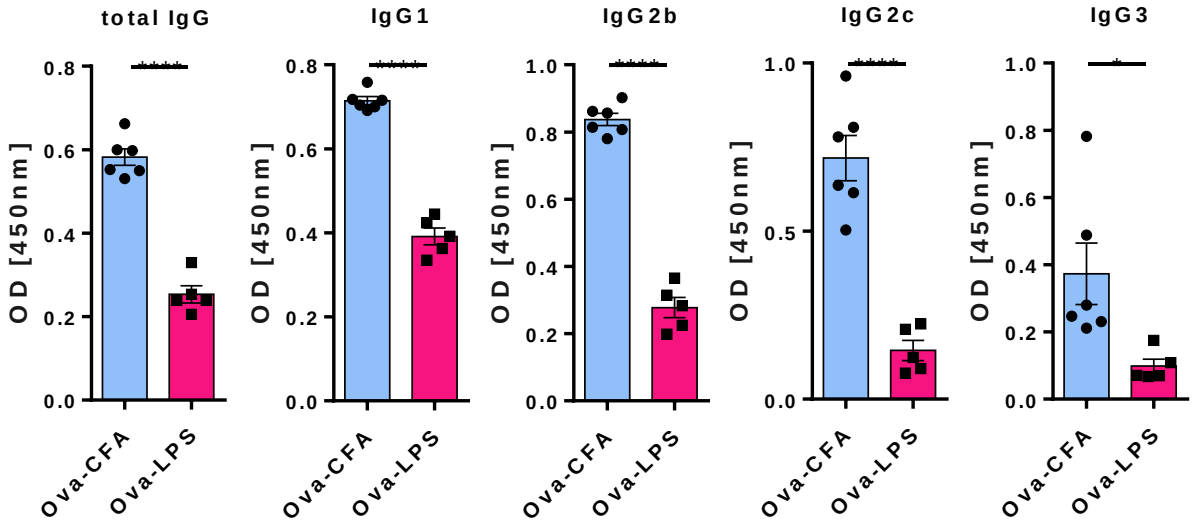

Figure 18: OVA-eCFA treatment results in significantly higher IgG production than OVA-LPS treatment upon boost immunization. Vert-X mice were immunized *i.p.* with 100 µg OVA emulsified in enriched CFA or 100 µg OVA in 30 µg LPS and 28d later challenged with 100 µg OVA, n=5-6 per group. Quantification of OVA-specific serum Ab levels for all IgG subclasses after indicated immunizations. Antibody subclasses were identified by HRP-coupled anti-subclass Abs. Data are representative of 2 independent experiments. Students unpaired t-test was used for all comparisons and data are presented as mean +/- SEM, *P < 0.05, **P < 0.01, ***P < 0.001 and ****P<0.0001

Next, I analyzed the glycosyltransferase expression in splenic OVA^+IgG1^+ PCs. Interestingly, B4galt1 and St6gal1 expression levels strongly resembled their respective counterparts 8 days upon OVA-eCFA and OVA-LPS immunization (**Figure 19** A-D, see also **Figure 13** A-D). Here, splenic OVA^+IgG1^+ PCs of OVA-eCFA treated mice showed significantly less expression of B4galt1 and St6gal1 than $IgG1^+$ PCs under steady state conditions and OVA^+IgG1^+ PCs after OVA-LPS immunization. Since the B4galt1 expression correlates with antibody galactosylation and St6gal1 expression correlates with antibody sialylation, this indicates that the glycosylation of antigen-specific IgG Abs is stable and maintained, even throughout re-exposure to the antigen.

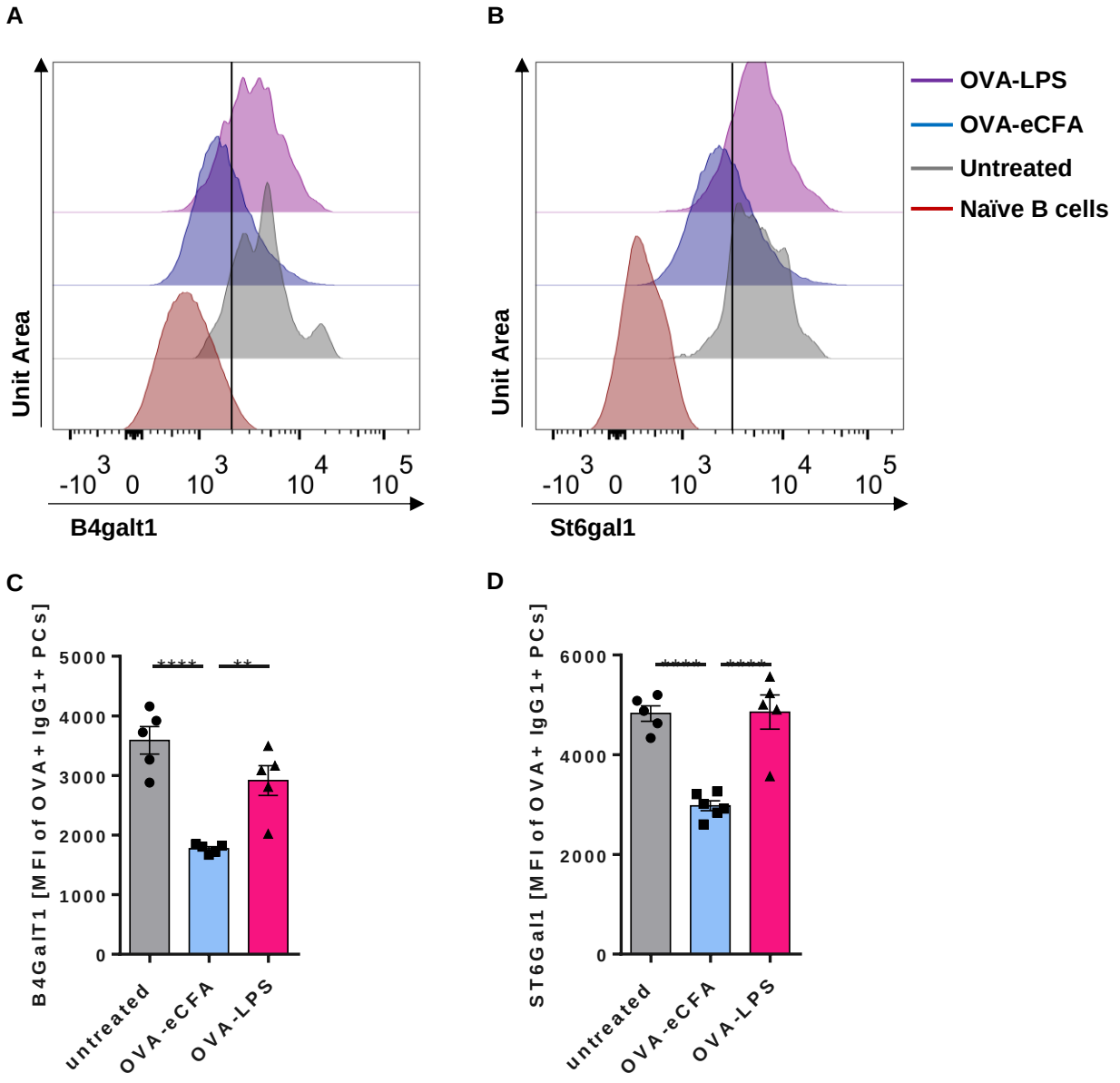

Figure 19: IgG antibody glycosylation is maintained upon re-exposure to antigen. Vert-X mice were immunized *i.p.* with 100 µg OVA emulsified in enriched CFA or 100 µg OVA in 30 µg LPS and 28 days later challenged with 100 µg OVA, n=5-6 per group. (A, B) Comparison of intracellular B4GalT1 (A) and ST6Gal1 (B) expression in splenic OVA^+IgG1^+ PCs after indicated immunizations, data are presented as histogram overlays of one representative mouse per group. (C, D) Comparison of intracellular B4GalT1 (C) and ST6Gal1 (D) expression in splenic OVA^+IgG1^+ PCs after indicated immunizations. Data are representative of 2 independent experiments. One-way ANOVA test was used for all comparisons and data are presented as mean +/- SEM, *P < 0.05, **P < 0.01, ***P < 0.001 and ****P<0.0001

To test if the produced Abs solely stem from newly formed PCs, generated from memory B cells upon re-exposure, I analyzed whether a significant portion of LLPCs in the BM were OVA-specific and could therefore contribute to the measured antibody repertoire. Since the frequency of LLPCs in the BM is capped to approximately 0.1%, I presumed that only a small portion of the produced IgG Abs could stem from these cells.

Surprisingly, approximately 10% of all LLPCs in the BM were OVA-specific at the time point of investigation (**Figure 20** B, D). Considering that these cells can produce large amounts of Abs, I cannot exclude that a substantial proportion of the produced IgG Abs stem from these cells. Utilizing the properties of the immunized Vert-X mice, I additionally checked whether the LLPCs in the BM are capable of producing the anti-inflammatory cytokine IL-10. Interestingly, the LLPCs of OVA-eCFA and OVA-LPS treated mice produced substantial and comparable amounts (~15%) of IL-10, 5d upon boost immunization. Since nearly none of the IL-10 producing cells were also antigen-specific, it raises the question, what the purpose of these IL-10 producing cells is (**Figure 20** B, C). Therefore, it would be of interest if these IL-10^{+} LLPCs have suppressive capacities and further experiments should be conducted to unravel the importance of those cells.

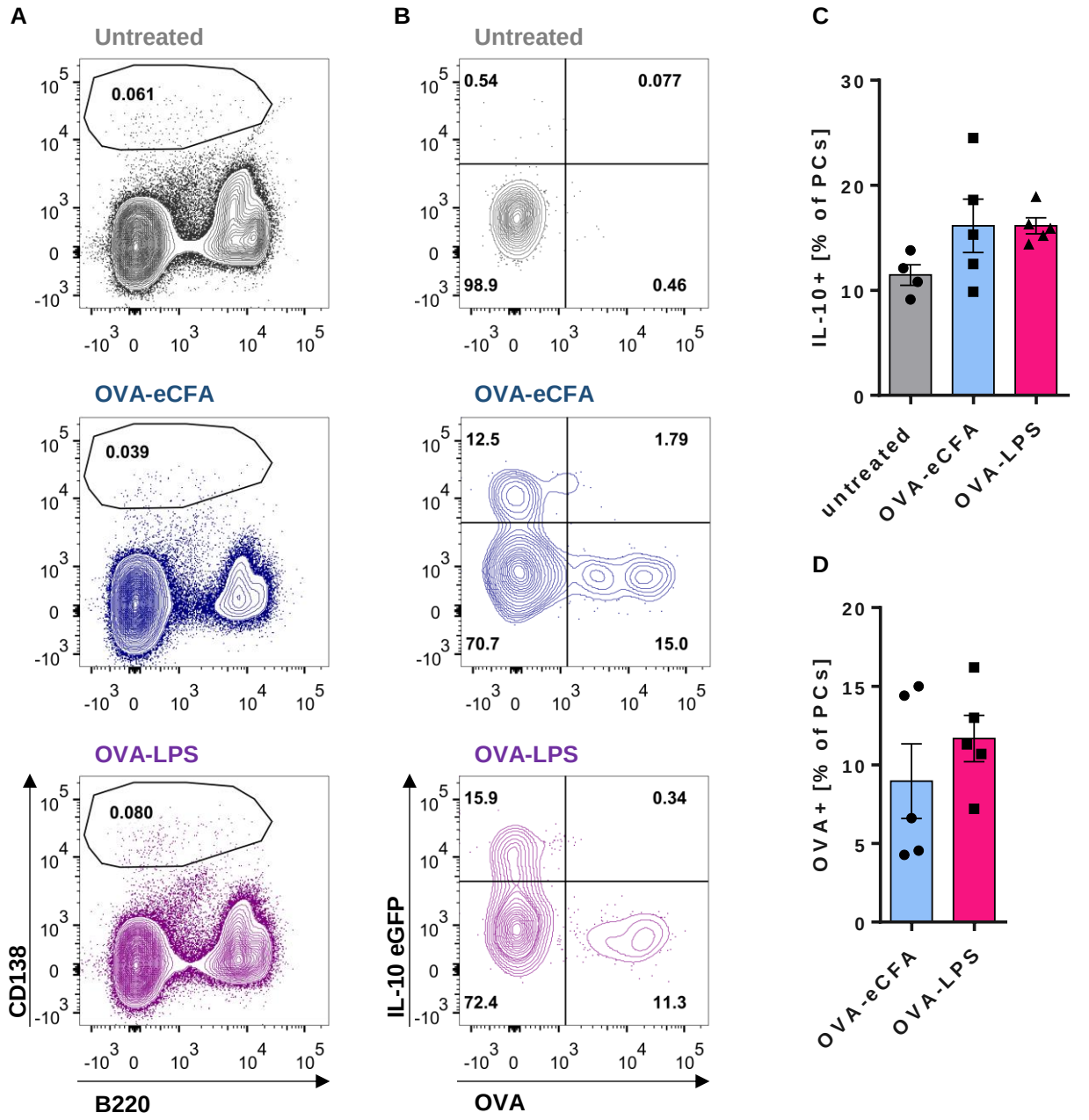

Figure 20: Comparable amounts of OVA$^+$ and IL-10$^+$ CD138$^+$ LLPCs in the BM upon boost immunization of OVA-eCFA and OVA-LPS treated mice. Vert-X mice were immunized *i.p.* with 100 µg OVA emulsified in enriched CFA or 100 µg OVA in 30 µg LPS and 28d later challenged with 100 µg OVA, n=5 per group. (A) Comparison of frequency of CD138$^+$ LLPCs 5d upon boost immunization of untreated, OVA-eCFA and OVA-LPS treated mice. (B-D) Comparison of frequencies of OVA$^+$ and IL-10$^+$ CD138$^+$ LLPCs 5d upon boost immunization of untreated, OVA-eCFA and OVA-LPS treated mice. Data are representative for 2 independent experiments. Students unpaired t-test (D) or One-way ANOVA test (C) were used for all comparisons and data are presented as mean +/- SEM, *P < 0.05, **P < 0.01, ***P < 0.001 and ****P<0.0001

To verify that antigen-specific IgG$^+$ Abs maintain their glycosylation profile even upon re-exposure to this antigen, I compared the glycosylation profiles of OVA-specific IgG$^+$ Abs at day 8 and day 14 upon immunization, and at day 33 upon a boost immunization with Ovalbumin. All tested immunizations lead to a similar G0 content of approximately 20-25% 8 days upon immunization. The G1 and G2 contents, characterized as IgG Abs with either one (G1) or 2 (G2) terminal galactose residues without further addition of sialic acid, were slightly higher in OVA-eCFA treated mice, compared with OVA and OVA-LPS treated mice. Surprisingly, all groups showed high sialylation of the OVA$^+$IgG$^+$ Abs. Here, OVA-eCFA treated mice had a sialic acid content (G1S1, G2S1 and G2S2) of ~20%, while OVA and OVA-LPS treated mice had a significantly higher content of ~30%. In contrast, Ab galactosylation and sialylation were severely reduced at day 14 and upon antigen re-exposure in OVA-eCFA treated mice, but not in OVA and OVA-LPS treated mice, indicating stark differences in the inflammatory conditions upon OVA-eCFA and OVA-LPS immunization (**Figure 21** A-C).

The markedly different glycoprofiles at day 8 might at least partially be contributed to an extrafollicular pathway of B cell activation, leading to the production of IgG antibodies by extrafollicular plasma blasts. Since GCs can take up to 6 days to fully develop, extrafollicular Abs could very well contribute to the observed glycoprofiles, whereas the glycoprofiles at day 14 would be much less impacted by such Abs. Moreover, the glycoprofiles of the antigen-specific IgG Abs at day 33 could be a mixture of produced Abs by newly formed splenic PCs and LLPCs in the bone marrow.

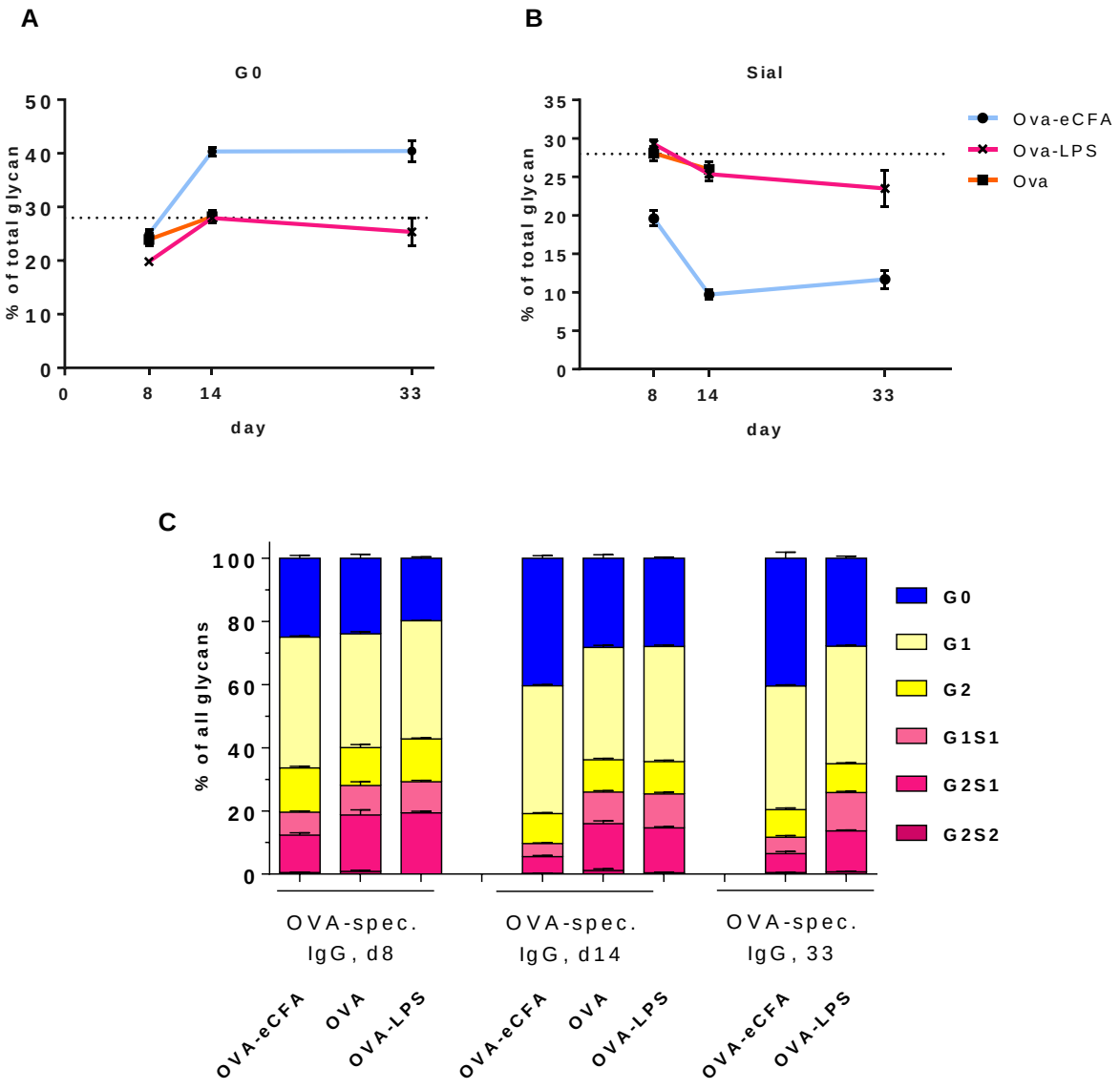

Figure 21: IgG antibody glycosylation is maintained upon re-exposure to antigen. Vert-X mice were immunized *i.p.* with 100 µg OVA emulsified in enriched CFA or 100 µg OVA in 30 µg LPS and 28d later challenged with 100 µg OVA. (A-C) Comparison of IgG glycoprofiles 8 days and 14 days upon immunization and 5 days upon boost immunization. Comparison of aglycosylated (GO) content (A) and of terminally sialylated (G1S1, G2S1 and G2S2) content (B) of OVA^+IgG^+ Abs, each dotted line is the mean of total IgG^+ Abs of untreated mice. (C) Overview about whole glycoprofiles of OVA^+IgG^+ Abs. Data are presented as mean +/- SEM of n=24 for untreated, n=18 for OVA-eCFA day 8, n=18 for OVA-eCFA day 14, n=12 for OVA-eCFA day 33, n=10 for OVA day 8, n=9 for OVA day 14, n=3 for OVA-LPS day 8, n=14 for OVA-LPS day 14, n=10 for OVA-LPS day 33.

Taken together, these data imply that the three OVA immunizations induce comparable early extrafollicular PC responses, but differ in their subsequent GC response. Furthermore, this suggests that a specific glycoprofile is imprinted into Abs being produced by antigen-specific plasma cells, that this glycoprofile is dependent on the co-stimulus (immunogenicity of the antigen) and that it is stable upon re-exposure to the same antigen. This indicates that memory B cells, which are poised to react to antigen re-exposure, differentiate into antigen-specific plasma cells, which produce high-affinity Abs exhibiting the same glycoprofile as the Abs produced upon first antigen contact.

To summarize, these data indicate that the IgG glycosylation is being regulated during the GC reaction, a process that is being controlled by T follicular helper cells. Since antigen immunogenicity seems to induce phenotypically distinct GC B cells, I next assessed whether similar immunization dependent differences can also be observed in the Tfh cell compartment.

3.5 Tfh cells during the GC response

Since the data point to a regulatory process within the GC, I next tried to delineate the mechanism leading to differentially glycosylated IgG^+ Abs. Therefore, I first analyzed the frequency of T follicular helper cells upon different immunizations utilizing the cell specific markers CD4, CXCR5 and ICOS (**Figure 22** A and B). To increase the specificity of my gating, I initially excluded $B220^+$ cells, which express high amounts of CXCR5, to decrease the frequency of falsely positive signals (**Figure 22** A). Next, I gated on $CD4^+$ cells, while simultaneously excluding $CD8^+$ cells (**Figure 22** B). I then gated on $CD4^+CXCR5^+ICOS^+$ cells, a marker combination which specifically characterizes T follicular helper cells (**Figure 22** C). To do that, I used FMO controls for CXCR5 and ICOS to only gate on cells, which are positive for those to markers (**Figure 22** D).

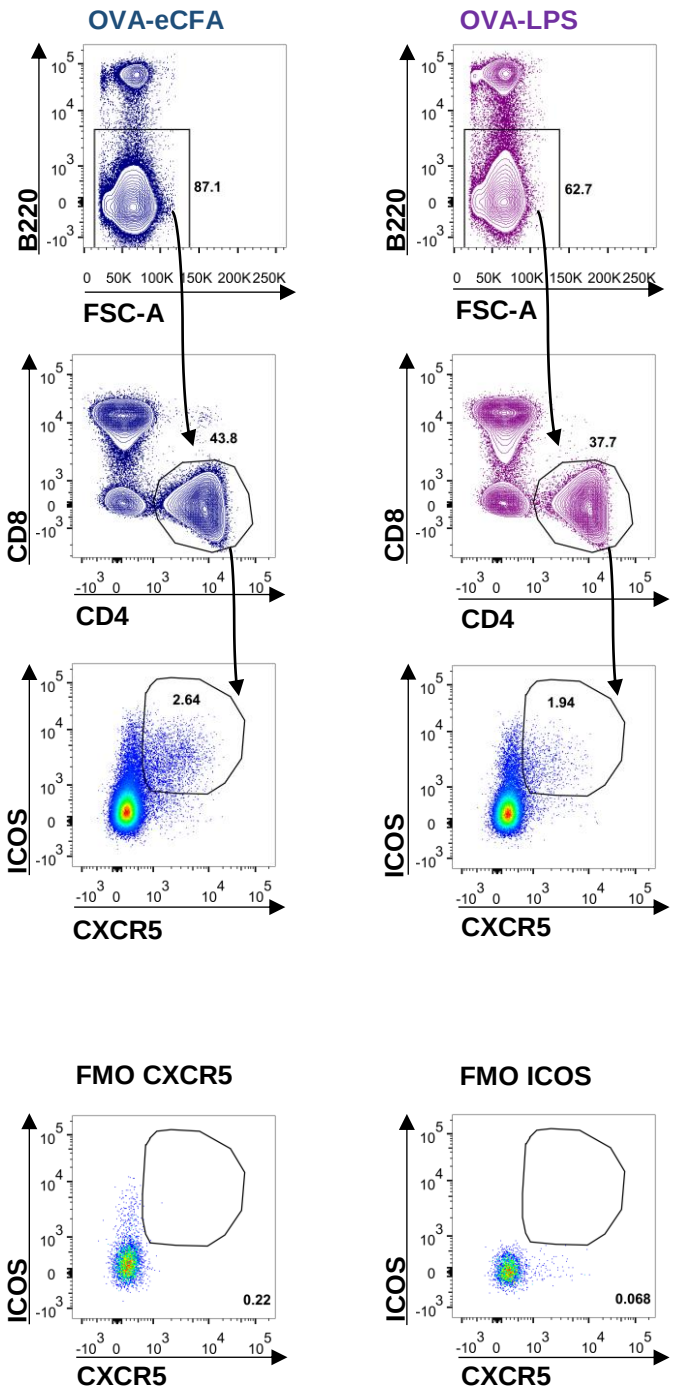

Figure 22: Characterization of T follicular helper cells. Vert-X mice were immunized *i.p.* with 100 µg OVA emulsified in enriched CFA or 100 µg OVA in 30 µg LPS, n=4 per group. Gating strategy to identify splenic $CD4^+CXCR5^+ICOS^+$ T follicular helper cells of either OVA-eCFA or OVA-LPS treated mice. FMO controls were used to reliably gate on $CXCR5^+$ and $ICOS^+$ cells.

OVA-eCFA treated mice had a significantly higher frequency (**Figure 23**) and cell number (data not shown) of Tfh cells, compared with OVA, OVA-LPS and untreated mice.

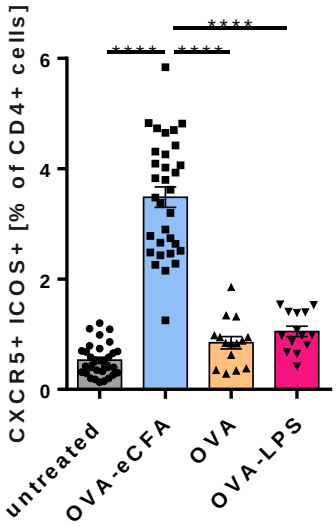

Figure 23: OVA-eCFA treatment results in substantial induction of T follicular helper cells. Vert-X mice were immunized *i.p.* with 100 µg OVA emulsified in enriched CFA, 5mg OVA or 100 µg OVA in 30 µg LPS and sacrificed at d8. Comparison of the frequency of splenic T follicular helper cells upon indicated immunizations. Data are combined of up to 5 independent experiments. One-way ANOVA test was used for all comparisons and data are presented as mean +/- SEM of n=33 for untreated mice, n=32 for OVA-eCFA treated mice, n=15 for OVA treated mice and n=14 for OVA-LPS treated mice, *P < 0.05, **P < 0.01, ***P < 0.001 and ****P<0.0001

OVA and OVA-LPS treated mice resulted in higher Tfh frequencies than steady state conditions in untreated mice, though this difference didn't reach statistical significance. Interestingly, the frequency of Tfh cells correlates with the frequency of (OVA-specific) GC B cells and PCs (**Figure 6** A and B and **Figure 8** A). The highest Tfh, GC B cell and PC frequencies were observed upon pro-inflammatory OVA-eCFA treatment. This is probably due to decreased intra- and interclonal competition of GC B cells for T cell help, since Tfh cells are available at a higher abundance. Therefore, more B cell clones and also those with a low relative affinity for the cognate antigen are able to undergo iterative rounds of affinity maturation, SHM and CSR, resulting in higher GC B cell and PC numbers.

To further delineate the influence of T follicular helper cells on GC B cells, I analyzed the production of the pro-inflammatory cytokines IFN-γ and IL-17A by Tfh cells. For this, I immunized C57BL/6 mice with OVA-eCFA or OVA-LPS and sacrificed them at the peak of the GC response at day 6. I found that splenic Tfh cells of OVA-eCFA treated mice produce substantial amounts of IL-17A and relatively low amounts of IFN-γ. Tfh cells of OVA-LPS treated mice on the other hand produced significantly less IL-17A, but substantially more IFN-γ (**Figure 24** A, B and **Figure 25** A, B). Interestingly, IFN-γ and IL-17A production seem to be mutually exclusive upon both immunizations, since I couldn't find any IFN-γ/IL-17A double positive Tfh cells. This suggests that IFN-γ^+ and IL-17-A^+ Tfh cells are phenotypically distinct and indicates that they could act on specific targets. On the other hand, GC B cells possess receptors for both cytokines, pointing to an interaction of those cells (Jackson et al. 2016; Domeier et al. 2016; Hsu et al. 2008). Since approximately 25% of the Tfh cells produced IFN-γ upon OVA-LPS immunization, I further checked whether these cells also express other cytokines. Since similar findings have been shown for Tr1 cells, I tested if these Tfh cells are able to simultaneously produce IL-10. By utilizing the eGFP signal of Vert-X mice, I found that a profound percentarge of all Tfh cells produce IL-10 and that this percentage depended on the immunization (**Figure 25** C). Here, Tfh cells of OVA-LPS treated mice produced significantly more IL-10 than those of OVA-eCFA treated mice. Moreover, I found a high percentage of IFN-γ/IL-10 double positive cells, and this percentage was significantly higher in OVA-LPS treated mice (~3%) than in OVA-eCFA treated mice (~0.5%), pointing to a more suppressive Tfh phenotype upon low-inflammatory OVA-LPS immunization (**Figure 25** C, D). These data point to an important role of Tfh derived cytokines to modulate and control the GC response.

Since GC reactions need to be efficiently regulated to prevent detrimental effects like autoimmunity, a variety of regulatory mechanisms have been proposed. Especially Tfr cells have been implicated to efficiently regulate the GC response through different mechanisms, including secretion of anti-inflammatory cytokines IL-10 and TGF-β. To further address how GC reactions are regulated, I next analyzed the abundance of Tfh and Tfr cells, as well as their respective cytokine production.

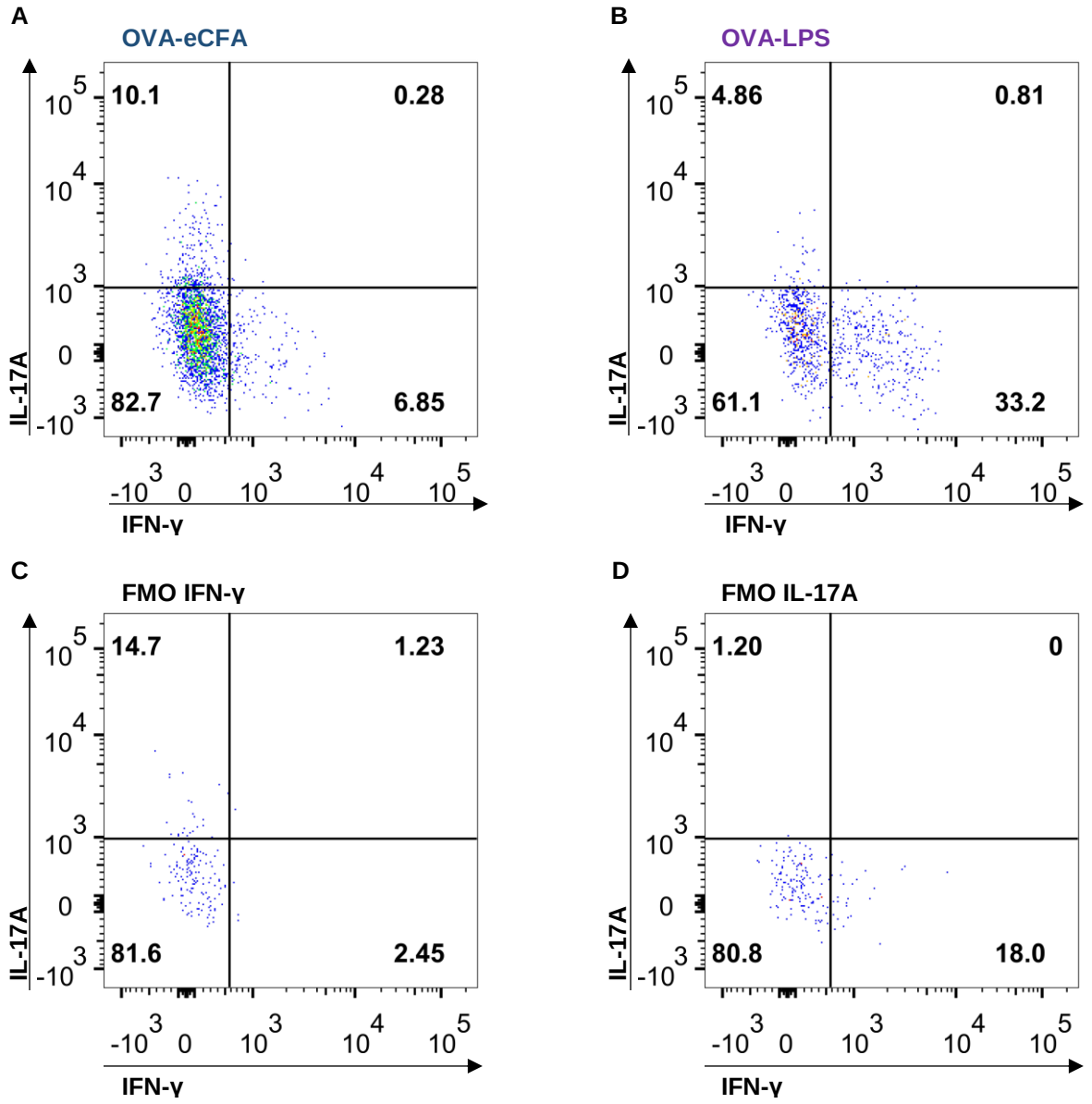

Figure 24: T follicular helper cells produce substantial amounts of the pro-inflammatory cytokines IFN-γ and IL-17A. Vert-X mice were immunized *i.p.* with 100 µg OVA emulsified in enriched CFA or 100 µg OVA in 30 µg LPS, n=4 per group. Gating strategy to characterize IFN-γ and IL-17A producing splenic $CD4^+CXCR5^+ICOS^+$ T follicular helper cells at day 8 after vaccination. (A, B) Cytokine production upon OVA-eCFA (A) and OVA-LPS (B) immunization. (C, D) FMO controls to set the gates for IFN-γ^+ (C) and IL-$17A^+$ (D) cells. Shown are representative dot plots of each group. All cells were activated with a cell activation complex consisting of PMA, Ionomycin, Brefeldin-A and Monensin and were incubated for 5h at 37°C prior to the staining.

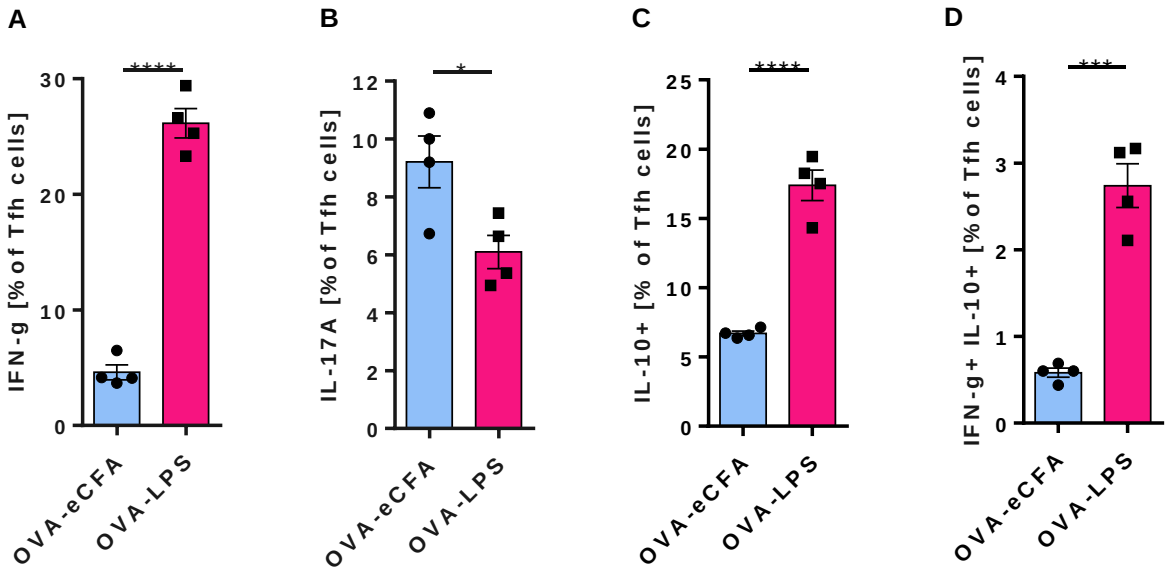

Figure 25: T follicular helper cells induced upon different stimuli are phenotypically distinct. Vert-X mice were immunized *i.p.* with 100 µg OVA emulsified in enriched CFA or 100 µg OVA in 30 µg LPS, n=4 per group. Comparison of the frequency of cytokine producing splenic T follicular helper cells at day 6 after vaccination. (A) Comparison of IFN-γ producing Tfh cells. (B) Comparison of IL-17A producing Tfh cells. (C) Comparison of IL-10 producing Tfh cells. (D) Comparison of IFN-γ/IL-10 producing Tfh cells. Data are representative of 2 independent experiments. Students t-test was used for all comparisons and data are presented as mean +/- SEM, *P < 0.05, **P < 0.01, ***P < 0.001 and ****P<0.0001

To further characterize T follicular helper cells, I additionally stained for FoxP3 to discriminate between Tfh and Tfr cells. The latter cells are defined by a combination of different markers ($CD4^+CXCR5^+ICOS^+FoxP3^+$). These Tfr cells are thought to interact and inhibit Tfh and GC B cells and thereby regulate the ensuing GC response (Wing et al. 2014; Sage & Sharpe 2016; Sage & Sharpe 2015; Ramiscal & Vinuesa 2013).

First, I measured the frequency of Tfr cells during steady state conditions in untreated mice and upon immunization with OVA-eCFA, OVA and OVA-LPS. When gated on $CD4^+CXCR5^+ICOS^+$ cells, I found that OVA-eCFA treated mice showed significantly less FoxP3 production than steady state conditions in untreated mice and low-inflammatory OVA and OVA-LPS treated mice (**Figure 26** A, B). While pro-inflammatory OVA-eCFA resulted in approximately 20% regulatory Tfr cells, it also means that ~80% were stimulatory Tfh cells (Tfr/Tfh ratio of 0.25). This ratio is significantly more skewed towards suppressive Tfr cells in steady state conditions, OVA and also OVA-LPS treated mice, which all showed a comparable Tfr/Tfh ratio of ~0.43 (**Figure 26** B).

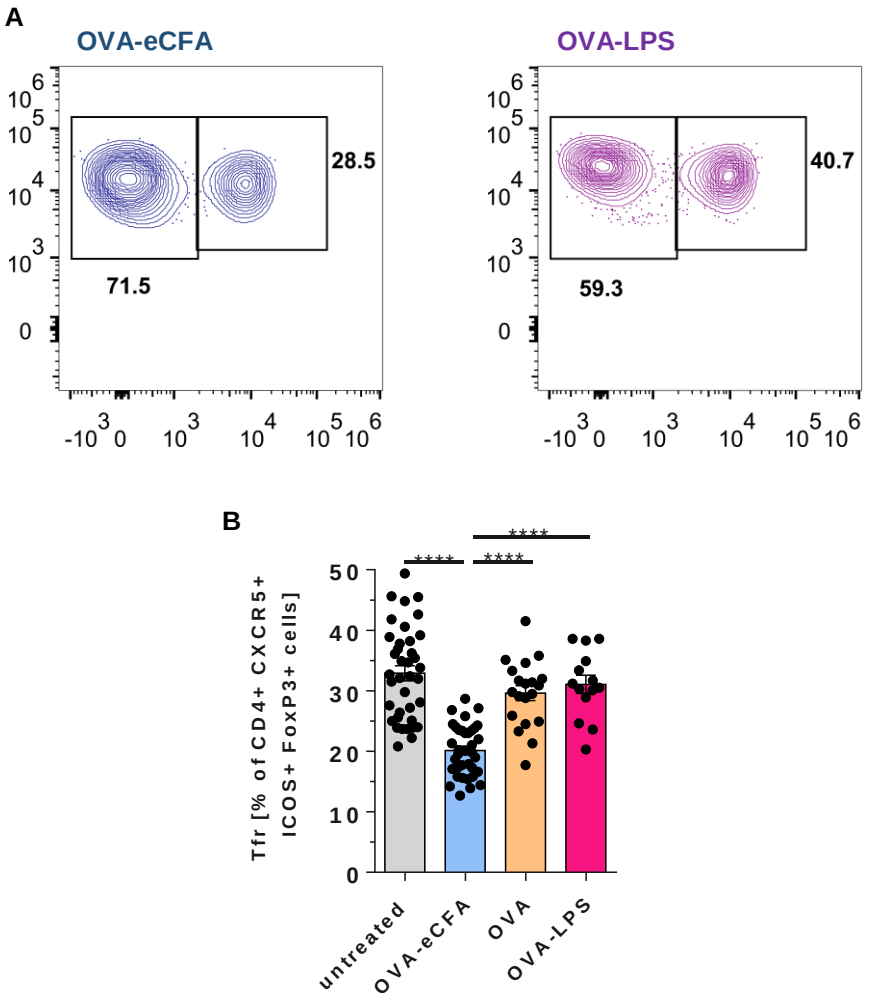

Figure 26: Tfr cells control the germinal center response. Vert-X mice were immunized *i.p.* with 100 µg OVA emulsified in enriched CFA, 5mg OVA or 100 µg OVA in 30 µg LPS. Comparison of the frequency of splenic Tfr cells at day 8 after vaccination. Gating strategy to identify Tfr cells, gated on $CD4^+CXCR5^+ICOS^+$ cells (A). Comparison of the frequency of Tfr cells (B). Data are pooled of up to 5 independent experiments. One-way ANOVA test was used for all comparisons and data are presented as mean +/- SEM of n=33 for untreated mice, n=32 for OVA-eCFA treated mice, n=15 for OVA treated mice and n=14 for OVA-LPS treated mice, *P < 0.05, **P < 0.01, ***P < 0.001 and ****P<0.0001

Taken together, these data indicate that GC reactions are likely modulated by T follicular helper cells. Since these cells directly interact with GC B cells, it is plausible that secreted cytokines and subsequent signal transduction further define the GC response and possibly glycosyltransferase expression and Ab glycosylation.

3.6 The pro-inflammatory cytokines IFN-γ and IL-17A alter IgG glycosylation

To investigate whether cytokine secretion and signal transduction during the germinal center reaction affects Ab glycosylation, I immunized wildtype, IL-17RA$^{-/-}$ and IL-17RA$^{-/-}$ **/** IFN-γRI$^{-/-}$ mice with pro-inflammatory OVA-eCFA and analyzed glycosyltransferase expression and IgG glycosylation. Since it has been shown that GC B cells express both the IL-17R and the IFN-γRI, it is possible that the GC reaction would be influenced if GC B cells lack those receptors (Domeier et al. 2016; Jackson et al. 2016; Hsu et al. 2008). Therefore, I assessed the strength of the germinal center response by analyzing the frequency of GC B cells and PCs. I found that IL-17RA$^{-/-}$ **/** IFN-γRI$^{-/-}$ double knockout mice had a significantly lower frequency of both cell types, compared with wildtype and IL-17RA$^{-/-}$ mice (**Figure 27** A, C). While the frequency of OVA^{+} GC B cells and PCs was comparable between all mouse strains, IL-17RA$^{-/-}$ **/** IFN-γRI$^{-/-}$ double knockout mice showed a profoundly reduced CSR towards IgG1 (**Figure 27** B, C, E, F). Since OVA-eCFA immunization of IL-17RA$^{-/-}$ mice didn't result in substantial changes of GC B cells and PCs, this suggests that signal transduction through the IFN-γRI contributes to the development or proliferation of these cells. To test whether these differences during the GC reaction also affect the IgG glycosylation, I analyzed the expression levels of B4galt1 and St6gal1 and the glycoprofiles of IgG^{+} Abs in the serum. First, I analyzed enzyme expression in OVA^{+}IgG1^{+} GC B cells. I found significantly higher glycosyltransferase expression in OVA-eCFA treated double knockout mice, compared with OVA-eCFA treated wildtype mice (**Figure 28** A-D). This indicates, that glycosyltransferase expression is influenced by IL-17RA and IFN-γRI signal transduction.

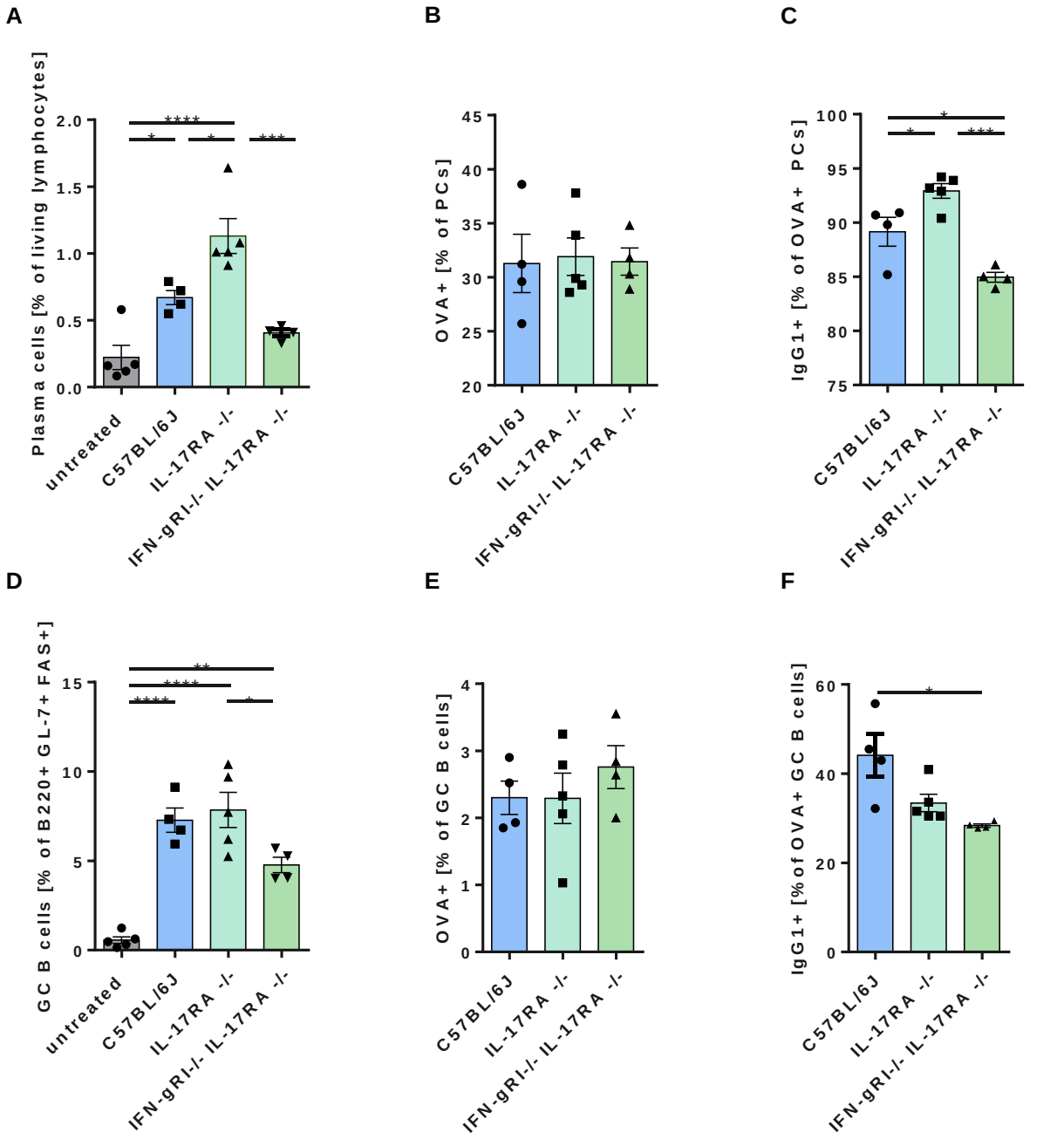

Figure 27: Lack of IFN-γ and IL-17A signal transduction alter the germinal center reaction. Wildtype, IL-17RA$^{-/-}$ and IL-17RA$^{-/-}$ **/** IFN-γRI$^{-/-}$ mice were immunized with OVA-eCFA, n=4-5 per group. (A-F) Comparison of the frequency of PCs (A), OVA^{+} PCs (B), OVA^{+}IgG1^{+} PCs (C), GC B cells (D), OVA^{+} GC B cells (E) and OVA^{+}IgG1^{+} GC B cells (F) at day 8 after vaccination. Data are representative of 2 independent experiments. One-way ANOVA was used for all comparisons and data are presented as mean +/- SEM, *P < 0.05, **P < 0.01, ***P < 0.001 and ****P<0.0001.

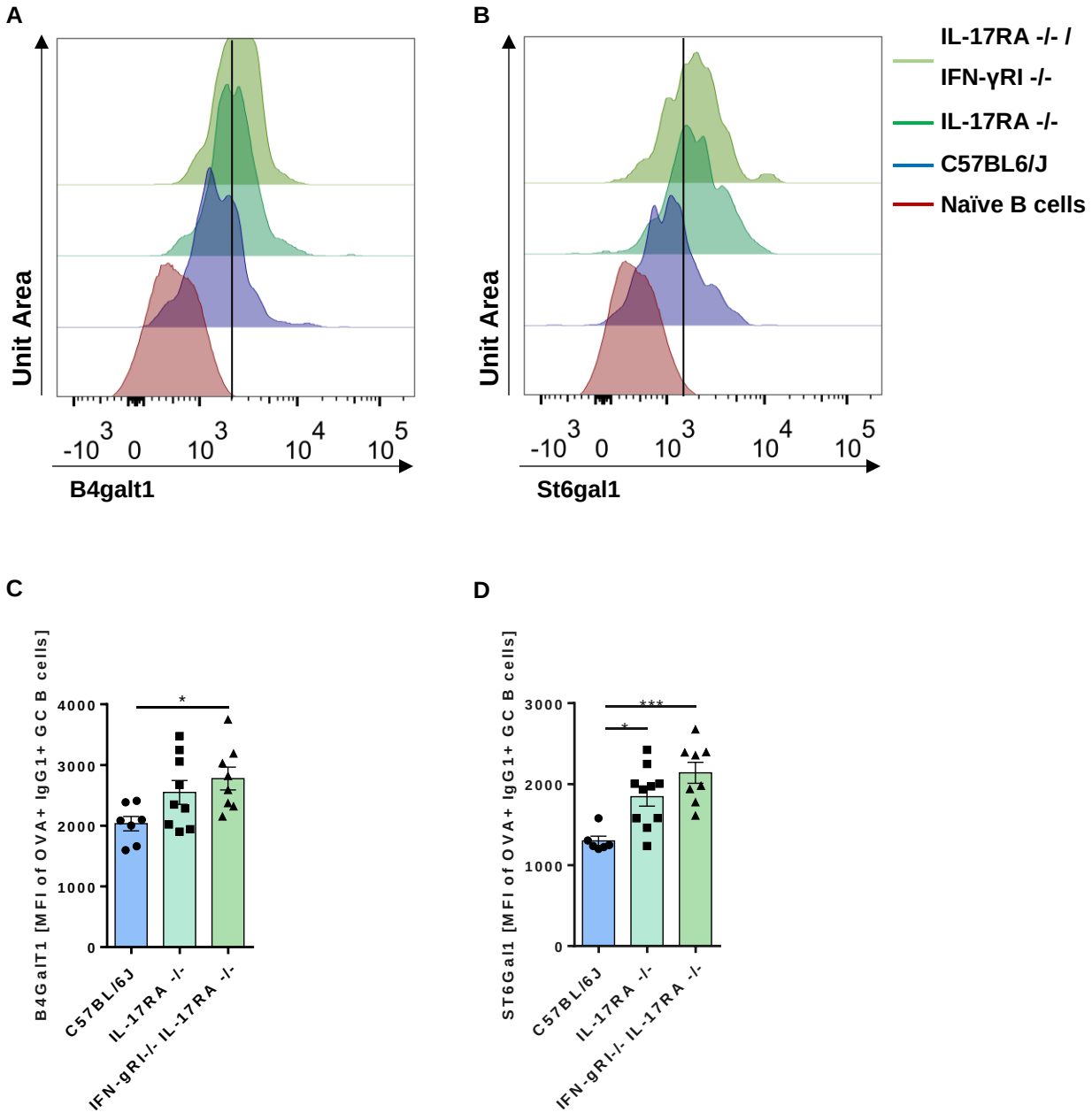

Figure 28: Lack of IFN-γ and IL-17A signal transduction alter expression of B4GalT1 and ST6Gal1 in GC B cells. Wildtype, IL-17RA$^{-/-}$ and IL-17RA$^{-/-}$ **/** IFN-γRI$^{-/-}$ mice were immunized with OVA-eCFA, n=7-9 per group. (A, B) Histogram overlays of B4Galt1 (A) and ST6Gal1 (B) expression in splenic naïve B cells and OVA^{+}IgG1^{+} GC B cells at day 8 after vaccination. (C, D) MFI of B4GalT1 and ST6Gal1 in OVA^{+}IgG1^{+} GC B cells at day 8 after vaccination. Data are representative of 2 independent experiments and data in C and D were pooled of up to 2 independent experiments. One-way ANOVA was used for all comparisons and data are presented as mean +/- SEM, *P < 0.05, **P < 0.01, ***P < 0.001 and ****P<0.0001.

To verify that these changes in B4galt1 and St6gal1 expression are maintained upon differentiation into Ab-secreting PCs, I analyzed enzyme expression in OVA^{+}IgG1^{+} PCs. I found similar expression levels in PCs as in GC B cells, with significantly higher values in double knockout mice compared with wildtype mice (**Figure 29**).

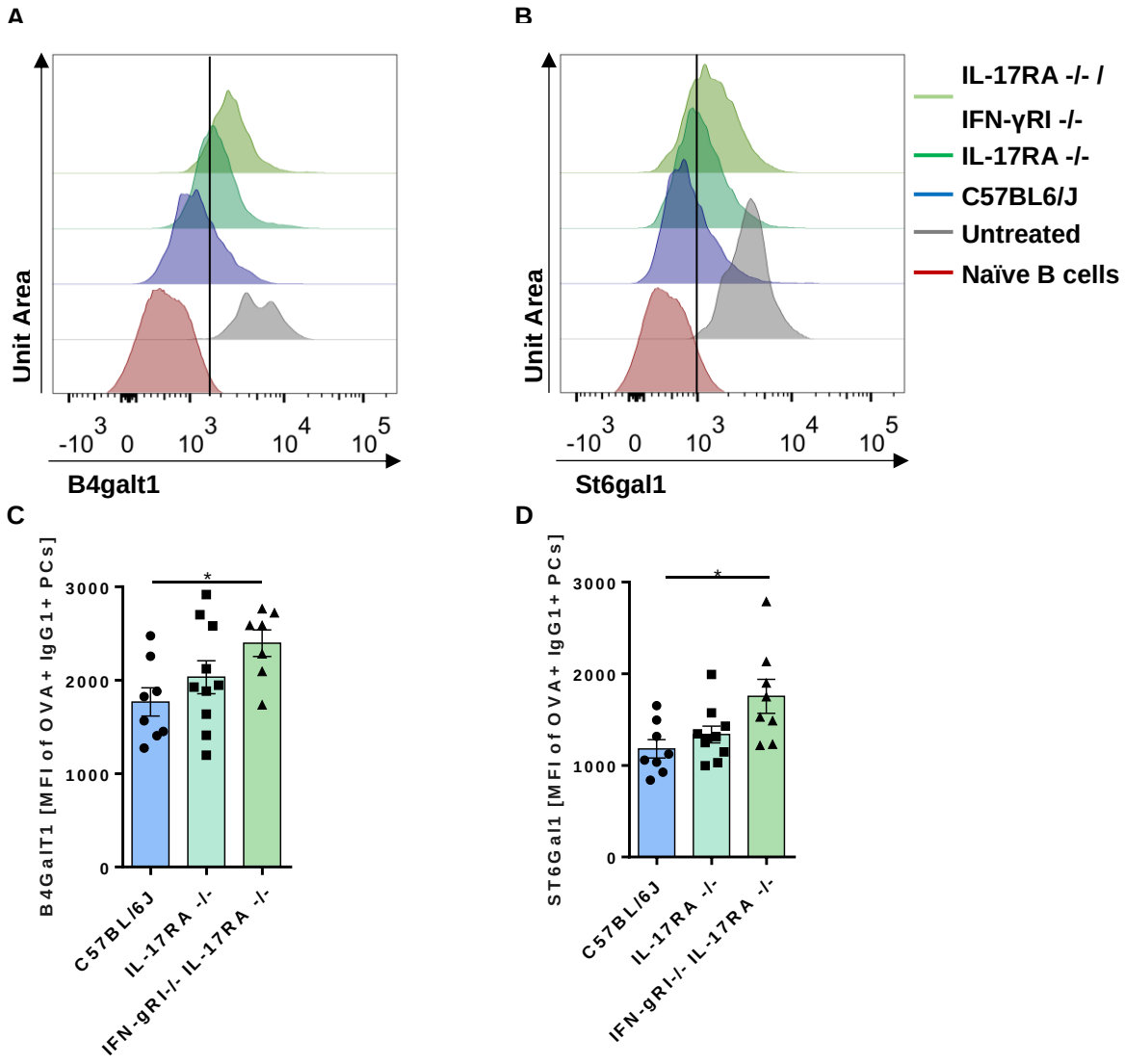

Figure 29: Lack of IFN-γ and IL-17A signal transduction alter expression of B4galt1 and St6gal1 in PCs. Wildtype, IL-17RA$^{-/-}$ and IL-17RA$^{-/-}$ **/** IFN-γRI$^{-/-}$ mice were immunized with OVA-eCFA, n=7-9 per group. (A, B) Histogram overlays of B4Galt1 (A) and St6gal1 (B) expression in splenic naïve B cells and OVA^{+}IgG1^{+} PCs at day 8 after vaccination. (C, D) MFI of B4GalT1 and St6gal1 in OVA^{+}IgG1^{+} PCs at day 8 after vaccination. Data are representative of at least 2 independent experiments and data in C and D were pooled of up to 2 independent experiments. One-way ANOVA was used for all comparisons and data are presented as mean +/- SEM, *P < 0.05, **P < 0.01, ***P < 0.001 and ****P<0.0001.

To assess whether these differences in B4galt1 and St6gal1 expression result in distinct IgG glycosylation patterns, I analyzed the Fc glycosylation of $OVA^{+}IgG^{+}$ Abs in the sera of OVA-eCFA treated mice. In accordance with their high expression of B4galt1 and St6gal1, OVA-eCFA immunization of IL-$17RA^{-/-}$ **/** IFN-$\gamma RI^{-/-}$ double knockout mice led to a substantially lower G0 content, a higher G1 and G2 content, as well as a higher G1S1 and G2S1 content (**Figure 30**).

Since GC B cells express the IL-17RA as well as the IFN-γRI and since I showed that T follicular helper cells are able to produce these cytokines, especially under pro-inflammatory conditions, it is likely that the signal transduction of these cytokines decreases B4galt1 and St6gal1 expression in GC B cells and PCs. Thus, these data suggest that the pro-inflammatory cytokines IL-17A and IFN-γ act on GC B cells during the GC reaction. While T follicular helper cells are a likely source of these cytokines, the GC microenvironment is also modulated by Tfr cells. Therefore, I next evaluated whether this regulatory T cell subset produces substantial amounts of anti-inflammatory cytokines IL-10 and TGF-β and if these cytokines influence the expression of B4galt1 and St6gal1 in GC B cells and PCs.

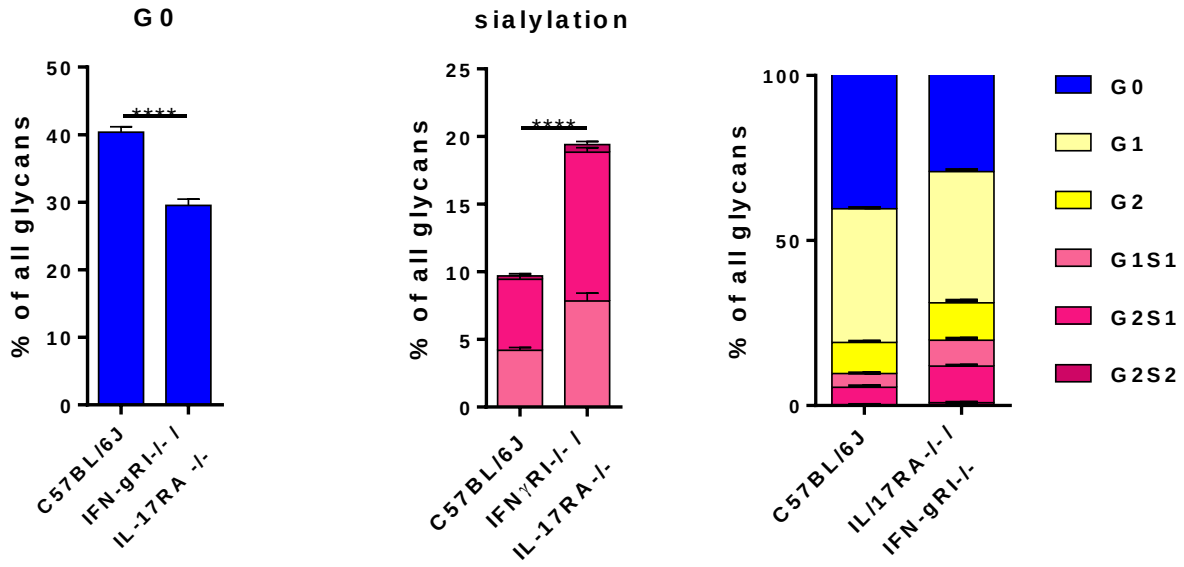

Figure 30: Lack of IFN-γ and IL-17A signal transduction alter IgG Ab glycosylation. C57BL/6J, IL-$17RA^{-/-}$ and IL-$17RA^{-/-}$ **/** IFN-$\gamma RI^{-/-}$ mice were immunized with OVA-eCFA. Comparison of IgG glycoprofiles 14 days upon immunization. One-way ANOVA test was used for all comparisons (added values for sialylation) and data are presented as mean +/- SEM of n=18 for OVA-eCFA immunized C57BL/6J mice and n=5 for OVA-eCFA immunized IL-17RA -/- **/** IFN-γRI-/- mice.

3.7 Tfr cells produce large amounts of the regulatory cytokines IL-10 and TGF-β

It has been proposed in recent studies, that regulatory Tfr cells are capable of effectively suppressing Tfh and GC B cells, thereby controlling the GC response. Although a variety of suppressive mechanisms have been proposed, including secretion of regulatory cytokines, cellular interaction with target cells, mechanical disruption, cytolysis and more, none have been formally verified (Sage & Sharpe 2015).

To assess the regulatory capacity of Tfr cells, I measured their production of suppressive cytokines IL-10 and TFG-β. Therefore, I immunized Vert-X mice with pro-inflammatory OVA-eCFA, low-inflammatory OVA and OVA-LPS. I used the produced eGFP signal as a surrogate marker for IL-10 production and LAP-1 as a surrogate marker for TGF-β production by these cells. Although all tested conditions strongly induced both cytokines in Tfr cells, OVA-eCFA immunization led to a substantially lower production of IL-10 and TGF-β. In all tested conditions, TGF-β was the predominant cytokine, while only a small portion of cells produced IL-10. Up to 35% of Tfr cells were capable of producing TGF-β, whereas only up to 10% were positive for eGFP (**Figure 31**).

Since these data were obtained without additional activation of the cells with PMA, Ionomycin and Brefeldin-A or Monensin, it is likely that an even higher proportion of Tfr cells are able to secrete these suppressive cytokines upon activation.

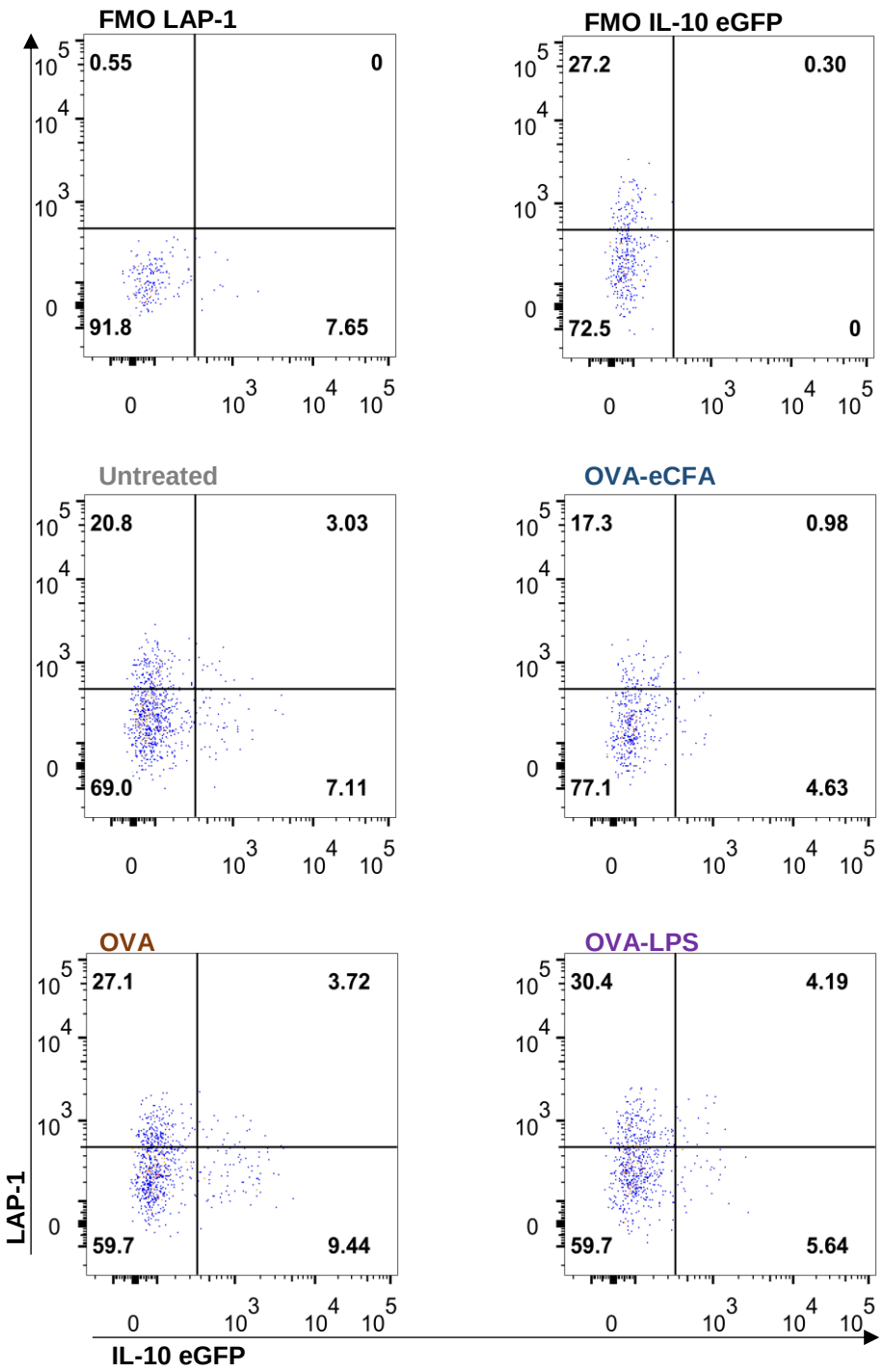

Figure 31: Tfr cells are capable of producing substantial amounts of TGF-β and IL-10. Vert-X mice were immunized *i.p.* with 100 µg OVA emulsified in enriched CFA, 5mg OVA or 100 µg OVA in 30 µg LPS, n=5 per group. Gating strategy to identify TGF-β$^+$ and IL-10$^+$ Tfr cells, gated on CD4$^+$CXCR5$^+$ICOS$^+$FoxP3$^+$ cells at day 8 after vaccination. Shown are representative dot plots for each immunization and FMO controls for LAP-1 and IL-10 gating.

To further assess the suppressive potential of Tfr cells and to be able to put it in context to other cell types, I evaluated and compared TGF-β and IL-10 production in regulatory T cells ($CD4^+FoxP3^+$), Tfh cells ($CD4^+CXCR5^+ICOS^+FoxP3^-$) and Tfr cells ($CD4^+CXCR5^+ICOS^+FoxP3^+$). All tested conditions led to a substantial production of the suppressive cytokine TGF-β with profound differences between the compared cell types. As expected, a substantial percentage of up to ~20% of regulatory T cells were capable of producing this suppressive cytokine, while only a small percentage of ~5% of Tfh cells were TGF-β positive.

Interestingly, a significantly higher percentage of ~30% of Tfr cells were capable of producing this cytokine, compared with both other cell types. Within the Treg cell population, the different immunizations led to different percentages of TGF-β^+ cells. While steady state conditions in untreated mice resulted in ~10% TGF-β^+ Treg cells, pro-inflammatory OVA-eCFA led to a significantly higher percentage of ~14% TGF-β^+ cells. OVA-eCFA immunization seems to result in a comparable percentage of cytokine producing cells, compared to low-inflammatory OVA (~12%) and OVA-LPS (~17%) treatment.

Only a small percentage of $CD4^+CXCR5^+ICOS^+FoxP3^-$ Tfh cells of up to ~7% were capable of producing TGF-β. Here, steady state conditions in untreated mice, low-inflammatory OVA and OVA-LPS immunizations resulted in a similar percentage of TGF-β^+ cells (~7%), while pro-inflammatory OVA-eCFA resulted in a significantly lower percentage (~2.5%) of TGF-β^+ cells. These data are consistent with the role of Tfh cells in the GC reaction, where they facilitate B cell activation, possibly via IFN-γ and IL-17 secretion, as shown before.

Tfr cells seem to be poised for the production of suppressive cytokines. Nearly a third of all cells produced TGF-β in steady state conditions and upon OVA and OVA-LPS treatment, while a significantly lower percentage of ~20% produced it upon OVA-eCFA immunization. Taken into account, that OVA-eCFA treatment also resulted in a significantly lower percentage and also amount of Tfr cells, compared with the other conditions, these data imply that the germinal center reaction upon pro-inflammatory OVA-eCFA is affected by mainly IFN-γ and IL-17 producing Tfh cells. Moreover, upon OVA-eCFA treatment only a small portion of the T follicular helper cells are regulatory Tfr cells, of which only ~20% produce the suppressive cytokine TGF-β, which further shifts the germinal center reaction towards B cell activation. (**Figure 32**)

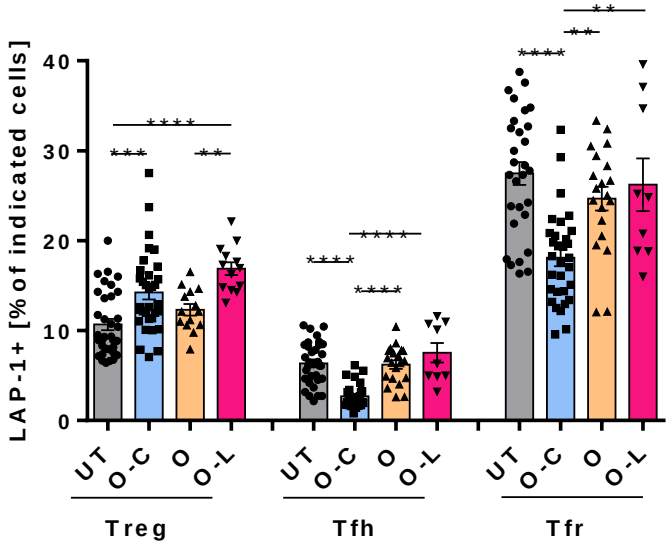

Figure 32: Tfr cells are poised to produce large amounts of suppressive cytokines. Vert-X mice were immunized *i.p.* with 100 µg OVA emulsified in enriched CFA, 5mg OVA or 100 µg OVA in 30 µg LPS. Comparison of the frequency of splenic TGF-β$^+$ Treg, Tfh and Tfr cells at day 8 after vaccination. Data are pooled of up to 5 independent experiments. One-way ANOVA test was used for all comparisons and data are presented as mean +/- SEM of n=29-39 for untreated, n=31-33 for OVA-eCFA, n=14-15 for OVA and n=9-14 for OVA-LPS, *P < 0.05, **P < 0.01, ***P < 0.001 and ****P<0.0001.

The IL-10 production of Treg, Tfh and Tfr cells is comparable to the TGF-β production by the respective cell types. Interestingly, Tfh cells and Treg cells seem to have similar percentages of IL-10$^+$ cells (~3-8%), with a strong tendency for higher IL-10 production in Tfh cells (**Figure 33**). Tfr cells had a significantly higher percentage of IL-10$^+$ cells (~10-15%), compared with Treg and Tfh cells. When gated on CD4$^+$FoxP3$^+$ Treg cells, the different immunizations only led to slight, but nonetheless significant differences. Steady state conditions in untreated mice and low-inflammatory OVA immunization led to approximately 3% IL-10 producing cells, while OVA-eCFA and OVA-LPS immunization resulted in ~5% IL-10 producing cells. Approximately 6-9% of CD4$^+$CXCR5$^+$ICOS$^+$FoxP3$^-$ Tfh cells were positive for IL-10 production upon steady state conditions, low-inflammatory OVA and OVA-LPS, while a significantly lower percentage of ~2% of Tfh cells were producing IL-10 upon OVA-eCFA immunization. Tfr cells, characterized as CD4$^+$CXCR5$^+$ICOS$^+$FoxP3$^+$ cells, showed a significantly higher percentage of IL-10 producing cells, again highlighting their immense suppressive potential. When immunized with OVA-eCFA, approximately 10% of splenic Tfr cells were prone to produce IL-10, while a substantially higher

percentage of cells did so upon OVA and OVA-LPS immunization (~12%). The highest percentage of ~15% of IL-10 producing Tfr cells were observed in steady state conditions in untreated mice. (**Figure 33**)

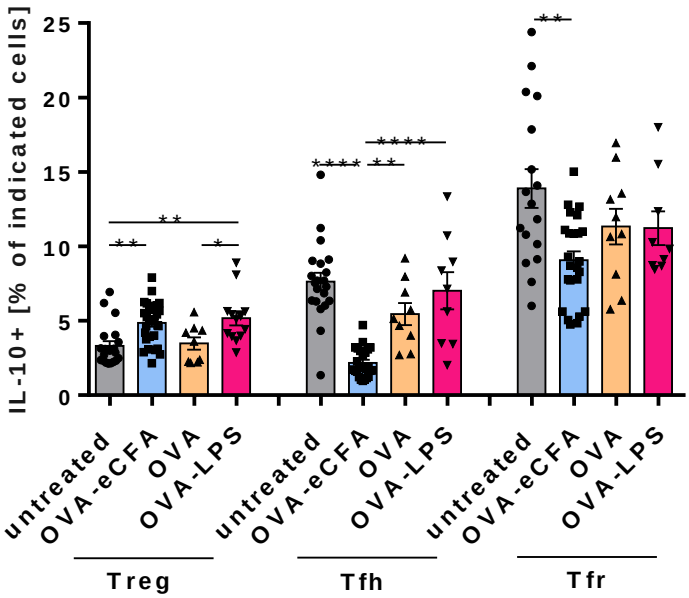

Figure 33: Tfr cells are poised to produce large amounts of suppressive cytokines. Vert-X mice were immunized *i.p.* with 100 µg OVA emulsified in enriched CFA, 5mg OVA or 100 µg OVA in 30 µg LPS. Comparison of the frequency of splenic TGF-β⁺ Treg, Tfh and Tfr cells at day 8 after vaccination. Data are pooled of up to 5 independent experiments. One-way ANOVA test was used for all comparisons and data are presented as mean +/- SEM of n=17-21 for untreated, n=24-29 for OVA-eCFA, n=9-10 for OVA and n=9-13 for OVA-LPS, *P < 0.05, **P < 0.01, ***P < 0.001 and ****P<0.0001.

Taken together, these data demonstrate the extensive regulatory capability of Tfr cells. When compared to Treg cells, Tfr cells showed a substantially higher suppressive proficiency. Even without prior activation of the cells, nearly half of all Tfr cells readily produced TGF-β, IL-10 or both regulatory cytokines.

Surprisingly, Tfr cells even seem to be phenotypically distinct upon different immunizations. While highly pro-inflammatory conditions (OVA-eCFA) led to a low percentage and amount of Tfr cells, which also produced significantly less anti-inflammatory cytokines, low-inflammatory conditions (OVA and OVA-LPS) and also steady state conditions led to a markedly higher Tfr/Tfh ratio and

substantially higher production of both cytokines. This is consistent with the strength of the GC response, characterized by the frequency of GC B cells and PCs and the amount of produced Abs. This suggests, that the Tfr/Tfh ratio, as well as the produced cytokines by both cell types regulate the germinal center response. A variety of studies have shown that Tfr cells don't act solely through cytokine secretion, but also through cell-cell contacts, thereby inhibiting the activation of APCs (Sage, Paterson, et al. 2014; Wing et al. 2014).

3.8 Tfr cells have a high suppressive capacity

To further assess the suppressive potential of Tfr cells, I measured the expression of the co-inhibitory receptor CTLA-4. This receptor is constitutively expressed on Treg cells and Tfr cells and actively upregulated on conventional T cells (Sage, Paterson, et al. 2014; Walker 2013). It shows a high structural homology to CD28, but is able to bind CD80 and CD86 with a much higher affinity and avidity (Walker & Sansom 2015; Walker 2015; Paterson et al. 2015). Therefore, target cells expressing those ligands are less likely to be activated through extended cell-cell contracts. Moreover, several studies showed a regulatory effect of CTLA-4 through transendocytosis of its target ligands CD80 and CD86 expressed on APCs. (Sage & Sharpe 2016; Sage & Sharpe 2015; Sage, Paterson, et al. 2014; Schildberg et al. 2016; Wing et al. 2014).

I found that nearly all Tfr cells express CTLA-4, while only a small portion of Treg and Tfh cells express this receptor. Regulatory T cells of OVA-eCFA immunized mice showed a significantly higher CTLA-4 expression (~50%) than those during steady state conditions and upon OVA and OVA-LPS immunization (~40%). The differences in Tfh cells were slimmer, with a slightly higher CTLA-4 expression upon OVA and OVA-LPS immunization, compared with OVA-eCFA. When gated on Tfr cells, I found no differences in CTLA-4 expression between all tested conditions (**Figure 34**). Taken together, I found few differences in expression level upon different immunizations, indicating that this is a highly conserved receptor, which is not prone to changes in expression levels.

Since the Tfr/Tfh ratio is lower upon pro-inflammatory OVA-eCFA (~0.25) than in low-inflammatory conditions (~0.43), this still points to a more suppressive environment in OVA and OVA-LPS treated mice.

To address whether CTLA-4 can exert cell extrinsic effects (direct interactions between CTLA-4 and its ligands), apart from IL-10 and TGF-β production, to downregulate B7 molecules on APCs

via transendocytosis (transfer of CD80 and CD86 from the surface of APCs into T cells), I assessed whether I can detect CD86 signals within different subsets of T cells.

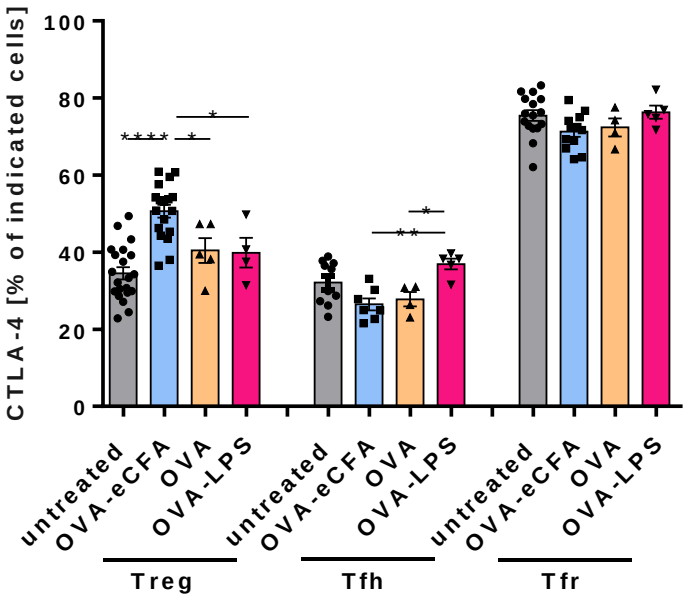

Figure 34: CTLA-4 is constitutively expressed on Treg and Tfr cells. Vert-X mice were immunized *i.p.* with 100 µg OVA emulsified in enriched CFA, 5mg OVA or 100 µg OVA in 30 µg LPS. Comparison of the frequency of CTLA-4 of splenic Treg, Tfh and Tfr cells at day 8 after vaccination. Data are pooled of up to 4 independent experiments. One-way ANOVA test was used for all comparisons and data are presented as mean +/- SEM for n=10-21 for untreated, n=7-18 for OVA-eCFA, n=4-5 for OVA and n=4-5 for OVA-LPS, *P < 0.05, **P < 0.01, ***P < 0.001 and ****P<0.0001.

Most of the CTLA-4 is located in intracellular compartments, rather than on the cell surface. Therefore, I co-stained intracellular CTLA-4 and CD86 in splenic T cells, characterized as $CD4^+CXCR5^-ICOS^-FoxP3^-$, regulatory T cells ($CD4^+$ $FoxP3^+$), Tfh cells ($CD4^+CXCR5^+ICOS^+FoxP3^-$) and Tfr cells ($CD4^+CXCR5^+ICOS^+FoxP3^+$) 8 days upon OVA-eCFA and OVA-LPS immunization. Interestingly, I found substantially higher $CD86^+$/$CTLA\text{-}4^+$ double positive signals in regulatory T cells and Tfr cells compared with T cells and Tfh cells, which is in accordance with their respective CTLA-4 expression (**Figure 35** A, upper right quadrants). Only a small percentage of T cells were positive for both CTLA-4 and CD86 (~3%) upon immunization with either OVA-eCFA and OVA-LPS.

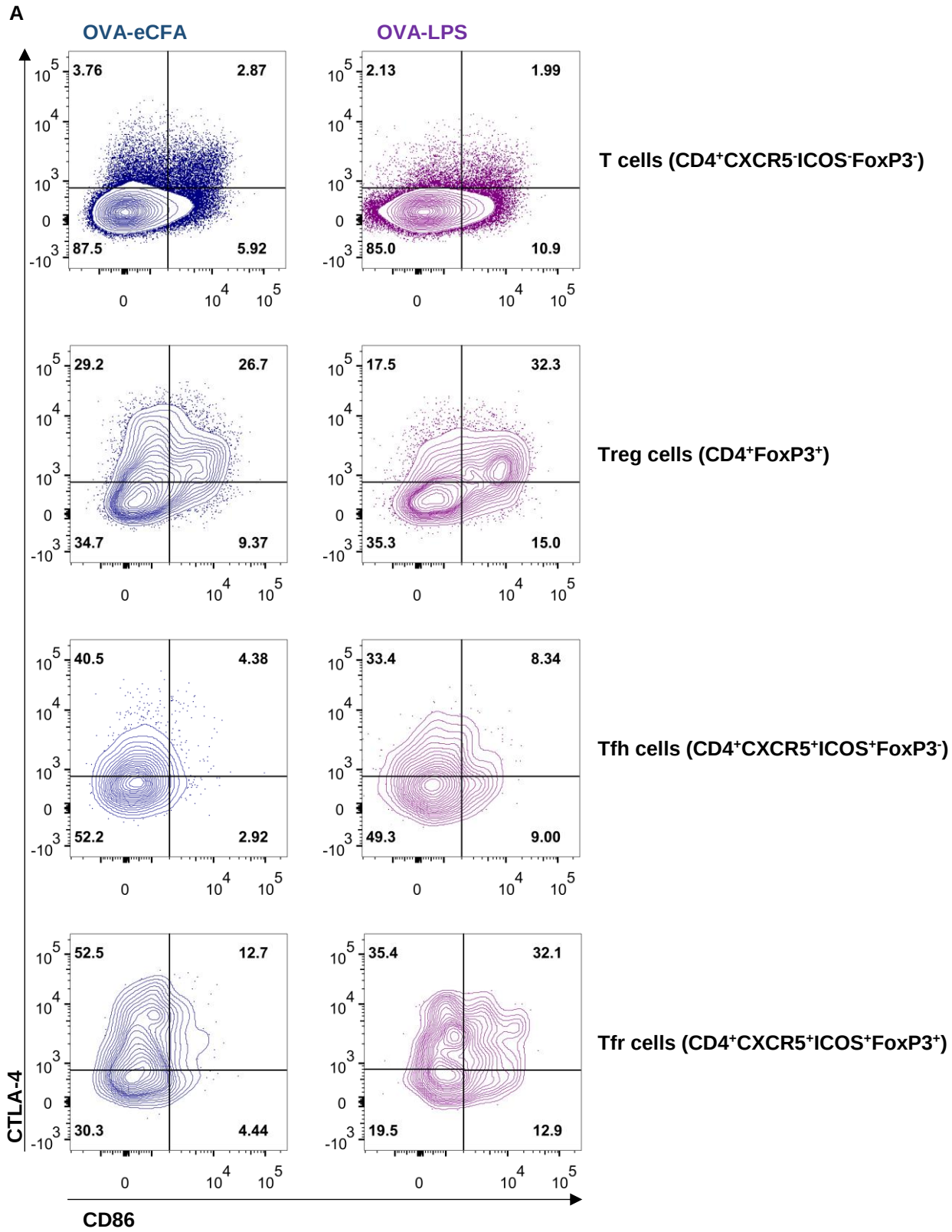
A
OVA-eCFA
OVA-LPS
3.76
2.87
87.5
5.92
2.13
1.99
85.0
10.9
T cells (CD4+CXCR5-ICOS-FoxP3-)
29.2
26.7
34.7
9.37
17.5
32.3
35.3
15.0
Treg cells (CD4+FoxP3+)
40.5
4.38
52.2
2.92
33.4
8.34
49.3
9.00
Tfh cells (CD4+CXCR5+ICOS+FoxP3-)
52.5
12.7
30.3
4.44
35.4
32.1
19.5
12.9
Tfr cells (CD4+CXCR5+ICOS+FoxP3+)
CTLA-4
CD86

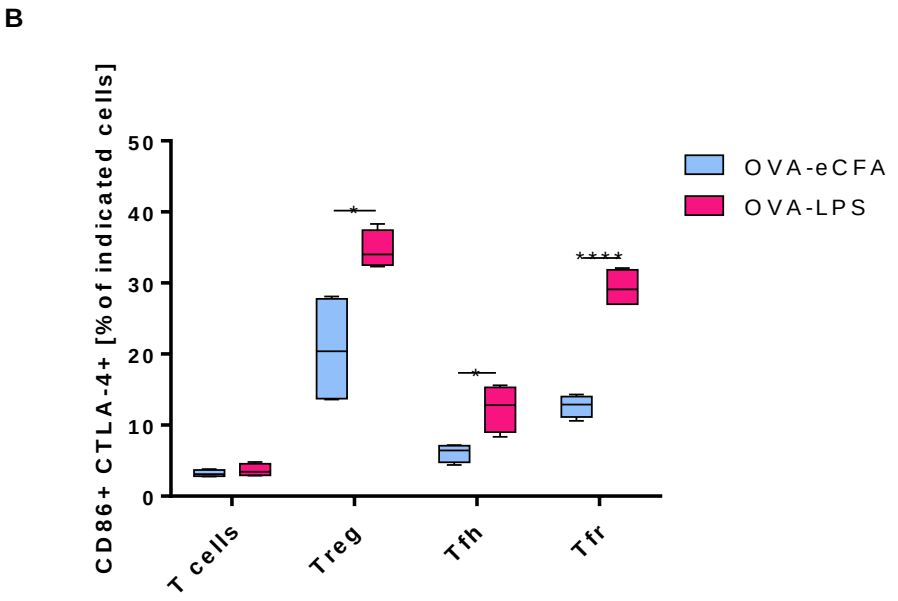

Figure 35: Treg and Tfr cells effectively suppress antigen presenting cells. Vert-X mice were immunized *i.p.* with 100 µg OVA emulsified in enriched CFA, 5mg OVA or 100 µg OVA in 30 µg LPS, n=4 per group. (A) Representative FACS plots for CTLA-4 expression and transendocytosis of CD86 in T-, Treg, Tfh and Tfr cells at day 8 after vaccination. Gates were set according to FMO controls (B) Comparison of the frequency of CTLA-4$^+$CD86$^+$ T-, Treg, Tfh and Tfr cells at day 8 after vaccination. Data are representative of 2 independent experiments. Students t-test was used for all comparisons and data are presented as 10-90 percentile, *P < 0.05, **P < 0.01, ***P < 0.001 and ****P<0.0001.

When gated on regulatory T cells, I found a substantially higher percentage of CTLA-4$^+$/CD86$^+$ cells and also significant differences between OVA-eCFA (~20%) and OVA-LPS (~35%) treated mice. These immunization dependent differences were also apparent in Tfh cells, though the overall percentage of CTLA-4$^+$/CD86$^+$ was much lower (~5% in OVA-eCFA treated mice to ~10% in OVA-LPS treated mice). Tfr cells showed the biggest immunization differences of CTLA-4$^+$/CD86$^+$ cells (~10% in OVA-eCFA treated mice to ~30% in OVA-LPS treated mice), while the overall percentages of double positive cells were comparable with those of Treg cells. These data indicate a cell-extrinsic effect of CTLA-4 expressing cells to downregulate B7 molecules on target APCs. Since most of the CD86$^+$ cells were also CTLA-4$^+$ this indicates a direct regulatory effect involving transendocytosis. Since I didn't find any differences regarding the CD86 expression on

antigen-specific IgG1$^+$GC B cells (data not shown), I hypothesize that CD86 is re-expressed swiftly.

Taken together, these data indicate that T follicular helper cells control the germinal center response through immunization-specific Tfr/Tfh ratios, secretion of stimulatory and inhibitory cytokines and expression of co-inhibitory receptors, through which the Tfr cells interact with GC B cells. Thus, Tfr cells are pivotal for the regulation of the GC response. To address if a transient depletion of Tfr cells during the peak of the GC reaction impacts the antigen-specific Ab response, I next immunized DEREG mice with low-inflammatory OVA. Importantly, it has been shown that a depletion of Treg cells also ensues a depletion of the Tfr compartment (Linterman et al. 2011; Wing et al. 2014)

3.9 Tfr cells are likely to alter IgG Ab glycosylation

To delineate, whether depletion of Treg cells and therewith Tfr cells is sufficient to impact the glycosylation of IgG$^+$ Abs, I transiently depleted the Tfr cell compartment before the immunization with low-inflammatory OVA and at the peak of the GC response at day 6.

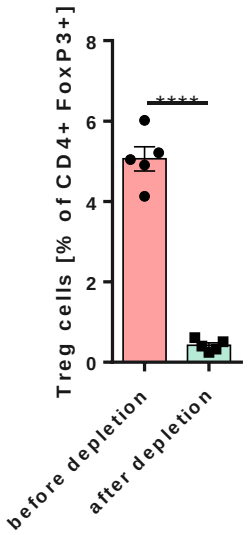

For optimal Tfr depletion, mice were treated with 1µg Diphtheria Toxin (DT) 6h before and 6 days after OVA immunization. To delineate a possible influence of this depletion on the Ab glycosylation, I analyzed intracellular glycosyltransferase expression at day 9 in OVA$^+$IgG1$^+$-GC B cells and -PCs, as well as the IgG glycosylation at day 14. Moreover, 2 days after the initial treatment with Diphtheria Toxin, I assessed whether the Treg/Tfr depletion was successful through analysis of the Treg frequency in the blood of treated mice (**Figure 36**). As expected, nearly all Treg cells were successfully depleted (~5% to ~0.5%).

Figure 36: **Treg cells are effectively depleted through Diphtheria Toxin.** DEREG mice were immunized *i.p.* with 1µg DT followed by immunization with 5mg OVA 6h later. Comparison of the frequency of Treg cells before and 2 days after DT treatment. Data are representative of 2 independent experiments. Students t-test was used for all comparisons and data are presented as mean +/- SEM, n=4-5 per group, *P < 0.05, **P < 0.01, ***P < 0.001 and ****P<0.0001.

Next, I assessed how depletion of Tfr cells affected the GC reaction. Therefore, I measured the frequency of OVA^+IgG1^+ -GC B cells and -PCs. The frequencies of PCs, OVA^+ PCs and OVA^+IgG1^+ PCs were all increased ~3-fold upon Tfr depletion compared with undepleted controls at day after OVA-immunization. Similar to PCs, depletion of Tfr cells also led to a significant 5-fold increase in GC B cells. Moreover, also OVA^+ GC B cells were significantly increased after depletion, as well as OVA^+IgG1^+ GC B cells. This suggests, that GC B cells are poised to undergo CSR towards IgG1 and that this preferential IgG1 commitment is translated to the PC compartment, when suppressive Tfr signals are missing (**Figure 37** A-F).

Altogether, transient depletion of Tfr cells during an ongoing immune reaction against a low-inflammatory antigen results in a substantially enhanced GC reaction, characterized by increased abundances of GC B cells and PCs. To test, if this altered GC response also impacts the long-term Ab response, I quantified the OVA^+IgG^+ Ab production via ELISA. According to the increased GC B cell and PC compartment, transient depletion of Tfr cells also significantly increased the amount of all IgG subclasses compared with undepleted controls. These observed differences in OVA-specific Ab production were most pronounced for the IgG2b and IgG2c subclasses, where a Tfr depletion led to a ~2-fold and ~3-fold increase respectively, while the IgG1 increase was more moderate, compared with undepleted controls. Of note, IgG1 is the predominant subclass upon OVA immunization, as evidenced by prior ELISA and flow cytometric analysis (**Figure 7** C, **Figure 9** B, **Figure 37** C), indicating that the majority of produced Abs are $IgG1^+$ Abs.

These data support the notion, that GC B cells are more prone to undergo CSR, when suppressive Tfr signals are absent (**Figure 38**). This effect is possibly caused by enhanced stimulatory signals by Tfh cells, which would lead to a decreased intra- and interclonal competition amongst GC B cells and a subsequently greater abundance of antigen-specific GC B cells and ultimately PCs.

Taken together, these data suggest, that an efficient, yet transient depletion of Tfr cells alters the GC response towards a TD antigen, resulting in an increased abundance of GC B cells, PCs, as well as serum Abs.

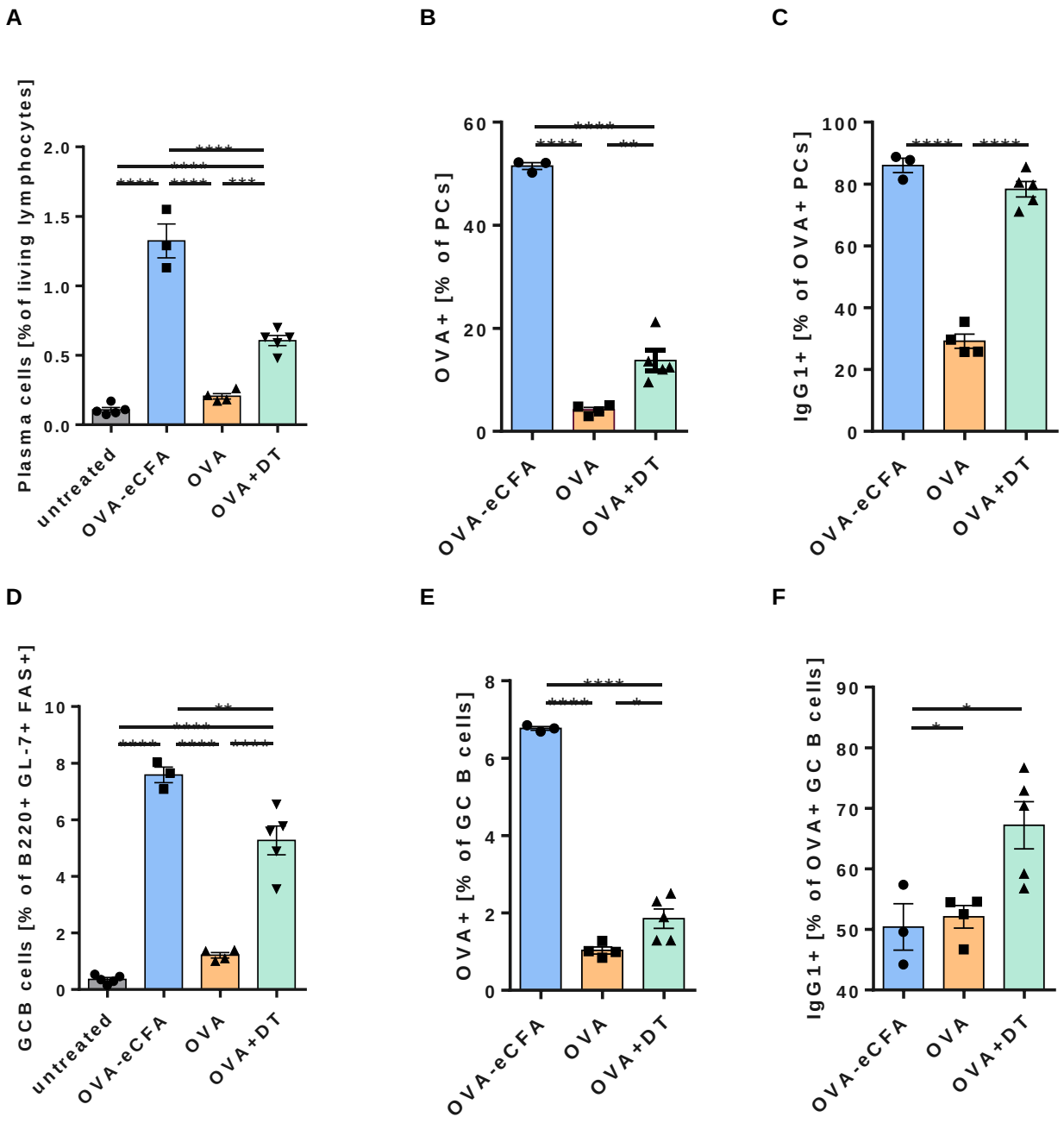

Figure 37: Tfr cells influence the GC response. DEREG mice were immunized *i.p.* with 1µg DT followed by immunization with 5mg OVA 6h later and another DT treatment at day 6, n=3-5 per group. (A-F) Comparison of the frequency of PCs (A), OVA$^+$ PCs (B), OVA$^+$IgG1$^+$ PCs (C), GC B cells (D), OVA$^+$ GC B cells (E) and OVA$^+$IgG1$^+$ GC B cells (F) at day 9 after vaccination. Data are representative of 2 independent experiments. One-way ANOVA was used for all comparisons and data are presented as mean +/- SEM, *P < 0.05, **P < 0.01, ***P < 0.001 and ****P<0.0001.

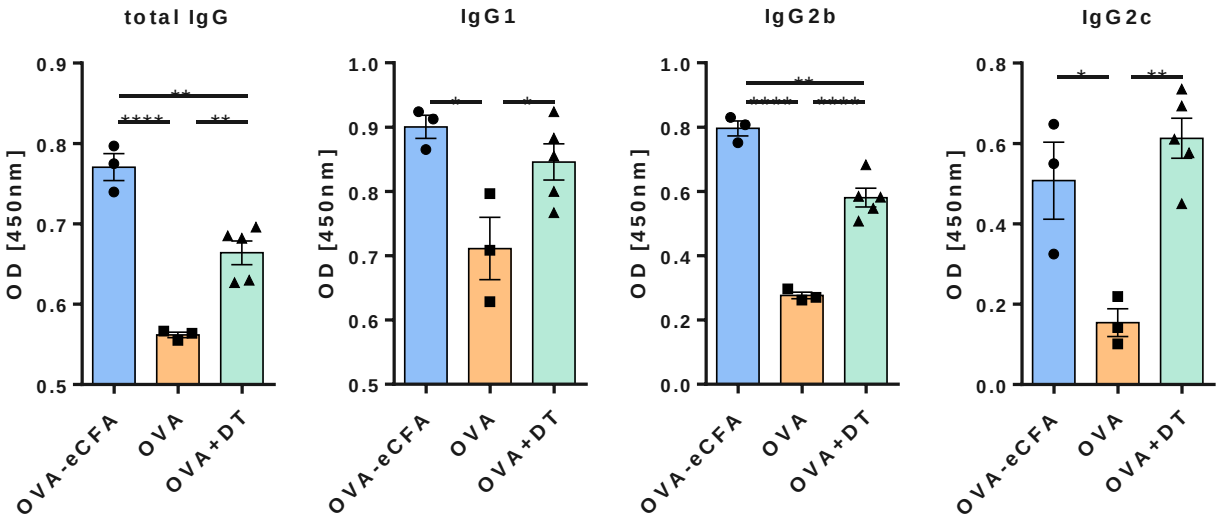

Figure 38: Treg/Tfr depletion results in enhanced IgG Ab production. DEREG mice were immunized *i.p.* with 1µg DT followed by immunization with 5mg OVA 6h later and another DT treatment at day 6, n=3-5 per group, Quantification of OVA-specific serum Ab levels for all IgG subclasses at day 14 after vaccination. Data are representative of 2 independent experiments. One-way ANOVA test was used for all comparisons and data are presented as mean +/- SEM, *P < 0.05, **P < 0.01, ***P < 0.001 and ****P<0.0001.

To assess whether a Tfr depletion also alters the glycosylation of the produced IgG$^+$ Abs, I measured the intracellular glycosyltransferase (B4galt1 and St6gal1) expression and further verified these results via antigen-specific IgG glycoanalysis. Since my data demonstrate, that the IgG glycosylation is regulated within the germinal center and GC B cells, I first determined the glycosyltransferase expression in those cells. OVA$^+$IgG1$^+$ GC B cells of mice, in which Tfr cells have been transiently depleted, expressed significantly less B4galt1 and St6gal1, when compared with undepleted controls. Moreover, the expression levels of both enzymes after Tfr depletion were comparable to those in OVA-eCFA treated mice (**Figure 39** A-D).

To verify whether these expression levels are maintained in Ab-secreting PCs, I also analyzed the enzyme expression in OVA$^+$IgG1$^+$ PCs. As expected, the expression profiles of both enzymes in OVA$^+$IgG1$^+$ PCs matched those in OVA$^+$IgG1$^+$ GC B cells. Also in PCs, B4galt1 and St6gal1 expression of OVA-eCFA treated mice were comparable to those in DT treated mice, in which Tfr cells were transiently depleted and significantly lower than in OVA treated mice and untreated mice (**Figure 40** A-D).

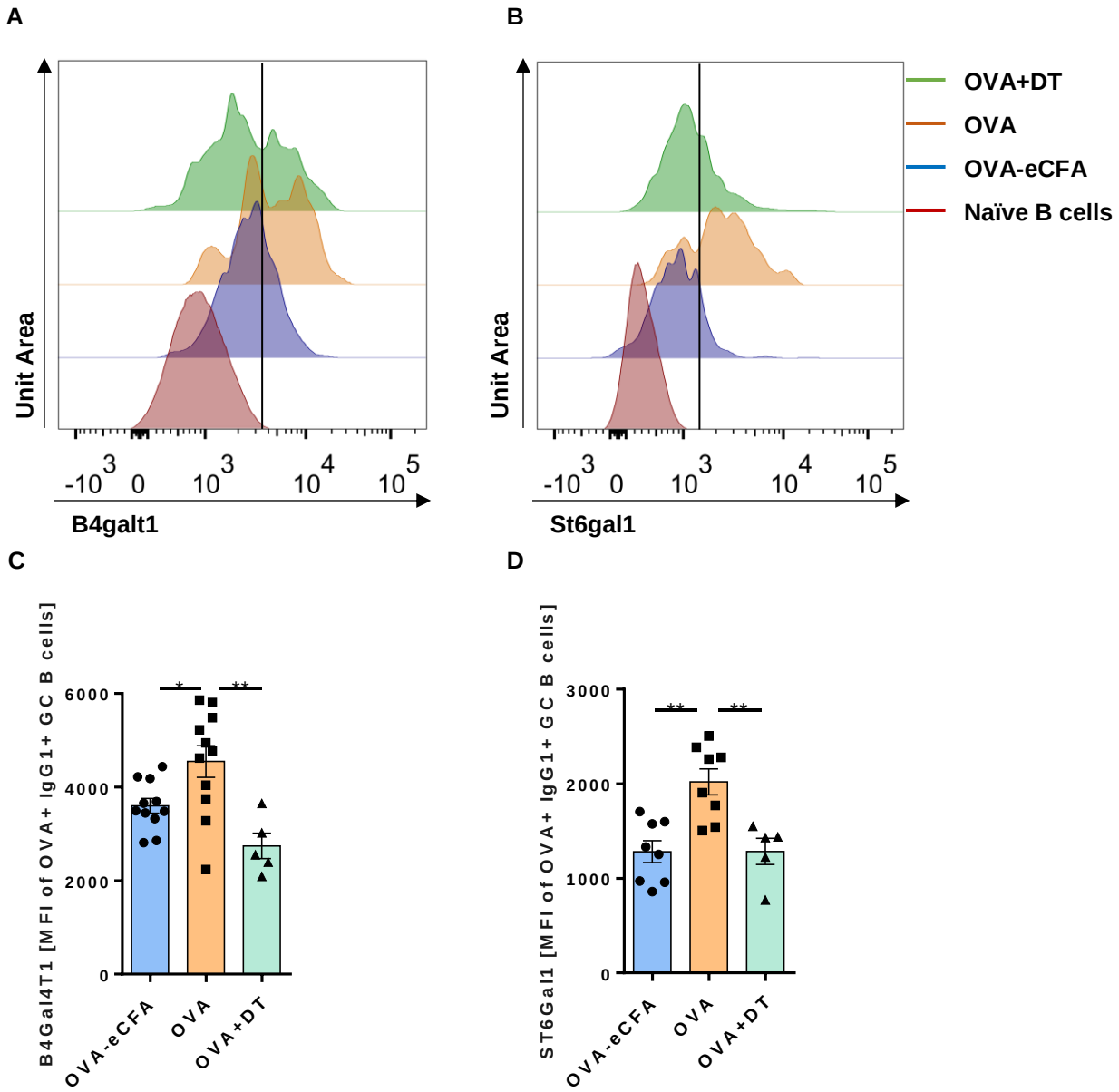

Figure 39: Tfr depletion alters transferase expression in GCs. DEREG mice were immunized *i.p.* with 1µg DT followed by immunization with 5mg OVA 6h later and another DT treatment at day 6. (A, B) Histogram overlays of B4Galt1 (A) and ST6Gal1 (B) expression in splenic naïve B cells and OVA$^+$IgG1$^+$ GC B cells at day 9 after vaccination. MFI of B4GalT1 (C) and ST6Gal1 (D) expression in OVA$^+$IgG1$^+$ GC B cells at day 9 after vaccination. Data were pooled of 2 independent experiments, with n=5-11 per group. One-way ANOVA test was used for all comparisons and data are presented as mean +/- SEM, *P < 0.05, **P < 0.01, ***P < 0.001 and ****P<0.0001.

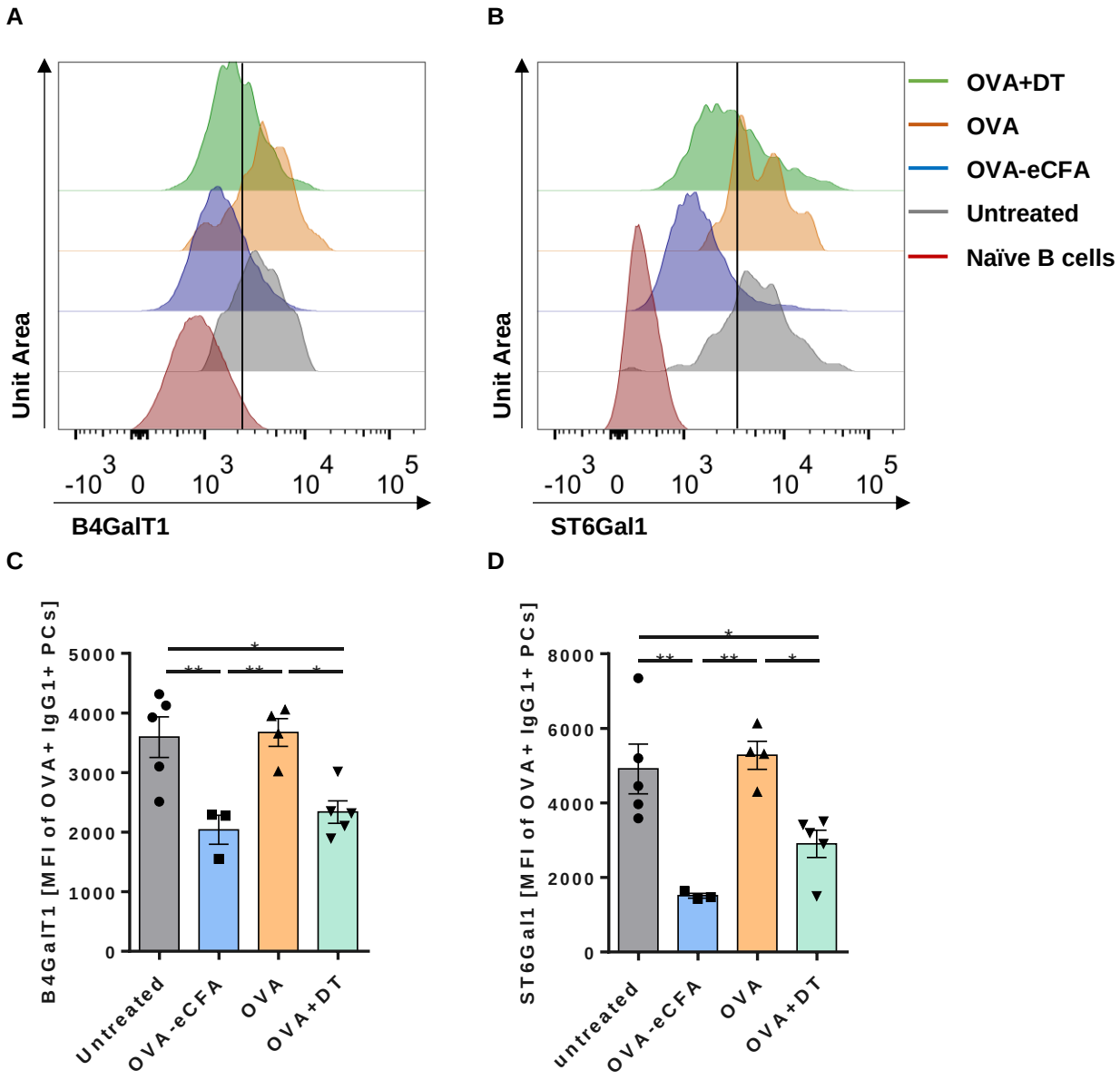

Figure 40: Tfr depletion alters transferase expression in PCs. DEREG mice were immunized *i.p.* with 1µg DT followed by immunization with 5mg OVA 6h later and another DT treatment at day 6, n=3-5 per group. Histogram overlays of B4Galt1 (A) and ST6Gal1 (B) expression in splenic naïve B cells and OVA^+IgG1^+ PCs at day 9 after vaccination. MFI of B4GalT1 (C) and ST6Gal1 (D) expression in OVA^+IgG1^+ PCs at day 9 after vaccination. Data are representative of 2 independent experiments. One-way ANOVA test was used for all comparisons and data are presented as mean +/- SEM, *P < 0.05, **P < 0.01, ***P < 0.001 and ****P<0.0001.

To demonstrate that these different glycosyltransferase expressions in GC B cells and PCs result in differentially glycosylated IgG$^+$ Abs, I analyzed the glycoprofile of OVA$^+$IgG$^+$ Abs in the serum at day 14 upon immunization. Transient depletion of Tfr cells led to a higher abundance of G0 content and to a substantially reduced abundance of terminally sialylated (G1S1, G2S1 and G2S2) IgG$^+$ Abs when compared with undepleted controls (**Figure 41**). This is in accordance with the observed expression levels of B4galt1 and St6gal1 in OVA$^+$IgG1$^+$-GC B cells and PCs.

Thus, Tfr depletion alters the GC reaction not only in quantity, but also in quality, suggesting that GC B cells, which lack suppressive signals by Tfr cells, are phenotypically distinct from GC B cells, that receive regulatory signals from Tfr cells. Taken together, these data indicate that a lack of Tfr cells during a germinal center response towards a low-inflammatory TD antigen culminates in the production of pro-inflammatory aglycosylated IgG Abs.

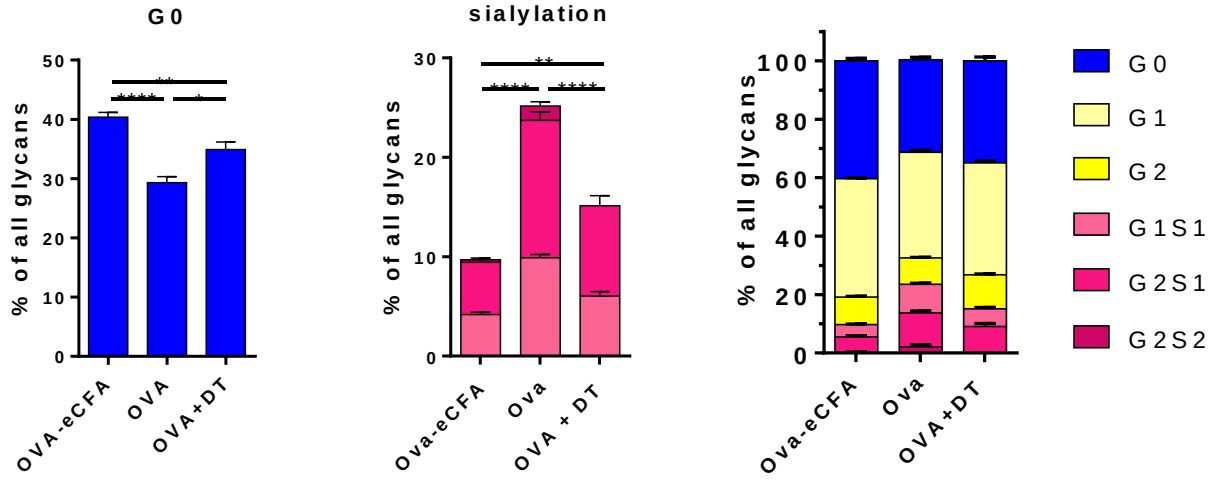

Figure 41: **Treg/Tfr depletion alters IgG glycosylation.** DEREG mice were immunized *i.p.* with 100 µg OVA emulsified in enriched CFA, 5mg OVA or with 1µg DT followed by immunization with 5mg OVA 6h later and another DT treatment at day 6. Comparison of IgG glycoprofiles 14 days upon immunization. One-way ANOVA test was used for all comparisons (added values for sialylation) and data are presented as mean +/- SEM of n=18 for OVA-eCFA, n=12 for OVA and n=5 for OVA+DT

Since a transient depletion of Tfr cells at the peak of the GC reaction skews the ensuing IgG$^+$ Ab response towards pro-inflammatory glycoforms, I next tested whether a profound increase of these cells via IL-2/JES6-1 therapy has an opposing effect, resulting in the production of a higher abundance of anti-inflammatory galactosylated and sialylated Abs.

3.10 IL-2/Jes6-1 complex strongly induces Tfr cells

Recent studies delineated the ability of low-dose IL-2 and IL-2/Jes6-1 complex treatments to severely reduce the disease activity in patients with autoimmunity or inflammatory conditions, by altering the Treg/Tcon ratio in favor of suppressive Treg cells (Klatzmann & Abbas 2015; Castela et al. 2014; Hartemann et al. 2013; Liao et al. 2013). Since I demonstrated that a transient depletion of Tfr cells decreases glycosyltransferase expression and shifts IgG Ab glycosylation towards pro-inflammatory glycoforms, I wanted to test if a massive induction of Tfr cells results in high glycosyltransferase expression and subsequent production of galactosylated and sialylated IgG^+ Abs. Therefore, I used the IL-2/Jes6-1 system to heavily induce regulatory T cells. Since Treg cells are the precursors of Tfr cells, I hypothesized that the abundance of Tfr cells would also profoundly increase. To induce a strong GC response to a specific antigen, I immunized mice with pro-inflammatory OVA-eCFA and additionally induced Treg/Tfr cells in one group with IL-2/Jes6-1 complex (**Figure 42**).

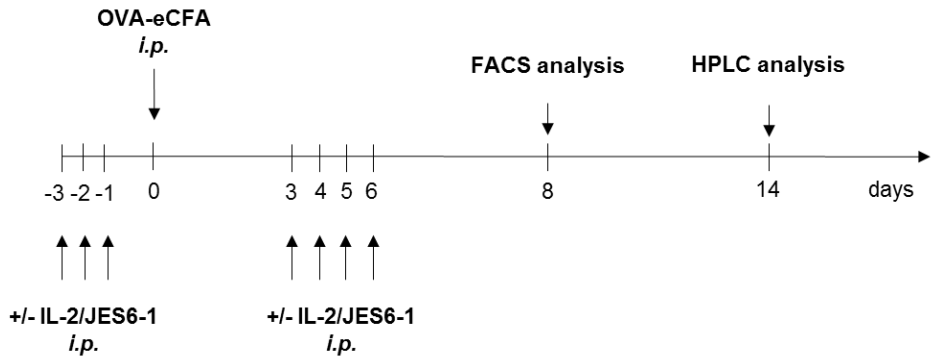

Figure 42: Experimental setup to induce Tfr cells. C57BL/6J or Vert-X mice were immunized i.p. with 100 µg OVA emulsified in enriched CFA at day 0, or 3 times with IL-2/Jes6-1 (day -3, -2 and -1) followed by 100 µg OVA emulsified in enriched CFA (day 0) and 4 additional IL-2/Jes6-1 (day 3-6) immunizations. Splenic cells were analyzed at day 8 via FACS and blood at day 14 for ELISA and HPLC analysis.

First, I assessed the strength of the GC response by measuring the frequency of GC B cells and PCs. The abundance of PCs was profoundly decreased upon IL-2/Jes6-1 treatment compared with OVA-eCFA treated mice, although it didn't reach statistical significance. When gated on OVA^+ PCs, I found a significant ~3-fold decrease, while OVA^+IgG1^+ PCs were decreased ~2-fold. As expected, induction of Tfr cells significantly decreased the strength of the GC response, characterized by a decrease in the frequency of GC B cells from ~5% to ~2%. While OVA^+ GC B cells

were slightly increased compared with OVA-eCFA treated mice, the frequency of class switched OVA^+IgG1^+ GC B cells was decreased nearly 2-fold (**Figure 43** A-F).

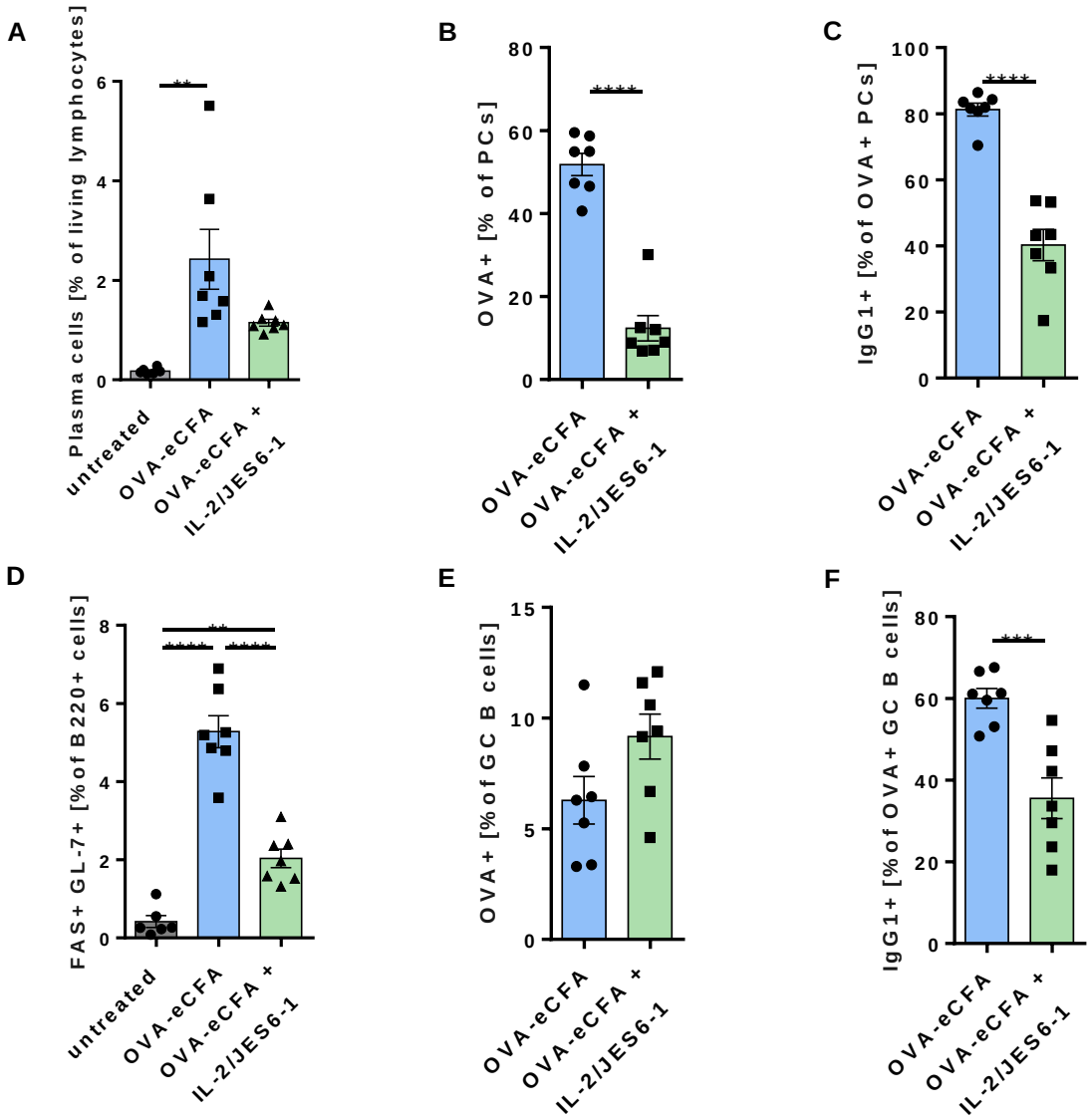

Figure 43: IL-2/Jes6-1 treatment suppresses the germinal center reaction. C57BL/6J or Vert-X mice were immunized i.p. with 100 µg OVA emulsified in enriched CFA at day 0, or 3 times with IL-2/Jes6-1 (day -3, -2 and -1) followed by 100 µg OVA emulsified in enriched CFA (day 0) and 4 additional IL-2/Jes6-1 (day 3-6) immunizations, n=7 per group. Comparison of the frequency of PCs (A), OVA^+ PCs (B), OVA^+IgG1^+ PCs (C), GC B cells (D), OVA^+ GC B cells (E) and OVA^+IgG1^+ GC B cells (F) at day 8 after vaccination. Data are representative of 2 independent experiments. One-way ANOVA or students t-test were used for all comparisons and data are presented as mean +/- SEM, *P < 0.05, **P < 0.01, ***P < 0.001 and ****P<0.0001.

In accordance with decreased frequencies of OVA^+IgG1^+ GC B cells and OVA^+IgG1^+ PCs, I found substantially decreased IgG Ab titers upon IL-2/Jes6-1 treatment, compared with OVA-eCFA treated control mice (**Figure 44**). Importantly, this observed decrease in Ab-titer was likely due to substantially diminished IgG1 production, since all other subclasses only showed mild trends towards lower titers, which didn't reach statistical significance (**Figure 44**).

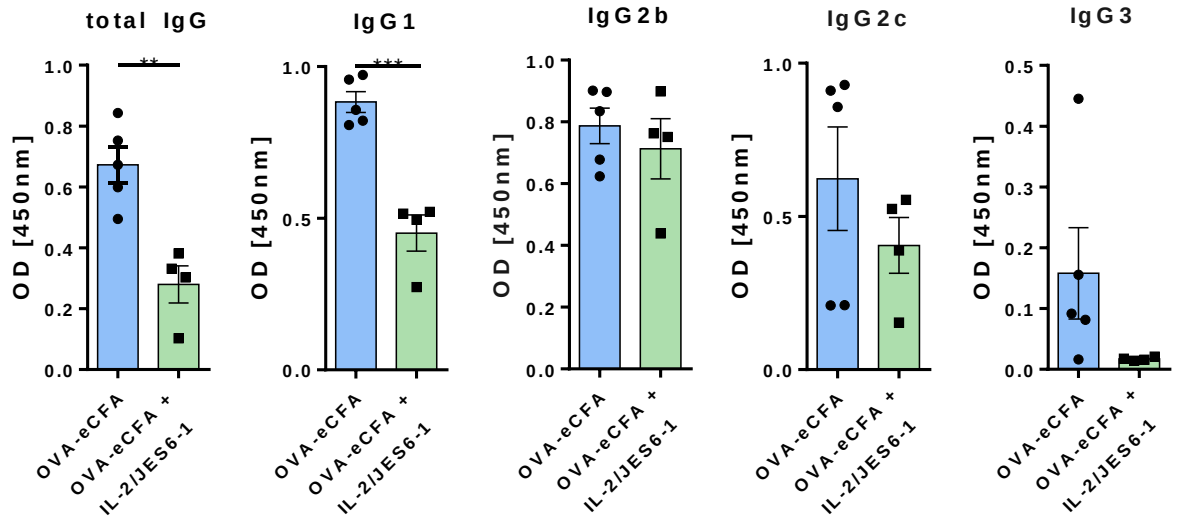

Figure 44: **IL-2/Jes6-1 treatment leads to decreased IgG production.** C57BL/6J or Vert-X mice were immunized i.p. with 100 µg OVA emulsified in enriched CFA at day 0, or 3 times with IL-2/Jes6-1 (day -3, -2 and -1) followed by 100 µg OVA emulsified in enriched CFA (day 0) and 4 additional IL-2/Jes6-1 (day 3-6) immunizations. Quantification of OVA-specific serum Ab levels for all IgG subclasses after indicated immunizations at day 11, n=4-5 per group. Data are representative of 2 independent experiments. One-way ANOVA test was used for all comparisons and data are presented as mean +/- SEM, *P < 0.05, **P < 0.01, ***P < 0.001 and ****P<0.0001.

Hence, Tfr induction substantially suppresses CSR towards IgG^+ subclass Abs, as well as B cell activation. To verify that these observed differences really stem from an increase in Tfr cells, I analyzed the Tfr/Tfh ratio, as well the production of regulatory cytokines and co-inhibitory receptors by Tfr cells. I found that OVA-eCFA+IL-2/Jes6-1 treatment results in a ~3-fold increase in regulatory T cells compared with OVA-eCFA treatment alone (**Figure 45** A). Next, I assessed the frequency of T follicular helper cells. As expected, the frequency of T follicular helper cells was significantly reduced (3.5% to 2.5%) upon IL-2/Jes6-1 treatment (**Figure 45** B). Strikingly, the Tfr/Tfh ratio substantially shifted in favor of Tfr cells, from a ~0.25 ratio upon OVA-eCFA to nearly 0.5 ratio upon OVA-eCFA+IL-2/Jes6-1 treatment (**Figure 45** C).

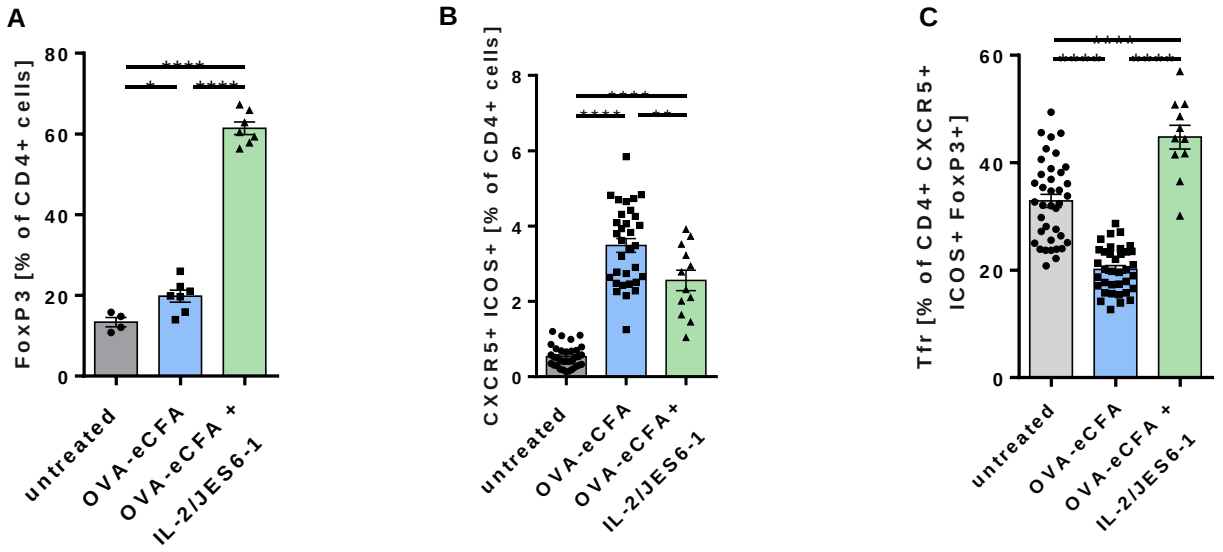

Figure 45: IL-2/Jes6-1 treatment results in substantial increases in Treg and Tfr cells. C57BL/6J or Vert-X mice were immunized i.p. with 100 µg OVA emulsified in enriched CFA at day 0, or 3 times with IL-2/Jes6-1 (day -3, -2 and -1) followed by 100 µg OVA emulsified in enriched CFA (day 0) and 4 additional IL-2/Jes6-1 (day 3-6) immunizations. Comparison of the frequency of Treg cells (A), n=4-7 per group, T follicular helper cells, n=12-29 per group (B) and Tfr cells, n=11-38 per group (C) at day 8 after vaccination. Data are representative of 2 independent experiments. One-way ANOVA test was used for all comparisons and data are presented as mean +/- SEM, *P < 0.05, **P < 0.01, ***P < 0.001 and ****P < 0.0001.

Since IL-2/Jes6-1 treatment massively induces Tfr cells, I next assessed the suppressive potential of these cells. To be able to rate the regulatory potential and to put it in context to other cell types, I evaluated and compared TGF-β and IL-10 production in regulatory T cells ($CD4^+FoxP3^+$), Tfh cells ($CD4^+CXCR5^+ICOS^+FoxP3^-$) and Tfr cells ($CD4^+CXCR5^+ICOS^+FoxP3^+$). I found that IL-2/Jes6-1 treatment substantially increased the percentage of TGF-β producing cells. While the percentage of TGF-β producing Treg cells was increased ~3-fold upon OVA-eCFA+IL-2/Jes6-1 treatment compared with OVA-eCFA treated mice, Tfh cells showed a nearly 9-fold increase in TGF-β producing cells. Although the IL-2/Jes6-1 mediated increase in TGF-β producing Tfr cells was only ~3-fold, approximately 60% of these cells readily produced this anti-inflammatory cytokine without further activation (**Figure 46**). As with TGF-β, IL2/Jes6-1 treatment resulted in significant increases in the percentages of IL-10 producing cells. The frequency of $IL\text{-}10^+$ Treg cells increased ~3-fold, while the frequency of IL-10 producing Tfh cells increased ~7-fold.

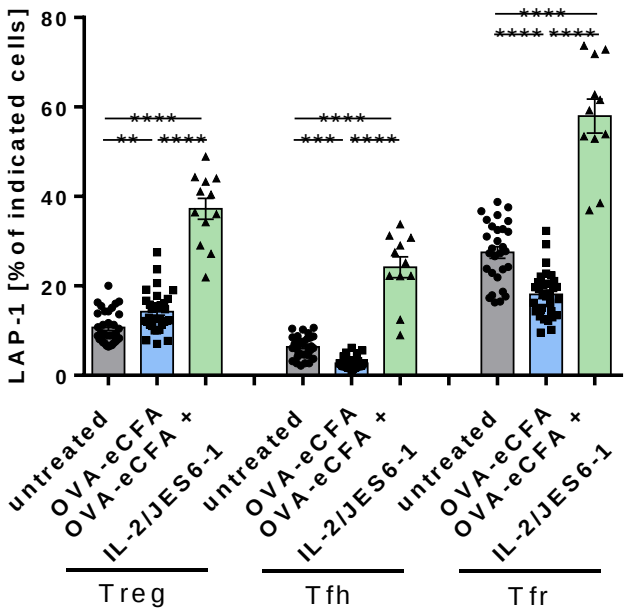

Figure 46: IL-2/Jes6-1 treatment induces TGF-β production. C57BL/6J or Vert-X mice were immunized i.p. with 100 µg OVA emulsified in enriched CFA at day 0, or 3 times with IL-2/Jes6-1 (day -3, -2 and -1) followed by 100 µg OVA emulsified in enriched CFA (day 0) and 4 additional IL-2/Jes6-1 (day 3-6) immunizations. Comparison of the frequency of splenic TGF-β$^+$ Treg, Tfh and Tfr cells at day 8 after vaccination. Data are pooled of up to 5 independent experiments. One-way ANOVA test was used for all comparisons and data are presented as mean +/- SEM for n=29-34 for untreated, n=31-33 for OVA-eCFA and n=11-12 for OVA-eCFA+IL-2/Jes6-1, *P < 0.05, **P < 0.01, ***P < 0.001 and ****P<0.0001.

Interestingly, when gated on Tfr cells, nearly 30% produced IL-10 upon IL-2/Jes6-1 treatment, leading to an accumulation of ~90% of Tfr cells producing either TGF-β, IL-10 or both anti-inflammatory cytokines (**Figure 47**). Taken into account, that the treatment also resulted in a substantial increase of the Tfr cell compartment, this leads to a highly suppressive milieu within the GC. This is in accordance with the decreased abundance of T follicular helper cells, GC B cells, PCs, as well as serum Abs.

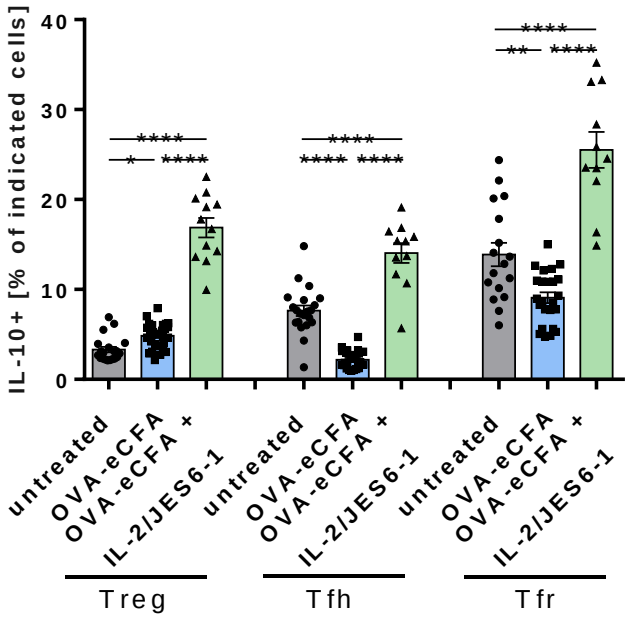

Figure 47: IL-2/Jes6-1 treatment induces IL-10 production. C57BL/6J or Vert-X mice were immunized i.p. with 100 µg OVA emulsified in enhanced CFA at day 0, or 3 times with IL-2/Jes6-1 (day -3, -2 and -1) followed by 100 µg OVA emulsified in enriched CFA (day 0) and 4 additional IL-2/Jes6-1 (day 3-6) immunizations. Comparison of the frequency of splenic IL-10$^+$ Treg, Tfh and Tfr cells at day 8 after vaccination. Data are pooled of up to 5 independent experiments. One-way ANOVA test was used for all comparisons and data are presented as mean +/- SEM for n=17-20 for untreated, n=24-29 for OVA-eCFA and n=11-12 for OVA-eCFA+IL-2/Jes6-1, *P < 0.05, **P < 0.01, ***P < 0.001 and ****P<0.0001.

To substantiate the regulatory potential of Treg and Tfr cells upon IL-2/Jes6-1 treatment, I analyzed the expression of the co-inhibitory receptor CTLA-4 on those cells. I found that it was significantly increased on both cell types, but with an even more substantial expression on Tfr cells (**Figure 48** A-C). Since a very high percentage (~90%) of Tfr cells also readily produced the anti-inflammatory cytokines TGF-β and IL-10, I next assessed whether these cytokine producing cells also expressed higher levels of CTLA-4.

Surprisingly, I found that Tfr cells, which simultaneously produced both cytokines, also expressed the highest levels of CTLA-4 (**Figure 48** D). Taken together, these data demonstrate that IL-2/Jes6-1 treatment results in a substantially altered Tfr/Tfh ratio in favor of Tfr cells, in a profoundly increased production of regulatory cytokines and in increased expression levels of the co-inhibitory receptor CTLA-4.

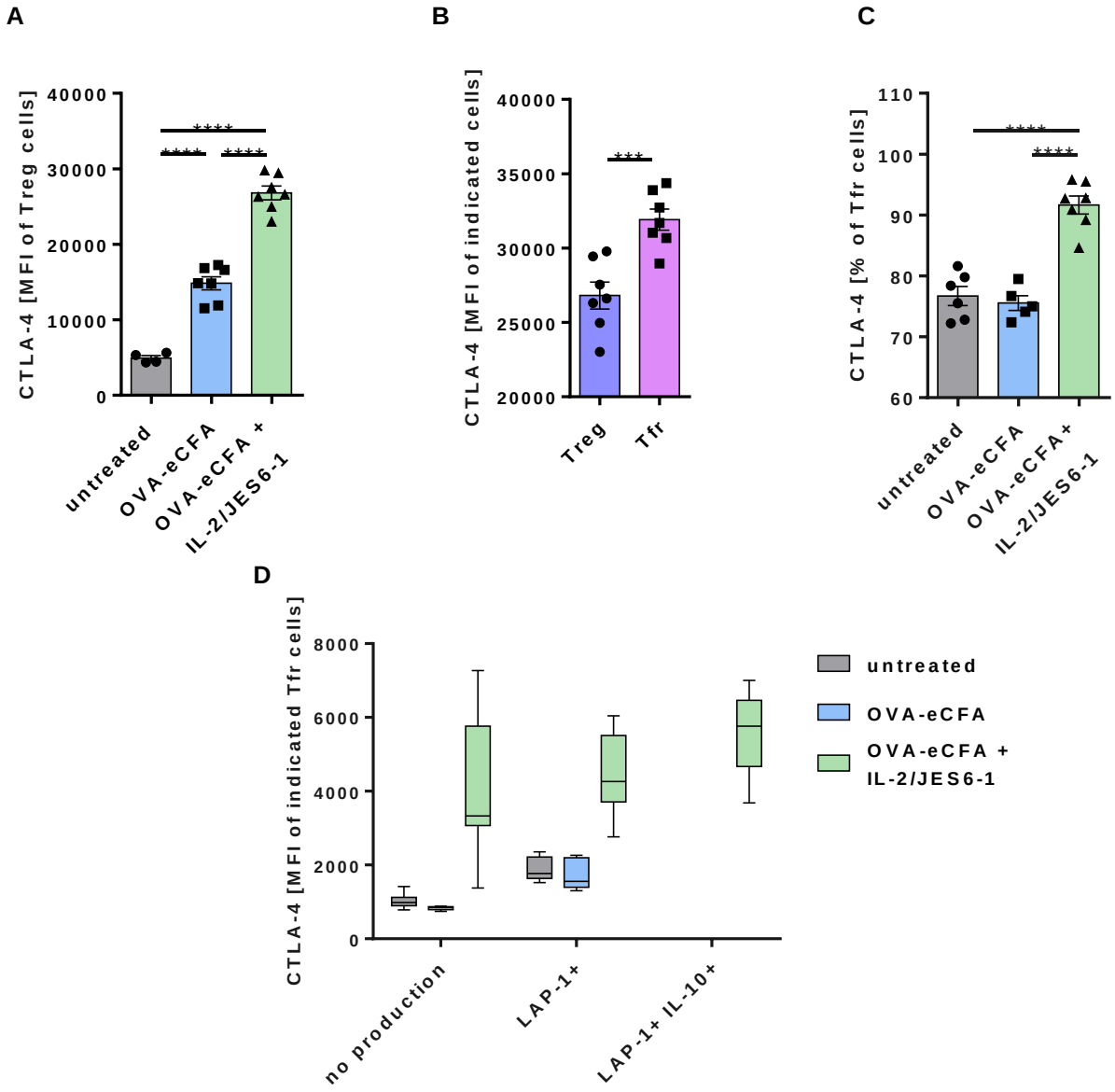

Figure 48: IL-2/Jes6-1 treatment induces the co-inhibitory receptor CTLA-4 on Treg and Tfr cells. C57BL/6J or Vert-X mice were immunized i.p. with 100 µg OVA emulsified in enriched CFA at day 0, or 3 times with IL-2/Jes6-1 (day -3, -2 and -1) followed by 100 µg OVA emulsified in enriched CFA (day 0) and 4 additional IL-2/Jes6-1 (day 3-6) immunizations, n=4-7 per group. Comparison of the frequency of CTLA-4 expression on Treg cells (A), Treg and Tfr cells upon OVA-eCFA+IL-2/Jes6-1 treatment (B), Tfr cells (C) and cytokine producing Tfr cells (D) at day 8 after vaccination. Data are representative of 2 independent experiments. One-way ANOVA test was used for all comparisons and data are presented as mean +/- SEM (A-C) and 10-90 percentile (D), *P < 0.05, **P < 0.01, ***P < 0.001 and ****P<0.0001.

Since a profound increase of Tfr cells resulted in a substantially altered GC reaction, I next investigated whether these cells are able to inhibit activation of GC B cells during an ongoing GC response. Therefore, I measured the expression of the stimulatory receptor CD86 on antigen-specific GC B cells. I found that splenic OVA^+IgG1^+ GC B cells of mice, which were treated with OVA-eCFA+IL-2/Jes6-1 expressed significantly less CD86 compared with OVA-eCFA treated mice (**Figure 49** A, B).

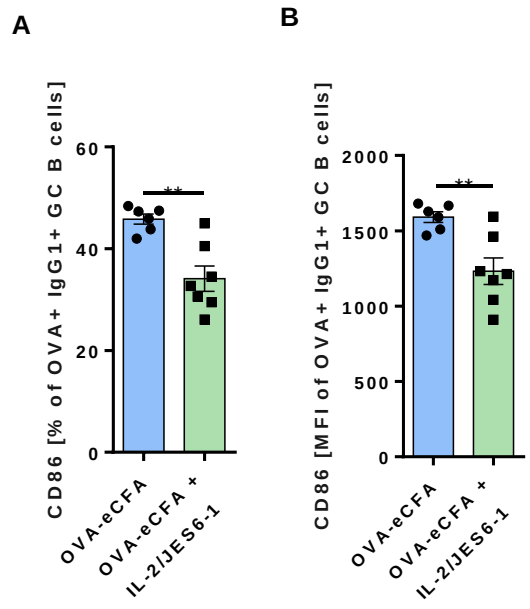

These data indicate that Tfr cells, which are induced upon IL-2/Jes6-1 treatment are highly suppressive and are able to successfully inhibit the activation of antigen-specific GC B cells. Since I showed that these Tfr cells heavily express CTLA-4, the reduction of CD86 is possibly mediated via transendocytosis, as demonstrated before (**Figure 35**).

Figure 49: **IL-2/Jes6-1 treatment results in reduced CD86 expression on GC B cells.** C57BL/6J or Vert-X mice were immunized i.p. with 100 µg OVA emulsified in enriched CFA at day 0, or 3 times with IL-2/Jes6-1 (day -3, -2 and -1) followed by 100 µg OVA emulsified in enriched CFA (day 0) and 4 additional IL-2/Jes6-1 (day 3-6) immunization, n=6-7 per group. Comparison of the frequency (A) and MFI (B) of CD86 expression on OVA^+IgG1^+ GC B Cells at day 8 after vaccination. Data are representative of 2 independent experiments. Students t-test was used for all comparisons and data are presented as mean +/- SEM, *P < 0.05, **P < 0.01, ***P < 0.001 and ****P<0.0001.

Taken together, these data demonstrate that IL-2/Jes6-1 treatment substantially influences the GC reaction by inhibiting GC B cells and PCs, decreasing CSR, modulating the Tfr/Tfh ratio, increasing anti-inflammatory cytokines secretion and suppressing B cell activation. To further assess whether these changes also affect Ab glycosylation, I analyzed the glycoprofile of OVA^+IgG^+

Abs 11 days upon immunization. I found that IL-2/Jes6-1 treatment markedly reduced the abundance of the G0 content, while galactosylation (G1) and sialylation (G1S1 and G2S1) were substantially enhanced (**Figure 50**).

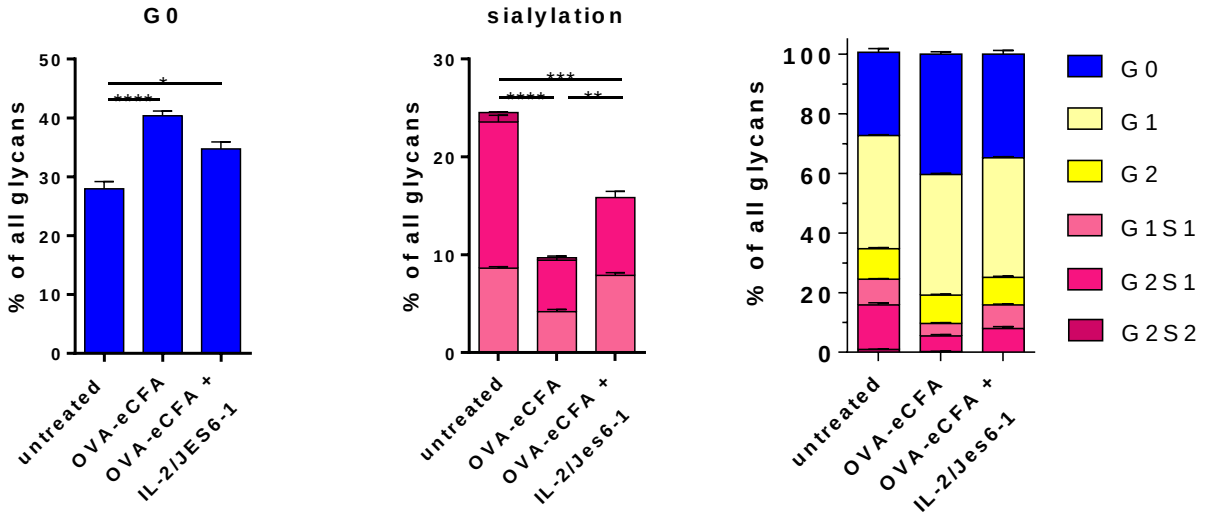

Figure 50: IL-2/Jes6-1 treatment alters IgG Ab glycosylation. C57BL/6J or Vert-X mice were immunized i.p. with 100 µg OVA emulsified in enriched CFA at day 0, or 3 times with IL-2/Jes6-1 (day -3, -2 and -1) followed by 100 µg OVA emulsified in enriched CFA (d0) and 4 additional IL-2/Jes6-1 (day 3-6) immunizations. Comparison of IgG glycoprofiles 11 days upon immunization. Data are presented as mean +/- SEM of n=4 for untreated, n=5 for OVA-eCFA and n=4 for OVA-eCFA+IL-2/Jes6-1.

These data indicate that IL-2/Jes6-1 treatment alters the glycosylation of newly formed antigen-specific antibodies towards more heavily galactosylated and sialylated glycoforms. Since a depletion of Tfr cells led to an opposite effect, it is plausible that IgG glycosylation is dependent on the abundance of Tfh and Tfr cells, as well as its secreted cytokines and expression of co-inhibitory receptors. The fact that antigen-specific GC B cells express specific and differential levels of the glycosyltransferases B4galt1 and St6gal1 further supports the notion, that IgG glycosylation is adjusted during the GC reaction. Since T follicular helper cells directly interact with GC B cells, it is likely that changes in glycosyltransferase expression and therewith in Ab glycosylation are mediated by Tfh and Tfr cells.

To summarize, the GC reaction is characterized by a complex interaction of GC B cells and T follicular helper cells. This interplay is pivotal for the induction of an effective humoral immune response towards TD antigens. My data indicate, that the glycosylation of antigen-specific IgG$^+$

Abs is being regulated during this process and that it is dependent on the expression of the glycosyltransferases B4GalT and St6gal1. Furthermore, conjunction of the pro-inflammatory eCFA with a TD-antigen resulted in a high abundance of agalactosylated and asialylated IgG^+ Abs, which act in a pro-inflammatory manner, whereas low-inflammatory OVA alone or in conjunction with LPS primarily induced anti-inflammatory galactosylated and sialylated IgG Abs. These distinct glycoprofiles were even maintained upon antigen re-exposure, although newly formed PCs as well as LLPCs contributed to the ensuing IgG^+ Ab response. Moreover, T follicular helper cells, which facilitate B cell help during the GC reaction were shown to produce profound amounts of the pro-inflammatory cytokines IL-17A and IFN-γ, which likely act directly on GC B cells. Accordingly, mice which lacked the receptors for both cytokines showed a significantly altered glycoprofile in favor of galactosylated and sialylated IgG^+ Abs. Besides stimulatory Tfh cells, also regulatory Tfr cells control the GC response. I could delineate the substantial suppressive capacity of these cells, which produce large amounts of the anti-inflammatory cytokines TGF-β and IL-10. Furthermore, I could demonstrate a direct interaction of these cells with GC B cells, which were inhibited by CTLA-4 mediated transendocytosis of the stimulatory molecule CD86. Moreover, transient depletion of Tfr cells during low-inflammatory conditions resulted in a markedly altered GC reaction, characterized by high abundances of GC B cells, PCs, as well as pro-inflammatory IgG^+ Abs. Accordingly, a massive induction of suppressive Tfr cells during pro-inflammatory conditions had an opposing effect and resulted in lower abundances of GC B cells, PCs and strikingly, a higher abundance of galactosylated and sialylated IgG^+ Abs.

4 Discussion

Although IgG glycosylation has been implicated in modulating key aspects of the immune response like CDC, vaccine efficacy or auto-Ab production in autoimmunity (Quast et al. 2015; Wang et al. 2015; Schwab et al. 2015), the precise mechanism, by which the glycosylation process is being regulated has remained elusive. Here, I propose a model, in which IgG Ab glycosylation is actively controlled by expression levels of B4galt1 and St6gal1 in GC B cells and is being influenced by the abundance of Tfh and Tfr cells, their ratio towards one another, as well as their secreted cytokines (**Figure 51**). I find that IL-2/Jes6-1 immunization induces highly suppressive Treg and Tfr cells, which are characterized by substantial production of anti-inflammatory cytokines IL-10 and TGF-β. Moreover, I also provide evidence that CTLA-4 on these highly suppressive Tfr cells potently inhibits CD28 mediated Tfh cell activation via downregulation of CD86 on antigen-specific GC B cells.

I demonstrated that different co-stimuli in conjunction with a TD antigen alter the ensuing GC reaction. Pro-inflammatory co-stimuli induced GCs, characterized by a high abundance of (antigen-specific IgG1$^+$) GC B cells and PCs, which expressed low levels of the glycosyltransferases B4galt1 and St6gal1, whereas low-inflammatory co-stimuli induced (antigen-specific IgG1$^+$) GC B cells and PCs with high expression levels of those enzymes. This was also reflected in the glycosylation pattern of OVA$^+$IgG$^+$ Abs in the serum, implying a correlation between enzyme expression and IgG Ab glycosylation. This is in accordance with recent publications, which have delineated the dependence of B4galt1 for galactosylation and St6gal1 for sialylation, although they have failed to assess the involved cell types and further regulating factors (Anthony et al. 2012; Shade & Anthony 2013; Onitsuka et al. 2012; Warnock et al. 2005; Wang et al. 2015). Of note, recent studies have implied the necessity of St6gal1 expression in B cells and PCs respectively for ensuing IgG$^+$ Ab sialylation (Ohmi et al. 2016; Oefner et al. 2012), which further supports my results. Moreover, it has been demonstrated that agalactosylated and especially asialylated IgG$^+$ Abs exert pro-inflammatory properties, while galactosylated and sialylated IgG$^+$ Abs act in an anti-inflammatory manner (Ohmi et al. 2016; Quast et al. 2015; Wang et al. 2015; Washburn et al. 2015; Ackerman et al. 2013; Ercan et al. 2010)

I obtained similar results upon antigen re-exposure, where newly formed OVA$^+$IgG1$^+$ PCs showed distinct glycosyltransferase expression and OVA$^+$IgG$^+$ serum Abs specific glycosylation patterns, dependent on initial immunization. Further analysis demonstrated that the observed OVA$^+$IgG$^+$

Ab Fc glycosylation stem from a mixture of produced Abs by newly formed splenic PCs and LLPCs in the BM. The Abs, secreted by these cells could have further influenced the GC reaction, thus altering B cell clone selection in favor of higher affinity BCRs, due to increased interclonal competition for the cognate antigen, as has been suggested in various studies (Zhang et al. 2013; Wang et al. 2015). This provides a possible and plausible mechanism for a rapid and effective B cell clone selection and subsequent production of high affinity class switched Abs, especially upon antigen re-exposure.

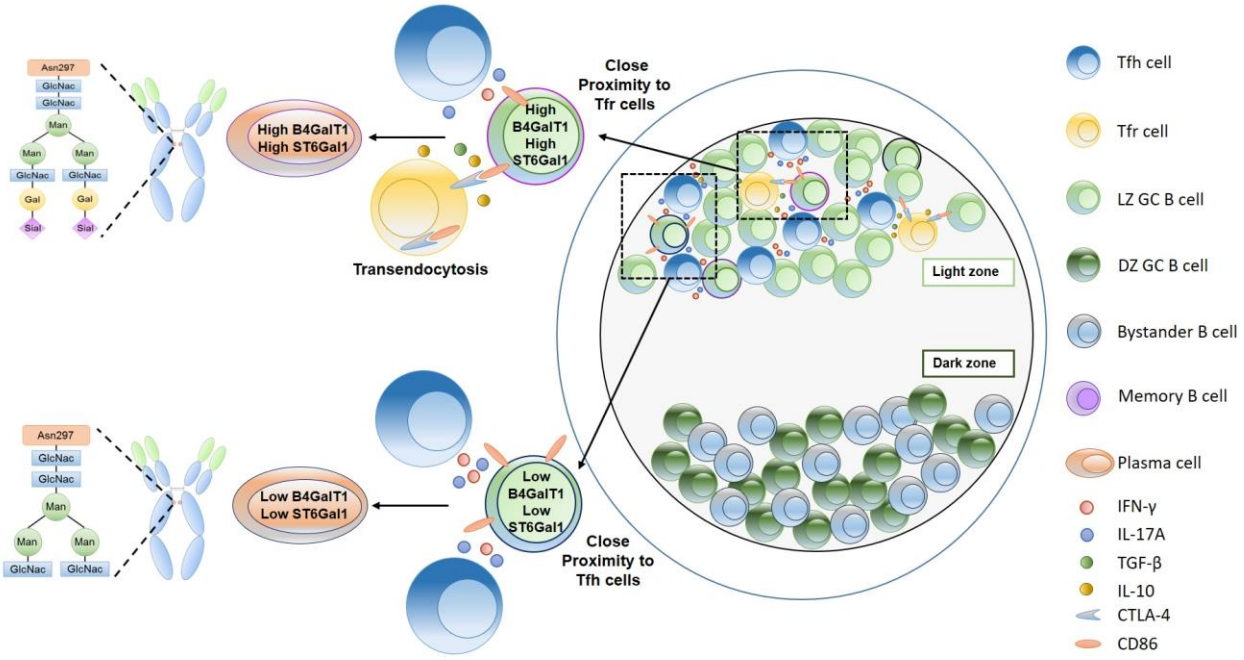

Figure 51: Schematic of the GC reaction in response to a TD antigen, resulting in the production of high abundances of either pro- or anti-inflammatory IgG⁺ Abs. A GC forms in response to a TD antigen but differs dependent on the co-stimulus. Pro-inflammatory co-stimuli result in a high abundance of GC B cells, Tfh cells and ultimately PCs. This high abundance of Tfh cells promotes positive GC B cell selection through cell-cell contacts and production of pro-inflammatory cytokines IFN-γ and IL-17RA. GC B cells, which develop in this microenvironment are defined by low expression levels of B4galt1, as well as St6gal1 (dark blue circled), which is transferred to the PC compartment and results in a high abundance of pro-inflammatory (agalactosylated and asialylated IgG⁺ Abs). Low-inflammatory co-stimuli on the other hand result in a lower abundance of GC B cells, probably due to an enhanced Tfr/Tfh ratio. These Tfr cells highly express the co-inhibitory receptor CTLA-4, as well as substantial amounts of the anti-inflammatory cytokines TGF-β and IL-10. GC B cells, which develop under these conditions are characterized by high expression levels of B4galt1 and St6gal1 (magenta circled), which are again translated into the PC compartment leading to higher abundances of anti-inflammatory (galactosylated and sialylated) IgG⁺ Abs.

The immunization dependent glycoprofiles of OVA^+IgG^+ Abs at day 33 (5 days after antigen re-exposure) were comparable to those of day 14 after vaccination, implying that the glycosyltransferase expression in newly formed splenic GCs and PCs, as well as LLPCs in the BM also remained stable.

This contrasts with the observed glycoprofiles at day 8, which were characterized by higher abundances of sialylated Abs (**Figure 21** A-C). While it is unlikely, that extrafollicular OVA^+IgG1^+ plasma blasts substantially contributed to the glycoprofiles at day 14 and day 33, it is possible that they markedly altered the Ab glycosylation patterns at day 8 after immunization and provide reasonable explanation for the increased levels of especially sialylated IgG^+ Abs upon OVA-eCFA treatment. In support of this notion, recent studies have indicated a similar mechanism upon influenza vaccination, where early formed plasma blasts were implied to profoundly contribute to the production of early, sialylated IgG^+ Abs (Wang et al. 2015). Thus, it seems like IgG^+ Ab glycosylation is maintained over long periods of time, which should be considered in vaccination studies, which up until now mostly focus on Ab levels, rather than Ab glycosylation.

Apart from substantial differences in the GC B cell and PC compartments, I also observed an altered T follicular helper cell response dependent on the immunization (**Figure 23**, **Figure 24**, **Figure 25**). Not only the abundance of these cells, but also their produced cytokines were immunization dependent. While it has been demonstrated that Tfh cells are able to produce a variety of cytokines (Weinstein et al. 2016; Qi 2016; Sage, Alvarez, et al. 2014; Carola G. Vinuesa et al. 2016), I observed profound vaccination-dependent differences in IFN-γ and IL-17A production. Interestingly, both of these cytokines or rather GC B cell signal transduction of the respective receptors IFN-γRI and IL-17RA have been implicated to potentially result in autoimmunity (Domeier et al. 2016; Jackson et al. 2016; Hsu et al. 2008), but are also pivotal for CSR (Weinstein et al. 2016; Reinhardt et al. 2009). Importantly, further experiments with $IL\text{-}17RA^{-/-}$/$IFN\text{-}\gamma RI^{-/-}$ double knockout mice demonstrated the dependency of signal transduction through these receptors in GC B cells to effectively downregulate the glycosyltransferases B4galt1 and St6gal1 and produce pro-inflammatory IgG^+ Abs, as has been partly suggested recently by our own research group (Hess et al. 2013), as well as others (Pfeifle et al. 2016). I found that Tfh cells produced significantly larger amounts of IFN-γ, but less IL-17A upon low-inflammatory OVA-LPS, compared with pro-inflammatory OVA-eCFA. Although excessive IFN-γRI signal transduction has been associated with development of autoimmunity, I found that a large percentage of the IFN-γ producing Tfh cells, were also secreting anti-inflammatory IL-10, which could pose a potential precaution to

prevent the development of autoimmune diseases, while simultaneously ensuring B cell isotype switching.

Moreover, IFN-γ has been shown to substantially increase the expression of PD-L1, which interacts with the co-inhibitory receptor PD-1 on T cells and upon ligation, leads to effective dephosphorization of CD28 via recruitment of the cytosolic tyrosine phosphatases Shp-1 and Shp-2, thereby suppressing T cell function (Kamphorst et al. 2017). Since PD-1 is expressed by both Tfh and Tfr cells (**Table 1**), this is indicative of a reciprocal regulation of GC B cells, Tfh and Tfr cells. Of note, PD-L1 has been demonstrated to induce iTregs and to enhance and sustain FoxP3 expression (Francisco et al. 2009). Interestingly, I found substantially upregulated expression of PD-L1 on $OVA^{+}IgG1^{+}$ GC B cells and of PD-1 on Tfh and Tfr cells upon OVA-LPS immunization, compared with OVA-eCFA (data not shown). This is indicative of a dual role of PD-L1, sustaining Tfr cell function via maintenance of FoxP3 on the one hand, while simultaneously inhibiting excessive Tfh and Tfr cell function by inactivating the CD28 signaling cascades on the other hand.

This suggests that cytokine production by Tfh cells plays a pivotal, yet precisely regulated role, balancing between insufficient and excessive B cell activation.

Additionally, I observed that Tfr cells are able to produce substantial amounts of the anti-inflammatory cytokines TGF-β and IL-10, which likely poses a mechanism to effectively control GC reactions by inhibiting Tfh and GC B cells. This secretion of regulatory cytokines possibly adds another layer of protection against the autoimmune disease development, since *in vitro* experiments have shown that Tfr cells significantly reduce Tfh cell cytokine production, reduce CSR in B cells, as well as suppress Ab production (Sage, Alvarez, et al. 2014; Wallin et al. 2014).

Although it has been implied, that Tfr cells can suppress Tfh and GC B cells, it still remains elusive how they exert these regulatory effects. Accordingly, recent studies have proposed several suppressive pathways for Tfr cells, including production of IL-10 and TGF-β (Sage & Sharpe 2015). IL-10 has been shown to alter Ab production and B.7 levels *in vivo* (Cai et al. 2012; Ding et al. 1993; Nova-Lamperti et al. 2016; Schildberg et al. 2016), whereas TGF-β has been implied to directly inhibit Tfh cells (McCarron & Marie 2014). This is in support of my data, since I observed lower Tfh cell, GC B cell, as well as PC numbers, but higher IL-10 and TGF-β production by Tfr cells upon low-inflammatory OVA-LPS treatment, compared with pro-inflammatory OVA-eCFA. Although the IgG subclass distribution was comparable between these different treatments, OVA-

eCFA vaccination led to significantly higher IgG^+ Ab levels compared with OVA-LPS. This is likely due to a combination of a different Tfr/Tfh ratio and their produced cytokines, which directly influenced the GC reaction and therefore led to distinct numbers of OVA^+ GC B cells and Ab-secreting PCs. A low Tfr/Tfh cell ratio with high levels of pro-inflammatory IL-17A, moderate levels of IFN-γ and low levels of TGF-β and IL-10 seems to favor the development of GC B cells. This is probably due to a high abundance of Tfh-GC B cell interactions resulting in a high level of stimulatory Tfh signals, facilitating positive B cell clone selection. Due to the high numbers of Tfh cells with simultaneous low numbers of Tfr cells, it is also likely that B cell clones with a lower relative BCR affinity for the respective antigen receive stimulatory signals and therefore undergo affinity maturation, SHM, as well as CSR. This would also result in high numbers of antigen-specific- and class switched PCs, all of which is in accordance with my data. Furthermore, this could also result in the production of not only high-affinity IgG^+ Abs, but also a fraction of low or medium-affinity IgG^+ Abs and if completely unregulated possibly in positive selection of self-reactive B cell clones and thus autoimmunity.

In support of this notion, a recent study has delineated a model, in which Tfr cells inhibit bidirectional co-stimulation between Tfh and GC B cells, as well as induce a suppressive epigenetic B cell state, in which CSR and glycolysis were severely disrupted, thereby efficiently suppressing the ensuing Ab response (Sage et al. 2016). Interestingly, this Tfr cell induced suppressive state could be overcome by production of IL-21 by Tfh cells (Sage et al. 2016).

Of note, all of these aforementioned criteria, specifically the Tfr/Tfh ratio, as well as their respective cytokine secretion, seem to substantially affect glycosyltransferase expression in class switched OVA^+GC B cells and therefore IgG^+ Ab glycosylation, further supporting the notion, that the glycosylation process is being regulated during the GC response. However, the exact contributions of each of these specific factors to Ab glycosylation are complicated to deduce, and further experiments are necessary to specifically characterize the impact of each of them on IgG^+ Ab glycosylation.

The ratio of stimulatory/regulatory signals during the GC response seems to be carefully balanced to ensure effective humoral immunity, while preventing excessive and unspecific B cell clone selection, which could lead to autoimmunity. Therefore, it is plausible that the cytokines, produced by Tfh and Tfr cells are transmitted through an immunological synapse during cell contacts with GC B cells. It has been shown that Tfh cells interact with GC B cells through TCR-MHCII complex,

ICOS-ICOSL, as well as CD-CD40L signaling (Crotty 2011; Gitlin et al. 2014). Although CD40L is mainly stored in intracellular vesicles, it can be rapidly transported to the cell surface upon ICOS co-stimulation, which facilitates an entangled contact (Qi 2016; Liu et al. 2015). This could also explain the relatively low amounts of produced cytokines by Tfh cells I observed, compared with other Th cell subsets, since a transport over an immunological synapse would be much more specific than cytokine secretion into the surrounding milieu, as has also been suggested in other studies (Qi 2016). This way it could also be ensured that only GC B cells with a high affinity for the cognate antigen receive stimulatory cytokine signals by Tfh cells, since those GC B cells could engage in long and specific contacts with Tfh cells via MHC-II-TCR interactions. A similar mechanism could be possible for Tfr cells, since these cells globally express CTLA-4, which has a high affinity for B.7 ligands that are expressed on GC B cells. Thus, Tfh as well as Tfr cells can remain in close contact with GC B cells and selectively exert either stimulatory or regulatory signals. Due to the higher abundance of T follicular helper cells with a simultaneous low Tfr/Tfh ratio upon pro-inflammatory OVA-eCFA immunization, it is much more likely that GC B cells interact with stimulatory Tfh cells, rather than suppressive Tfr cells and therefore receive positive selection signals. Since Tfr cells also secrete less TGF-β and IL-10 under these pro-inflammatory conditions, compared with low-inflammatory OVA-LPS, this moreover indicates a low rate of Tfh suppression, further facilitating positive B cell clone selection, leading to high abundances of Ab-secreting PCs. An exaggerated stimulation of GC B cells by Tfh cells could on the other hand have detrimental effects resulting in positive selection of self-reactive B cell clones and thus in autoimmunity. Therefore, GC reactions have to be carefully balanced by the Tfr/Tfh ratio to ensure an effective humoral Ab response, while simultaneously preventing the production of auto-Abs.

Since these results demonstrate, that the Tfr/Tfh ratio critically controls the GC reaction, I assessed the impact of Tfr deficiency in further experiments. Therefore, I utilized DEREG mice, in which DT immunization rapidly depleted Treg cells. Since Treg cell are the precursors of Tfr cells, the latter should be depleted alongside Treg cells. This is in accordance with recent publications, in which the same procedure was used to efficiently deplete Tfr cells (Wing et al. 2014; Linterman et al. 2011). I found that a transient depletion of Tfr cells before OVA immunization and at the peak of the GC reaction at day 6 resulted in significantly enhanced GC B cell-, OVA^+ GC B cell- and OVA^+IgG1^+ GC B cell- frequencies, as well as decreased B4galt1 and St6gal1 expression compared with undepleted control mice. These changes in GC B cells were directly translated to the PC compartment, where I observed similar increases in PCs, OVA^+ PCs, as well as

OVA^+IgG1^+ PCs. Moreover, this transient Tfr depletion also resulted in substantially increased OVA^+IgG^+ Ab production and markedly altered glycoprofiles towards pro-inflammatory Abs. It is likely that the observed differences stem from a profoundly reduced Tfr/Tfh ratio, possibly increasing the availability of B7 molecules on GC B cells, resulting in massively enhanced stimulatory capacities of Tfh cells. Although I cannot distinguish between the effects of Treg cell deficiency and Tfr cell deficiency in this study, it seems likely that the observed effects are facilitated due to a lack of Tfr cells, since these cells directly control the GC reaction and the observed effects are all GC related. Furthermore, it has been suggested that Tfr cells take a longer time to recover from transient depletion than Treg cells and that longer periods of depletion result in reduced numbers of antigen-specific Abs (Wing et al. 2014). Although this seems to be paradox initially, it has been implied that this reduction is due an uncontrolled expansion and positive selection of non-specific B cell clones, which ultimately outcompete antigen-specific clones and therefore result in reduced numbers of antigen-specific Abs, but massive abundances of potentially self-reactive auto-Abs (Wing et al. 2014). Considering the critical role of Tfr cells in suppressing the GC reaction, this seems reasonable and should be considered in potential therapeutic approaches to increase vaccination efficacy. I have not tested whether a long term Tfr depletion would also result in reduced expression of B4galt1 and St6gal1 in GC B cells and PCs, but it seems likely, since these changes are probably facilitated by the lack of Tfr cell suppression and therefore enhanced stimulation by Tfh cells. Moreover, it has been implicated that an early depletion of Treg cells could affect the expansion of Tfh cells, since Treg cells might regulate DCs, which are critical for Tfh cell development (Wing et al. 2014). Thus, direct effects related to Treg or Tfr cell depletion are complicated to uncouple.

I showed that Tfr cells are pivotal to control the GC response, although it is not yet clear whether secretion of anti-inflammatory cytokines, CTLA-4 mediated suppression or a combination of them critically regulates excessive GC formation.To further delineate possible suppressive pathways by Tfr cells, I next altered the Tfr/Tfh ratio in favor of Tfr cells via IL-2/Jes6-1 immunization.

I found that a substantial induction in Tfr cells has opposing effects to the transient depletion experiments. The Tfr/Tfh ratio upon pro-inflammatory OVA-eCFA immunization was at ~0.25, while OVA-eCFA+IL-2/Jes6-1 immunized mice had a substantially higher Tfr/Tfh ratio of 0.5. Thus, the ratio shifted substantially towards suppressive Tfr cells, which showed an immense regulatory capacity, marked by secretion of massive amounts of the anti-inflammatory cytokines TGF-β and IL-10 (**Figure 46**, **Figure 47**). Moreover, these highly suppressive Tfr cells were also

defined by significantly higher expression levels of the co-inhibitory receptor CTLA-4, compared with OVA-eCFA treated mice. The observed decreases in the frequencies of (OVA^+IgG1^+) GC B cells and PCs upon IL-2/Jes6-1 immunization, compared with OVA-eCFA treatment, are therefore most likely the result of this highly suppressive GC microenvironment, characterized by a high Tfr/Tfh ratio, substantial anti-inflammatory cytokine production, as well as high expression of CTLA-4 on these cells. I found that Tfr cells globally express CTLA-4, but that also a high percentage of Treg and Tfh cells express this co-inhibitory molecule, pointing to a pivotal role of this co-inhibitory receptor in the regulation of B cell responses. Accordingly, mice lacking CTLA-4 on Tregs either constitutively or conditionally have been shown to rapidly develop a lymphoproliferative disease and mulitorgan damage (Wing et al. 2008). I also found a significant decrease of the stimulatory molecule CD86 on OVA^+IgG1^+ GC B cells upon IL-2/Jes6-1 treatment. This decrease is most likely the result of the highly suppressive GC microenvironment. The availability of CD86 during the GC reaction is therefore significantly reduced, possibly through cell extrinsic mechanisms of CTLA-4 (transendocytosis), as has been shown before (**Figure 35** A, B). This would negatively affect the stimulatory potential of Tfh cells. Moreover, it has been shown that IL-2 signaling induces BLIMP-1, as well as STAT-5, both of which result in an inhibition of Tfh cell development through Bcl-6 repression (Johnston et al. 2012; Ballesteros-Tato et al. 2012; Nurieva et al. 2012).

Together with the massively increased abundance of Tfr cells and availability of anti-inflammatory cytokines, it is likely that Tfh cells as well as GC B cells are being further suppressed, explaining the reduced frequencies of GC B cells, PCs, as well as IgG^+ Abs. Taken together, these data could substantiate the mode of action of IL-2/Jes6-1 autoimmune therapy by adding further particulars regarding alterations in the GC reaction and especially regarding the induction of highly suppressive Tfr cells.

The observed decrease in CD86 is in accordance with recent studies, in which CTLA-4 mediated downregulation of CD86 has been observed in B cells, although outside of the GC (Sage, Paterson, et al. 2014), as well as in *in vitro* studies, in which CD80 and CD86 on B cells were efficiently downregulated by CTLA-4 (Wing et al. 2014). The disparity between the findings, that CTLA-4 mediated downregulation of CD86 occurred inside or outside of the GC reaction probably stems from the fact, that I induced a large abundance of highly suppressive Tfr cells with markedly increased CTLA-4 expression and anti-inflammatory cytokine production via IL-2/Jes6-1 immunization (**Figure 45**, **Figure 46**, **Figure 47**, **Figure 48**). Thus, IL-2/Jes6-1 induced Tfr cells showed

a higher capacity to inhibit GC B cell activation, since also IL-10 and TGF-β have been implicated to downregulate CD86 on B cells (Nova-Lamperti et al. 2016; Schildberg et al. 2016). Moreover, ablation of CTLA-4 on Treg cells has been shown to result in an increase of IL-10 producing Treg cells, posing a possible compensatory mechanism for the loss of CTLA-4 (Paterson et al. 2015). To further support this notion, my results also revealed no significant differences in CD86 expression on OVA^+IgG1^+GC B cells after pro-and low-inflammatory immunizations, although the Tfr/Tfh ratio differed significantly (data not shown). This substantiates the possibility, that only a high abundance of highly suppressive Tfr cells leads to an effective and long-term downregulation of CD86 on GC B cells, especially since CD80 and CD86 have been shown to be rapidly re-expressed (Schildberg et al. 2016). Therefore, it is possible that a long-term downregulation of these stimulatory molecules on GC B cells can only be obtained by a combination of direct (transendocytosis) and indirect effects (cytokine mediated downregulation).

I also found a significant downregulation of OVA^+IgG^+ Abs upon IL-2/Jes6-1 treatment, probably facilitated by prior decrease in GC B cells, class switched (OVA^+IgG1^+) GC B cells and also PCs. It is likely, that this reduction in antigen-specific GC B cells, PCs, as well as IgG^+ Abs was due to increased abundances of highly suppressive Tfr cells and decreased abundances of Tfh cells. The ensuing increase in Interclonal competition among GC B cells could be a result of decreased stimulatory signals from Tfh cells, due to a markedly altered Tfr/Tfh ratio upon IL-2/Jes6-1 treatment. This would result in a reduced number of GC B cells undergoing iterative circles of positive selection, affinity maturation, SHM, as well as CSR, ultimately leading to a lower number of IgG^+ Ab-secreting PCs. Accordingly, transient depletion of Tfr cells led to a significant increase in GC B cells, OVA^+ GC B cells, as well as OVA^+IgG1^+ GC B cells. This increase was directly translated to the PC compartment and resulted in substantial increases in IgG^+ Abs, suggesting an opposite mechanism to the Tfr increase upon IL-2/Jes6-1 therapy. Importantly, IL-2/Jes6-1 immunization also altered the glycosylation profile of the produced IgG^+ Abs towards a higher abundance of anti-inflammatory galactosylated and sialylated Abs.

Of note, IL-2/Jes6-1 therapy has also been effectively utilized to treat a variety of autoimmune diseases in mice, among them collagen-induced arthritis (CIA) (Lee et al. 2012). This disease is also dependent on antigen-specific IgG^+ Ab production. While (Lee et al. 2012) reasoned that the amelioration in arthritis onset was due to increased Treg abundances and decreased antigen-specific IgG^+ Ab production, they failed to directly link this effect to alterations in the Tfr compart-

ment, which would directly affect the GC response and therefore also antigen-specific Ab production. Another recent study delineated the importance of sialylated antigen-specific Abs in the amelioration of CIA, as well as in the suppression of CIA development (Ohmi et al. 2016).

Since my data indicate that IgG^+ Ab glycosylation is amongst other factors dependent on the Tfr/Tfh ratio, this suggests that the disease onset and severity of CIA and possibly other Ab-dependent autoimmune diseases could be ameliorated by altering this Tfr/Tfh ratio towards Tfr cells, resulting in higher abundances of anti-inflammatory sialylated IgG^+ Abs. Thus, my data may provide important particulars and increase the understanding of IL-2 based autoimmune therapy.

To summarize, my findings demonstrate that IgG^+ Ab galactosylation and sialylation are being regulated during the GC response through distinct expression levels of the respective glycosyltransferases B4galt1 and St6gal1. This enzyme expression in GC B cells appears to be actively modulated and seems to be dependent on a variety of factors. My data indicate that GC reactions, which are characterized by a low Tfr/Tfh ratio, profound Tfh cell production of pro-inflammatory cytokines IFN-γ and IL-17A without simultaneous co-production of IL-10, high availability of the stimulatory receptor CD86, as well as low Tfr cell production of anti-inflammatory cytokines TGF-β and IL-10, lead to a low expression level of B4galt1 and St6gal1 in GC B cells and ultimately results in a high abundance of pro-inflammatory (agalactosylated and asialylated) IgG^+ Abs.

On the other hand, GC reactions, which are defined by a high Tfr/Tfh ratio, low Tfh cell production of IL-17A and co-production of IFN-γ and IL-10, as well as high Tfr cell production of TGF-β and IL-10 lead to a high expression level of B4galt1 and St6gal1 in GC B cells and therefore result in a high abundance of anti-inflammatory (galactosylated and sialylated) IgG^+ Abs.

Thus, TD antigen-specific IgG^+ Ab glycosylation is a process that can be actively modulated through alterations of the Tfr/Tfh ratio and the production of their respective cytokines. This determines the stimulatory potential of Tfh cells and entails B cell clone selection, abundance of GC B cells and PCs and ultimately the quantity and quality of the humoral Ab response.

In conclusion, my findings offer insights into how IgG Ab glycosylation is regulated, reveal pivotal roles for Tfh and Tfr cells in this process, and to shed light on potential therapeutic strategies, i.e. to further boost protective Ab production for vaccination or for the treatment of several Ab-dependent autoimmune diseases.

5 Abbreviations

Ab	Antibody
ADCC	Antibody-dependent cellular cytotoxicity
ADCP	Antibody-dependent cellular phagocytosis
Ag	Antigen
AID	Activation-induced cytidine deaminase
APC	Antigen presenting cell
Asn297	Asparagine 297
B4galt1	β-1,4 galactosyltransferase 1
BC	B cell
Bcl-6	B-cell lymphoma 6
BCR	B cell receptor
Blimp-1	B lymphocyte-induced maturation protein-1
CDC	Complement dependent cytotoxicity
CFA	Complete Freund´s Adjuvant
CIA	Collagen induced arthritis
CSR	Class switch recombination
CTLA-4	Cytotoxic T-lymphocyte-associated protein 4
CXCR5	Chemokine receptor CXC receptor 5
DC	Dendritic cell

DT	Diphtheria Toxin
DTH	Delayed type hypersensitivity
EBA	Epidermolysis bullosa aquisita
FcR	Fc receptor
FcRn	Neonatal Fc receptor
FcγR	Fc γ receptor
FoxP3	Forkhead-Box-Protein 3
GC	Germinal Center
GlcNac	N-Acetyl glucosamine
i.p.	intraperitoneally
ICOS	Inducible T cell co-stimulator
IF	Interfollicular zone
IFN-γ	Interferon-γ
IFN-γRI	Interferon-γ Receptor 1
Ig	Immunoglobulin
IL	Interleukin
IL-17RA	Interleukin-17 Receptor A
ITAM	Immunoreceptor tyrosine-based activation motif
ITIM	Immunoreceptor tyrosine-based inhibition motif
ITP	Immunothrombocytopenia

Ko	knockout
LLPC	Long lived plasma cells
Man	Mannose
MBC	Memory B cell
MFI	Mean fluorescence intensity
MHC-II	Major histocompatibility complex II
MZ	Marginal zone
OVA	Ovalbumin
PC	Plasma cell
PD-1	Programmed cell death protein 1
SEM	Standard error of mean
SHIP	SH-2-domain-containing inositol phosphatases
SHM	Somatic hypermutation
SLE	Systemic lupus erythematosus
St6gal1	α-2,6-sialyltransferase 1
STAT	Signal transducer and activator of transcription
TB	T cell – B cell border
TCR	T cell receptor
TD	T cell dependent antigen
Tfh	T follicular helper cell

Tfr	T follicular regulatory cell
TGF-β	Tumor growth factor β
Th	T helper cell
TI	T cell independent antigen
Treg	Regulatory T cell
WT	wild type

6 References

Abrams, D. et al., 2009. Interleukin-2 therapy in patients with HIV infection. *The New England journal of medicine*, 361(16), pp.1548–59.

Ackerman, M.E. et al., 2013. Natural variation in Fc glycosylation of HIV-specific antibodies impacts antiviral activity. *Journal of Clinical Investigation*, 123(5), pp.2183–2192.

Albert, H. et al., 2008. In vivo enzymatic modulation of IgG glycosylation inhibits autoimmune disease in an IgG subclass-dependent manner. *Proceedings of the National Academy of Sciences of the United States of America*, 105(39), pp.15005–15009.

Allman, D. & Pillai, S., 2008. Peripheral B cell subsets. *Curr Opin Immunol*, 20(2), pp.149–157.

Aloulou, M. et al., 2016. Follicular regulatory T cells can be specific for the immunizing antigen and derive from naive T cells. *Nature communications*, 7, p.10579.

Amigorena, S. et al., 1989. Fc gamma RII expression in resting and activated B lymphocytes. *European journal of immunology*, 19(8), pp.1379–85.

Anderson, A.C., Joller, N. & Kuchroo, V.K., 2016. Lag-3, Tim-3, and TIGIT: Co-inhibitory Receptors with Specialized Functions in Immune Regulation. *Immunity*, 44(5), pp.989–1004.

Anthony, R.M., Wermeling, F., et al., 2008. Identification of a receptor required for the anti-inflammatory activity of IVIG. *Proceedings of the National Academy of Sciences of the United States of America*, 105(50), pp.19571–8.

Anthony, R.M., Nimmerjahn, F., et al., 2008. Recapitulation of IVIG anti-inflammatory activity with a recombinant IgG Fc. *Science*, 320(5874), pp.373–6.

Anthony, R.M., Wermeling, F. & Ravetch, J. V., 2012. Novel roles for the IgG Fc glycan. *Annals of the New York Academy of Sciences*, 1253(1), pp.170–180.

Arce Vargas, F. et al., 2017. Fc-Optimized Anti-CD25 Depletes Tumor-Infiltrating Regulatory T Cells and Synergizes with PD-1 Blockade to Eradicate Established Tumors. *Immunity*, pp.577–586.

Arenas-Ramirez, N., Woytschak, J. & Boyman, O., 2015. Interleukin-2: Biology, Design and Application. *Trends in Immunology*, 36(12), pp.763–777.

Arlauckas, S.P. et al., 2017. In vivo imaging reveals a tumor-associated macrophage–mediated resistance pathway in anti–PD-1 therapy. , pp.1–10.

Bakema, J.E. & Egmond, M. Van, 2014. Fc Receptors. , 382, pp.373–392.

Ballesteros-Tato, A. et al., 2012. Interleukin-2 Inhibits Germinal Center Formation by Limiting T Follicular Helper Cell Differentiation. *Immunity*, 36(5), pp.847–856.

Ballesteros-Tato, A. et al., 2016. T Follicular Helper Cell Plasticity Shapes Pathogenic T Helper 2 Cell-Mediated Immunity to Inhaled House Dust Mite. *Immunity*, 44(2), pp.259–273.

Baumjohann, D. et al., 2013. Persistent Antigen and Germinal Center B Cells Sustain T Follicular Helper Cell Responses and Phenotype. *Immunity*, 38(3), pp.596–605.

Blackburn, S.D. et al., 2009. Coregulation of CD8+ T cell exhaustion by multiple inhibitory receptors during chronic viral infection. *Nature immunology*, 10(1), pp.29–37.

Boyd, P.N., Lines, A.C. & Patel, A.K., 1995. The effect of the removal of sialic acid, galactose and total carbohydrate on the functional activity of Campath-1H. *Molecular Immunology*, 32(17–18), pp.1311–1318.

Boyman, O. et al., 2006. Selective stimulation of T cell subsets with antibody-cytokine immune complexes. *Science*, 311(5769), pp.1924–1927.

Boyman, O. & Sprent, J., 2012. The role of interleukin-2 during homeostasis and activation of the immune system. *Nature Reviews Immunology*, 12(3), pp.180–190.

Bruhns, P. & Jönsson, F., 2015. Mouse and human FcR effector functions. *Immunological Reviews*, 268(1), pp.25–51.

Butt, D. et al., 2015. FAS Inactivation Releases Unconventional Germinal Center B Cells that Escape Antigen Control and Drive IgE and Autoantibody Production. *Immunity*, 42(5), pp.890–902.

Cai, G. et al., 2012. A regulatory role for IL-10 receptor signaling in development and B cell help of T follicular helper cells in mice. *Journal of immunology (Baltimore, Md.: 1950)*, 189(3), pp.1294–302.

Campbell, I.K. et al., 2014. Therapeutic effect of IVIG on inflammatory arthritis in mice is dependent on the Fc portion and independent of sialylation or basophils. *J Immunol*, 192(11), pp.5031–5038.

Cannons, J.L., Lu, K.T. & Schwartzberg, P.L., 2013. T follicular helper cell diversity and plasticity. *Trends in Immunology*, 34(5), pp.200–207.

Carsetti, R., Rosado, M.M. & Wardmann, H., 2004. Peripheral development of B cells in mouse and man. *Immunol Rev*, 197, pp.179–191.

Castela, E. et al., 2014. Effects of low-dose recombinant interleukin 2 to promote T-regulatory cells in alopecia areata. *JAMA dermatology*, 150(7), pp.748–51. Available at: http://www.ncbi.nlm.nih.gov/pubmed/24872229.

Chan, A.C. & Carter, P.J., 2010. Therapeutic antibodies for autoimmunity and inflammation. *Nature reviews. Immunology*, 10(5), pp.301–316.

Chan, T.D. et al., 2009. Antigen affinity controls rapid T-dependent antibody production by driving the expansion rather than the differentiation or extrafollicular migration of early plasmablasts. *Journal of immunology (Baltimore, Md. : 1950)*, 183(5), pp.3139–49.

Chen, W. et al., 2003. Conversion of peripheral CD4+CD25- naive T cells to CD4+CD25+ regulatory T cells by TGF-beta induction of transcription factor Foxp3. *The Journal of experimental medicine*, 198(12), pp.1875–86.

Chung, Y. et al., 2011. Follicular regulatory T cells expressing Foxp3 and Bcl-6 suppress germinal center reactions. *Nature medicine*, 17(8), pp.983–988.

Cilio, C.M. et al., 1998. Cytotoxic T lymphocyte antigen 4 is induced in the thymus upon in vivo activation and its blockade prevents anti-CD3-mediated depletion of thymocytes. *The Journal of experimental medicine*, 188(7), pp.1239–46.

Crotty, S., 2015. A brief history of T cell help to B cells. *Nature reviews. Immunology*, 15(3), pp.185–9.

Crotty, S., 2011. Follicular helper CD4 T cells (TFH). *Annual review of immunology*, 29(1), pp.621–663.

Crotty, S., 2014. T Follicular Helper Cell Differentiation, Function, and Roles in Disease. *Immunity*, 41(4), pp.529–542.

Cunningham-Rundles, C. et al., 1992. Restoration of immunoglobulin secretion in vitro in common variable immunodeficiency by in vivo treatment with polyethylene glycol-conjugated human recombinant interleukin-2. *Clinical Immunology and Immunopathology*, 64(1), pp.46–56.

Cunningham, A.F. et al., 2004. Loss of CD154 impairs the Th2 extrafollicular plasma cell response but not early T cell proliferation and interleukin-4 induction. *Immunology*, 113(2), pp.187–193.

Dedeoglu, F. et al., 2004. Induction of activation-induced cytidine deaminase gene expression by IL-4 and CD40 ligation is dependent on STAT6 and NFκB. *International Immunology*, 16(3), pp.395–404.

Dibble, C.C. & Cantley, L.C., 2015. Regulation of mTORC1 by PI3K signaling. *Trends in Cell Biology*, 25(9), pp.545–555.

Ding, L. et al., 1993. IL-10 inhibits macrophage costimulatory activity by selectively inhibiting the up-regulation of B7 expression. *Journal of immunology (Baltimore, Md.: 1950)*, 151(3), pp.1224–1234.

Domeier, P.P. et al., 2016. IFN-γ receptor and STAT1 signaling in B cells are central to spontaneous germinal center formation and autoimmunity. *The Journal of Experimental Medicine*, p.jem.20151722.

Ercan, A. et al., 2010. Aberrant IgG galactosylation precedes disease onset, correlates with disease activity, and is prevalent in autoantibodies in rheumatoid arthritis. *Arthritis and Rheumatism*, 62(8), pp.2239–2248.

Esplugues, E. et al., 2011. Control of TH17 cells occurs in the small intestine. *Nature*, 475(7357), pp.514–8.

Espy, C. et al., 2011. Sialylation levels of anti-proteinase 3 antibodies are associated with the activity of granulomatosis with polyangiitis (Wegener's). *Arthritis and Rheumatism*, 63(7), pp.2105–2115.

Fairfax, K.C. et al., 2015. IL-4-Secreting Secondary T Follicular Helper (Tfh) Cells Arise from Memory T Cells, Not Persisting Tfh Cells, through a B Cell-Dependent Mechanism. *Journal of immunology (Baltimore, Md. : 1950)*, 194(7), pp.2999–3010.

Fazilleau, N. et al., 2009. Follicular Helper T Cells: Lineage and Location. *Immunity*, 30(3), pp.324–335.

Fontenot, J.D., Gavin, M. a & Rudensky, A.Y., 2003. Foxp3 programs the development and function of CD4+CD25+ regulatory T cells. *Nature immunology*, 4(4), pp.330–6.

Francisco, L.M. et al., 2009. PD-L1 regulates the development, maintenance, and function of induced regulatory T cells. *The Journal of experimental medicine*, 206(13), pp.3015–29.

Friedmann, M.C. et al., 1996. Different interleukin 2 receptor beta-chain tyrosines couple to at least two signaling pathways and synergistically mediate interleukin 2-induced proliferation. *Proceedings of the National Academy of Sciences of the United States of America*, 93(5), pp.2077–82.

Furness, A.J.S. et al., 2014. Impact of tumour microenvironment and Fc receptors on the activity of immunomodulatory antibodies. *Trends in Immunology*, 35(7), pp.290–298.

Gatto, D. & Brink, R., 2010. The germinal center reaction. *Journal of Allergy and Clinical Immunology*, 126(5), pp.898–907.

van de Geijn, F.E. et al., 2009. Immunoglobulin G galactosylation and sialylation are associated with pregnancy-induced improvement of rheumatoid arthritis and the postpartum flare: results from a large prospective cohort study. *Arthritis research & therapy*, 11(6), p.R193.

Gitlin, A.D., Shulman, Z. & Nussenzweig, M.C., 2014. Clonal selection in the germinal centre by regulated proliferation and hypermutation. *Nature*, 509(7502), pp.637–40.

Goenka, R. et al., 2011. Cutting edge: dendritic cell-restricted antigen presentation initiates the follicular helper T cell program but cannot complete ultimate effector differentiation. *Journal of immunology (Baltimore, Md. : 1950)*, 187(3), pp.1091–5.

Goodnow, C.C. et al., 2010. Control systems and decision making for antibody production. *Nat Immunol*, 11(8), pp.681–688.

Hamilton, S.E. et al., 2010. IL-2 complex treatment can protect naive mice from bacterial and viral infection. *Journal of immunology (Baltimore, Md. : 1950)*, 185(11), pp.6584–6590.

Hartemann, A. et al., 2013. Low-dose interleukin 2 in patients with type 1 diabetes: a phase 1/2 randomised, double-blind, placebo-controlled trial. *The lancet. Diabetes & endocrinology*, 1(4), pp.295–305.

Hess, C. et al., 2013. T cell – independent B cell activation induces immunosuppressive sialylated IgG antibodies. *The Journal of Clinical Investigationrnal of Clinical*, 123(9), pp.3788–3796.

Holmdahl, R., Malmström, V. & Burkhardt, H., 2014. Autoimmune priming, tissue attack and chronic inflammation - The three stages of rheumatoid arthritis. *European Journal of Immunology*, 44(6), pp.1593–1599.

Hsu, H.-C. et al., 2008. Interleukin 17-producing T helper cells and interleukin 17 orchestrate autoreactive germinal center development in autoimmune BXD2 mice. *Nature immunology*, 9(2), pp.166–75.

Irani, V. et al., 2015. Molecular properties of human IgG subclasses and their implications for designing therapeutic monoclonal antibodies against infectious diseases. *Molecular Immunology*, 67(2), pp.171–182.

Jackson, S.W. et al., 2016. B cell IFN-γ receptor signaling promotes autoimmune germinal centers via cell-intrinsic induction of BCL-6. *The Journal of Experimental Medicine*, p.jem.20151724.

Jefferis, R. & Lund, J., 2002. Interaction sites on human IgG-Fc for FcgammaR: current models. *Immunology letters*, 82(1–2), pp.57–65.

Johnston, R.J. et al., 2009. Bcl6 and Blimp-1 are reciprocal and antagonistic regulators of T follicular helper cell differentiation. *Science (New York, N.Y.)*, 325(5943), pp.1006–10.

Johnston, R.J. et al., 2012. STAT5 is a potent negative regulator of TFH cell differentiation. *Journal of Experimental Medicine*, 209(2), pp.243–250.

Kaji, T. et al., 2012. Distinct cellular pathways select germline-encoded and somatically mutated antibodies into immunological memory. *The Journal of experimental medicine*, 209(11), pp.2079–97.

Kamphorst, A.O. et al., 2017. Rescue of exhausted CD8 T cells by PD-1 – targeted therapies is CD28-dependent. , 683(March).

Kaneko, Y., Nimmerjahn, F. & Ravetch, J. V, 2006. Anti-Inflammatory Activity of Immunoglobulin G Resulting from Fc Sialylation Author(s): Yoshikatsu Kaneko, Falk Nimmerjahn and Jeffrey V. Ravetch Source: *Science*, 313(5787), pp.670–673.

Kao, D. et al., 2014. Targeting B cells and autoantibodies in the therapy of autoimmune diseases. *Seminars in Immunopathology*, 36(3), pp.289–299.

Karsten, C.M. et al., 2012. Anti-inflammatory activity of IgG1 mediated by Fc galactosylation and association of FcγRIIB and dectin-1. *Nature medicine*, 18(9), pp.1401–6.

Kasper, I.R. et al., 2016. Empowering Regulatory T Cells in Autoimmunity. *Trends in Molecular Medicine*, 22(9), pp.784–797.

Kerfoot, S.M. et al., 2011. Germinal Center B Cell and T Follicular Helper Cell Development Initiates in the Interfollicular Zone. *Immunity*, 34(6), pp.947–960.

King, I.L. & Mohrs, M., 2009. IL-4-producing CD4+ T cells in reactive lymph nodes during helminth infection are T follicular helper cells. *J Exp Med*, 206(5), pp.1001–1007.

Klatzmann, D. & Abbas, A.K., 2015. The promise of low-dose interleukin-2 therapy for autoimmune and inflammatory diseases. *Nature reviews. Immunology*, 15(5), pp.283–94.

Kovacs, J.A. et al., 1996. *Controlled trial of interleukin-2 infusions in patients infected with the human immunodeficiency virus.*,

Krieg, C. et al., 2010. Improved IL-2 immunotherapy by selective stimulation of IL-2 receptors on lymphocytes and endothelial cells. *Proceedings of the National Academy of Sciences of the United States of America*, 107(26), pp.11906–11.

Kühn, R., Rajewsky, K. & Müller, W., 2013. Generation and analysis of interleukin-4 deficient mice. *Science (New York, N.Y.)*, 254(5032), pp.707–710.

Lee, S.Y. et al., 2012. Interleukin-2/anti-interleukin-2 monoclonal antibody immune complex suppresses collagen-induced arthritis in mice by fortifying interleukin-2/STAT5 signalling pathways. *Immunology*, 137(4), pp.305–316.

Létourneau, S. et al., 2010. IL-2/anti-IL-2 antibody complexes show strong biological activity by avoiding interaction with IL-2 receptor alpha subunit CD25. *Proceedings of the National Academy of Sciences of the United States of America*, 107(5), pp.2171–6.

Levin, A.M. et al., 2012. Exploiting a natural conformational switch to engineer an interleukin-2 “superkine.” *Nature*, 484(7395), pp.529–533.

Liao, W., Lin, J.X. & Leonard, W.J., 2013. Interleukin-2 at the Crossroads of Effector Responses, Tolerance, and Immunotherapy. *Immunity*, 38(1), pp.13–25.

Lin, J.X. et al., 2012. Critical Role of STAT5 Transcription Factor Tetramerization for Cytokine Responses and Normal Immune Function. *Immunity*, 36(4), pp.586–599.

Linterman, M.A. et al., 2009. Follicular helper T cells are required for systemic autoimmunity. *The Journal of experimental medicine*, 206(3), pp.561–76.

Linterman, M. a et al., 2011. Foxp3+ follicular regulatory T cells control the germinal center response. *Nature medicine*, 17(8), pp.975–82.

Linterman, M. a et al., 2010. IL-21 acts directly on B cells to regulate Bcl-6 expression and germinal center responses. *The Journal of experimental medicine*, 207(2), pp.353–63.

Liu, D. et al., 2015. T-B-cell entanglement and ICOSL-driven feed-forward regulation of germinal centre reaction. *Nature*, 517(7533), pp.214–8.

Long, S.A. et al., 2012. Rapamycin/IL-2 combination therapy in patients with type 1 diabetes augments Tregs yet transiently impairs beta-cell function. *Diabetes*, 61(9), pp.2340–2348.

Malek, T.R. & Castro, I., 2010. Interleukin-2 Receptor Signaling: At the Interface between Tolerance and Immunity. *Immunity*, 33(2), pp.153–165.

de Man, Y.A. et al., 2008. Disease activity of rheumatoid arthritis during pregnancy: results from a nationwide prospective study. *Arthritis and rheumatism*, 59(9), pp.1241–1248.

Marengère, L.E. et al., 1996. Regulation of T cell receptor signaling by tyrosine phosphatase SYP association with CTLA-4. *Science (New York, N.Y.)*, 272(5265), pp.1170–3.

Masao, O. et al., 1997. Deletion of SHIP or SHP-1 reveals two distinct pathways for inhibitory signaling. *Cell*, 90(2), pp.293–301.

Matsumiya, S. et al., 2007. Structural Comparison of Fucosylated and Nonfucosylated Fc Fragments of Human Immunoglobulin G1. *Journal of Molecular Biology*, 368(3), pp.767–779.

Matsumoto, a et al., 2000. Autoantibody activity of IgG rheumatoid factor increases with decreasing levels of galactosylation and sialylation. *Journal of biochemistry*, 128(4), pp.621–628.

McCarron, M.J. & Marie, J.C., 2014. TGF-β prevents T follicular helper cell accumulation and B cell autoreactivity. *The Journal of clinical investigation*, 124(10), pp.4375–86.

McHeyzer-Williams, M. et al., 2012. Molecular programming of B cell memory. *Nature reviews. Immunology*, 12(1), pp.24–34.

Molloy, M.J., Zhang, W. & Usherwood, E.J., 2009. Cutting edge: IL-2 immune complexes as a therapy for persistent virus infection. *Journal of immunology (Baltimore, Md. : 1950)*, 182(8), pp.4512–4515.

Nakayamada, S. et al., 2011. Early Th1 Cell Differentiation Is Marked by a Tfh Cell-like Transition. *Immunity*, 35(6), pp.919–931.

Nimmerjahn, F. et al., 2005. FcγRIV: A novel FcR with distinct IgG subclass specificity. *Immunity*, 23(1), pp.41–51.

Nimmerjahn, F. & Ravetch, J. V, 2005. Divergent immunoglobulin g subclass activity through selective Fc receptor binding. *Science (New York, N.Y.)*, 310(5753), pp.1510–2.

Nimmerjahn, F. & Ravetch, J. V, 2007. The antiinflammatory activity of IgG: the intravenous IgG paradox. *The Journal of experimental medicine*, 204(1), pp.11–15.

Nimmerjahn, F. & Ravetch, J. V., 2008. Fcgamma receptors as regulators of immune responses. *Nature reviews. Immunology*, 8(1), pp.34–47.

Nova-Lamperti, E. et al., 2016. IL-10-produced by human transitional B-cells down-regulates CD86 expression on B-cells leading to inhibition of CD4(+)T-cell responses. *Scientific reports*, 6(January), p.20044.

Nurieva, R.I. et al., 2009. Bcl6 mediates the development of T follicular helper cells. *Science*, 325(5943), pp.1001–1005.

Nurieva, R.I. et al., 2012. STAT5 protein negatively regulates T follicular helper (Tfh) cell generation and function. *Journal of Biological Chemistry*, 287(14), pp.11234–11239.

Nutt, S.L. et al., 2015. The generation of antibody-secreting plasma cells. *Nature reviews. Immunology*, 15(3), pp.160–171.

O'Connor, B.P. et al., 2006. Imprinting the fate of antigen-reactive B cells through the affinity of the B cell receptor. *Journal of immunology (Baltimore, Md. : 1950)*, 177(11), pp.7723–7732.

Oefner, C.M. et al., 2012. Tolerance induction with T cell-dependent protein antigens induces regulatory sialylated IgGs. *Journal of Allergy and Clinical Immunology*, 129(6), pp.1647–1655.

Ohmi, Y. et al., 2016. Sialylation converts arthritogenic IgG into inhibitors of collagen-induced arthritis. *Nature communications*, 7, p.11205.

Onishi, Y. et al., 2008. Foxp3+ natural regulatory T cells preferentially form aggregates on dendritic cells in vitro and actively inhibit their maturation. *Proceedings of the National Academy of Sciences of the United States of America*, 105(29), pp.10113–8.

Onitsuka, M. et al., 2012. Enhancement of sialylation on humanized IgG-like bispecific antibody by overexpression of α2,6-sialyltransferase derived from Chinese hamster ovary cells. *Applied Microbiology and Biotechnology*, 94(1), pp.69–80.

Ono, M. et al., 1996. Role of the inositol phosphatase SHIP in negative regulation of the immune system by the receptor Fc(gamma)RIIB. *Nature*, 383(6597), pp.263–6.

Pali-Schöll, I. & Jensen-Jarolim, E., 2016. The concept of allergen-associated molecular patterns (AAMP). *Current Opinion in Immunology*, 42, pp.113–118.

Parekh, R.B. et al., 1985. Association of rheumatoid arthritis and primary osteoarthritis with changes in the glycosylation pattern of total serum IgG. *Nature*, 316(6027), pp.452–457.

Paterson, A.M. et al., 2015. Deletion of CTLA-4 on regulatory T cells during adulthood leads to resistance to autoimmunity. *The Journal of experimental medicine*, 212(10), pp.1603–1621.

Paus, D. et al., 2006. Antigen recognition strength regulates the choice between extrafollicular plasma cell and germinal center B cell differentiation. *The Journal of experimental medicine*, 203(4), pp.1081–91.

Pfeifle, R. et al., 2016. Regulation of autoantibody activity by the IL-23 – T H 17 axis determines the onset of autoimmune disease. , (November).

Phelan, J.D., Orekov, T. & Finkelman, F.D., 2008. Cutting edge: mechanism of enhancement of in vivo cytokine effects by anti-cytokine monoclonal antibodies. *Journal of immunology (Baltimore, Md. : 1950)*, 180(1), pp.44–8.

Pincetic, A. et al., 2014. Type I and type II Fc receptors regulate innate and adaptive immunity. *Nature immunology*, 15(8), pp.707–716.

Qi, H., 2016. T follicular helper cells in space-time. *Nature Reviews Immunology*.

Quast, I. et al., 2015. Sialylation of IgG Fc domain impairs complement-dependent cytotoxicity. *Journal of Clinical Investigation*, 125(11), pp.4160–4170.

Qureshi, O.S. et al., 2011. Trans-endocytosis of CD80 and CD86: a molecular basis for the cell-extrinsic function of CTLA-4. *Science*, 332, pp.600–3.

Rademacher, T.W., Williams, P. & Dwek, R.A., 1994. Agalactosyl glycoforms of IgG autoantibodies are pathogenic. *Proc Natl Acad Sci U S A*, 91(13), pp.6123–6127.

Ramiscal, R.R. & Vinuesa, C.G., 2013. T-cell subsets in the germinal center. *Immunol Rev*, 252(1), pp.146–155.

Reichert, J.M., 2016. Antibodies to watch in 2016. *mAbs*, 8(2), pp.197–204.

Reinhardt, R.L., Liang, H.-E. & Locksley, R.M., 2009. Cytokine-secreting follicular T cells shape the antibody repertoire. *Nature Immunology*, 10(4), pp.385–93.

Rombouts, Y. et al., 2015. Anti-citrullinated protein antibodies acquire a pro-inflammatory Fc glycosylation phenotype prior to the onset of rheumatoid arthritis. *Annals of the rheumatic diseases*, 74(1), pp.234–41.

Rosenberg, S.A., 2014. IL-2: the first effective immunotherapy for human cancer. *Journal of immunology (Baltimore, Md. : 1950)*, 192(12), pp.5451–8.

Saadoun, D. et al., 2011. Regulatory T-cell responses to low-dose interleukin-2 in HCV-induced vasculitis. *The New England journal of medicine*, 365(22), pp.2067–2077.

Sage, P.T., Alvarez, D., et al., 2014. Circulating T follicular regulatory and helper cells have memory-like properties. *Journal of Clinical Investigation*, 124(12), pp.5191–5204.

Sage, P.T. et al., 2015. Defective TFH Cell Function and Increased TFR Cells Contribute to Defective Antibody Production in Aging. *Cell Reports*, 12(2), pp.163–171.

Sage, P.T. et al., 2016. Suppression by TFR cells leads to durable and selective inhibition of B cell effector function. *Nature Immunology*, (October), pp.1–13.

Sage, P.T., Paterson, A.M., et al., 2014. The coinhibitory receptor CTLA-4 controls B cell responses by modulating T follicular helper, T follicular regulatory, and T regulatory cells. *Immunity*, 41(6), pp.1026–1039.

Sage, P.T. et al., 2013. The receptor PD-1 controls follicular regulatory T cells in the lymph nodes and blood. *Nature immunology*, 14(2), pp.152–61.

Sage, P.T. & Sharpe, A.H., 2016. T follicular regulatory cells. *Immunological Reviews*, 271(1), pp.246–259.

Sage, P.T. & Sharpe, A.H., 2015. T Follicular Regulatory Cells in the Regulation of B cell Responses. *Trends in immunology*, 36(7), pp.410–418.

Schatz, D.G. & Ji, Y., 2011. Recombination centres and the orchestration of V(D)J recombination. *Nature reviews. Immunology*, 11(4), pp.251–63.

Scherer, H.U. et al., 2010. Glycan profiling of anti-citrullinated protein antibodies isolated from human serum and synovial fluid. *Arthritis and Rheumatism*, 62(6), pp.1620–1629.

Schildberg, F.A. et al., 2016. Review Coinhibitory Pathways in the B7-CD28 Ligand-Receptor Family. *Immunity*, 44(5), pp.955–972.

Schmitt, N. et al., 2014. The cytokine TGF-β co-opts signaling via STAT3-STAT4 to promote the differentiation of human TFH cells. *Nature Immunology*, 15(9), pp.856–865.

Schwab, I., Lux, A. & Nimmerjahn, F., 2015. Pathways Responsible for Human Autoantibody and Therapeutic Intravenous IgG Activity in Humanized Mice. *Cell Reports*, 13(3), pp.1–11.

Schwab, I. & Nimmerjahn, F., 2013. Intravenous immunoglobulin therapy: how does IgG modulate the immune system? *Nature Reviews Immunology*, 13(3), pp.176–189.

Schwickert, T. a. et al., 2011. A dynamic T cell-limited checkpoint regulates affinity-dependent B cell entry into the germinal center. *Journal of Experimental Medicine*, 208(6), pp.1243–1252.

Shade, K.-T. & Anthony, R., 2013. Antibody Glycosylation and Inflammation. *Antibodies*, 2(3), pp.392–414.

Shields, R.L. et al., 2002. Lack of fucose on human IgG1 N-linked oligosaccharide improves binding to human FcγRIII and antibody-dependent cellular toxicity. *Journal of Biological Chemistry*, 277(30), pp.26733–26740.

Shih, T.-A.Y., Roederer, M. & Nussenzweig, M.C., 2002. Role of antigen receptor affinity in T cell-independent antibody responses in vivo. *Nature immunology*, 3(4), pp.399–406.

Shulman, Z. et al., 2014. Dynamic signaling by T follicular helper cells during germinal center B cell selection. *Science (New York, N.Y.)*, 345(6200), pp.1058–1062.

Shulman, Z. et al., 2013. T follicular helper cell dynamics in germinal centers. *Science*, 341(6146), pp.673–677.

De Silva, N.S. & Klein, U., 2015. Dynamics of B cells in germinal centres. *Nature Reviews Immunology*, 15(3), pp.137–148.

Smith, K.G.C. & Clatworthy, M.R., 2010. FcgammaRIIB in autoimmunity and infection: evolutionary and therapeutic implications. *Nature reviews. Immunology*, 10(5), pp.328–343.

von Spee-Mayer, C. et al., 2015. Low-dose interleukin-2 selectively corrects regulatory T cell defects in patients with systemic lupus erythematosus. *Annals of the Rheumatic Diseases*, p.annrheumdis-2015-207776..

Tai, X. et al., 2005. CD28 costimulation of developing thymocytes induces Foxp3 expression and regulatory T cell differentiation independently of interleukin 2. *Nature immunology*, 6(2), pp.152–162.

Takemori, T. et al., 2014. Generation of memory B cells inside and outside germinal centers. *European Journal of Immunology*, 44(5), pp.1258–1264.

Tang, Q. et al., 2008. Central Role of Defective Interleukin-2 Production in the Triggering of Islet Autoimmune Destruction. *Immunity*, 28(5), pp.687–697.

Tangye, S.G. et al., 2013. The good, the bad and the ugly - TFH cells in human health and disease. *Nature reviews. Immunology*, 13(6), pp.412–426.

Tarlinton, D. & Good-Jacobson, K., 2013. Diversity among memory B cells: origin, consequences, and utility. *Science (New York, N.Y.)*, 341(6151), pp.1205–11.

Tivol, E.A. et al., 1995. Loss of CTLA-4 leads to massive lymphoproliferation and fatal multiorgan tissue destruction, revealing a critical negative regulatory role of CTLA-4. *Immunity*, 3(5), pp.541–547.

Tomala, J. et al., 2009. In vivo expansion of activated naive CD8+ T cells and NK cells driven by complexes of IL-2 and anti-IL-2 monoclonal antibody as novel approach of cancer immunotherapy. *Journal of immunology (Baltimore, Md. : 1950)*, 183(8), pp.4904–12.

Victora, G.D. et al., 2010. Germinal center dynamics revealed by multiphoton microscopy with a photoactivatable fluorescent reporter. *Cell*, 143(4), pp.592–605.

Victora, G.D. & Nussenzweig, M.C., 2012. Germinal centers. *Annu Rev Immunol*, 30, pp.429–457.

Vidarsson, G., Dekkers, G. & Rispens, T., 2014. IgG subclasses and allotypes: From structure to effector functions. *Frontiers in Immunology*, 5(OCT).

Vinuesa, C.G. et al., 2005. A RING-type ubiquitin ligase family member required to repress follicular helper T cells and autoimmunity. *Nature*, 435(7041), pp.452–8.

Vinuesa, C.G. et al., 2016. Follicular Helper T Cells. , (February), pp.1–34.

Vinuesa, C.G. et al., 2016. Follicular Helper T Cells. *Annual review of immunology*, 34(1), p.annurev-immunol-041015-055605.

Vinuesa, C.G. & Cyster, J.G., 2011. How T cells earn the follicular rite of passage. *Immunity*, 35(5), pp.671–680.

Vokaer, B. et al., 2013. IL-17A and IL-2-Expanded Regulatory T Cells Cooperate to Inhibit Th1-Mediated Rejection of MHC II Disparate Skin Grafts. *PLoS ONE*, 8(10).

Walker, L.S.K., 2015. CTLA-4 and Autoimmunity: New Twists in the Tale. *Trends in Immunology*, 36(12), pp.760–762.

Walker, L.S.K. et al., 2003. Established T cell-driven germinal center B cell proliferation is independent of CD28 signaling but is tightly regulated through CTLA-4. *Journal of Immunology*, 170(1), pp.91–98.

Walker, L.S.K., 2013. Treg and CTLA-4: Two intertwining pathways to immune tolerance. *Journal of Autoimmunity*, 45, pp.49–57.

Walker, L.S.K. & Sansom, D.M., 2015. Confusing signals: recent progress in CTLA-4 biology. *Trends in immunology*, 36(2), pp.63–70.

Wallin, E.F. et al., 2014. Human T-follicular helper and T-follicular regulatory cell maintenance is independent of germinal centers. *Blood*, 124(17), pp.2666–2674.

Wang, T.T. et al., 2015. Anti-HA Glycoforms Drive B Cell Affinity Selection and Determine Influenza Vaccine Efficacy. *Cell*, 162(1), pp.160–169.

Warnock, D. et al., 2005. In vitro galactosylation of human IgG at 1 kg scale using recombinant galactosyltransferase. *Biotechnology and Bioengineering*, 92(7), pp.831–842.

Washburn, N. et al., 2015. Controlled tetra-Fc sialylation of IVIg results in a drug candidate with consistent enhanced anti-inflammatory activity. *Proceedings of the National Academy of Sciences of the United States of America*, 112(11), p.201422481.

Waterhouse, P. et al., 1995. Lymphoproliferative disorders with early lethality in mice deficient in Ctla-4. *Science (New York, N.Y.)*, 270(5238), pp.985–988.

Webster, K.E. et al., 2009. In vivo expansion of T reg cells with IL-2-mAb complexes: induction of resistance to EAE and long-term acceptance of islet allografts without immunosuppression. *The Journal of experimental medicine*, 206(4), pp.751–760.

Weinstein, J.S. et al., 2016. TFH cells progressively differentiate to regulate the germinal center response. *Nature Immunology*, (August).

Weisel, F.J. et al., 2016. A Temporal Switch in the Germinal Center Determines Differential Output of Memory B and Plasma Cells. *Immunity*, 44(1), pp.116–130.

Wieland, A. et al., 2015. Antibody effector functions mediated by Fcγ-receptors are compromised during persistent viral infection. *Immunity*, 42(2), pp.367–378.

Wing, J.B. et al., 2014. Regulatory T cells control antigen-specific expansion of Tfh cell number and humoral immune responses via the coreceptor CTLA-4. *Immunity*, 41(6), pp.1013–1025.

Wing, K. et al., 2008. CTLA-4 control over Foxp3+ regulatory T cell function. *Science*, 322(5899), pp.271–275.

Wollenberg, I. et al., 2011. Regulation of the germinal center reaction by Foxp3+ follicular regulatory T cells. *Journal of immunology (Baltimore, Md. : 1950)*, 187(9), pp.4553–60.

Wu, H. et al., 2016. Follicular regulatory T cells repress cytokine production by follicular helper T cells and optimize IgG responses in mice. *European Journal of Immunology*, pp.1–10.

Yu, A. et al., 2015. Selective IL-2 responsiveness of regulatory t cells through multiple intrinsic mechanisms supports the use of low-dose IL-2 therapy in type 1 diabetes. *Diabetes*, 64(6), pp.2172–2183.

Yu, D. et al., 2009. The Transcriptional Repressor Bcl-6 Directs T Follicular Helper Cell Lineage Commitment. *Immunity*, 31(3), pp.457–468.

Zhang, Y. et al., 2013. Germinal center B cells govern their own fate via antibody feedback. *Journal of Experimental Medicine*, 210(3), pp.457–464.

Zheng, S.G. et al., 2007. IL-2 is essential for TGF-beta to convert naive CD4+CD25- cells to CD25+Foxp3+ regulatory T cells and for expansion of these cells. *Journal of immunology (Baltimore, Md : 1950)*, 178(4), pp.2018–2027.

Zotos, D. et al., 2010. IL-21 regulates germinal center B cell differentiation and proliferation through a B cell-intrinsic mechanism. *The Journal of experimental medicine*, 207(2), pp.365–78.

PUBLICATIONS

Eschweiler, S. et al. Distinct inflammatory germinal center B cell responses determine the type of IgG antibody glycosylation, *Science Immunology, in revision.*

Epp, A.*, Hobusch, J.*, Bartsch, Y.*,…, **Eschweiler, S.** et al., 2016. Sialylation of IgG antibodies inhibits IgG-mediated allergic reactions. *Journal of Allergy and Clinical Immunology, in revision*.

Pagel, J., Hartz, A., Figge, J., Gille, C., **Eschweiler, S.** et al., 2016. Regulatory T cell frequencies are increased in preterm infants with clinical early-onset sepsis. *Clinical and Experimental Immunology*, 185(2), pp.219–227.